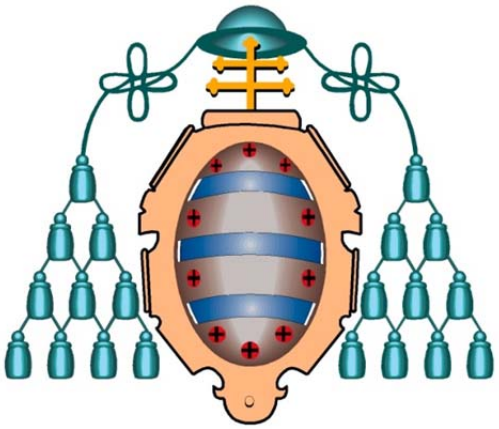

UNIVERSIDAD DE OVIEDO

DEPARTAMENTO DE INGENIERÍA QUÍMICA Y
TECNOLOGÍA DEL MEDIO AMBIENTE

INGENIERÍA DE PROCESOS Y AMBIENTAL

CINÉTICA Y CAPACIDAD DE SULFATACIÓN DE CaO EN LECHOS FLUIDIZADOS CIRCULANTES PARA CAPTURA DE CO_2

TESIS DOCTORAL

JOSÉ MARÍA CORDERO DÍAZ
2014

AGRADECIMIENTOS

Quiero expresar mi agradecimiento a la Doctora Mónica Alonso y al Investigador Científico Juan Carlos Abanades, por la Dirección de esta Tesis y por su apoyo y dedicación desde el principio hasta el final de su desarrollo.

Al Consejo Superior de Investigaciones Científicas (CSIC) por permitir la realización de esta Tesis en el Instituto Nacional del Carbón (INCAR) y a sus Directores durante el desarrollo del trabajo, Doctores Carlos Gutiérrez Blanco y Juan Manuel Díez Tascón.

Al Catedrático Fernando V. Díez Sanz, por aceptar ser tutor de esta Tesis.

Al Gobierno del Principado de Asturias, que a través del organismo FICYT ha concedido la beca predoctoral "Severo Ochoa".

A los proyectos que con su financiación han permitido el desarrollo de gran parte de los trabajos realizados en esta Tesis Doctoral: CaOling del 7º Programa Marco, y ReCaL.

A todo el "Grupo de Captura de CO_2" del INCAR, por su apoyo y colaboración con los trabajos llevados a cabo en esta Tesis. En especial quiero darle mi más sincero agradecimiento a Fernando Fuentes, tanto en lo laboral como en lo personal, pues ha sido un pilar de apoyo indiscutible.

A mis amigos y compañeros del INCAR, y a mis amigos de toda la vida, que siempre están ahí para escuchar y pasar buenos momentos.

A mi familia, en especial a mis padres y mi hermano, que han soportado frustraciones y alegrías por igual, y porque han demostrado que esté donde esté, sin importar los cambios que da la vida, siempre tendré un sitio con ellos.

RESUMEN

Uno de los principales retos a los que la humanidad se enfrentará en los próximos decenios es la mitigación del cambio climático. El principal causante es el CO_2 procedente del uso de combustibles fósiles para la obtención de energía. La captura y el almacenamiento de CO_2 sigue siendo una de las principales opciones de mitigación a corto y medio plazo. De entre las tecnologías emergentes de captura de CO_2 de grandes fuentes estacionarias, los procesos basados en CaO (Calcium Looping, CaL) para post-combustión han tenido un desarrollo muy rápido en los últimos años. Esto es debido a su potencial para reducir costes y penalizaciones energéticas cuando se les compara con otras tecnologías de captura más maduras. Otra de sus ventajas consiste en la posibilidad de eliminar la etapa de desulfuración al poder capturar simultáneamente SO_2 y CO_2 en el mismo reactor. Además, en este tipo de procesos, existe una sinergia entre el uso de la purga procedente del calcinador como agente desulfurante en el propio combustor.

Durante la investigación descrita en esta Tesis, se ha realizado un estudio cinético de la sulfatación de CaO en las condiciones relevantes de operación de los reactores que conforman un CaL. Para este estudio se ha empleado una termobalanza especialmente diseñada para llevar a cabo los ciclos de calcinación/carbonatación. Además, haciendo uso de una planta piloto experimental para captura de CO_2 se han llevado a cabo ensayos de

sulfatación simultáneos a la carbonatación y calcinación en continuo, para estudiar la co-captura de SO_2 y CO_2. Los resultados de estos trabajos se han validado a escala mayor, midiendo en termobalanza las velocidades de reacción y capacidades de sulfatación de un sorbente procedente de una purga de la planta experimental para captura de CO_2 de 1.7 MWt localizada en la Pereda. Finalmente, se han interpretado los datos experimentales obtenidos a escala de partícula mediante un modelo general de poro aleatorio (RPM, por sus siglas en inglés).

ABSTRACT

Climate change mitigation will present a major challenge for mankind in the near future. The CO_2 emitted from fossil fuel combustion is the principal source of greenhouse gases. CO_2 capture and storage continues to be one of the most important options for mitigating climate change in the medium to long term scales. Among the emerging technologies for capturing CO_2 from large-scale stationary sources, those based on CaO (Calcium Looping, CaO) in post-combustion processes have experienced rapid development in recent years. This is attributable to their enormous potential for reducing costs and energy penalties when compared to other more mature technologies. The possibility of avoiding the desulfuration stage by means of the simultaneous capture of CO_2 and SO_2 in the same reactor is another of their main advantages. Moreover, in processes of this kind, a synergy can be achieved if the CaO from the purge of the calciner is used as the source of the sorbent for desulfuration in the combustor.

A kinetic study of the sulfation of CaO in operating conditions typical of CaL reactors has been carried out in this Thesis. For this purpose, a thermogravimetric device specially designed for conducting calcination/carbonation cycles was used. In addition, in an experimental pilot plant consisting of two fluidized circulating interconnected beds experiments on simultaneous sulfation, carbonation and calcination were performed in continuous mode. The results of these studies have been validated at larger scales by measuring in a thermogravimetric apparatus the sulfation rates and

capacities of a sorbent obtained from a 1.7 MWt CO_2 capture pilot plant located in La Pereda. The experimental data have been interpreted by means of a random pore model (RPM).

ÍNDICE

Lista de Publicaciones

1. B. Arias, J.M. Cordero, M. Alonso, J.C. Abanades, "Sulfation rates of cycled CaO particles in the carbonator of a Ca-looping cycle for postcombustion CO_2 capture", AIChE Journal 58 (2012) 2262-2269.

2. B. Arias, J.M. Cordero, M. Alonso, M.E. Diego, J.C. Abanades, "Investigation of SO_2 Capture in a Circulating Fluidized Bed Carbonator of a Ca Looping Cycle", Industrial & Engineering Chemistry Research 52 (2013) 2700-2706.

3. M. Alonso, J.M. Cordero, B. Arias, J.C. Abanades, "Sulfation Rates of Particles in Calcium Looping Reactors", Chemical Engineering & Technology 37 (2014) 15-19.

4. J.M. Cordero, M. Alonso B, "Modeling of the kinetics of sulphation of CaO Particles under CaL Reactor Conditions", Chemical Engineering Journal (*in press*).

5. J.M. Cordero, M. Alonso, B. Arias, J.C. Abanades, "Sulfation Performance of CaO Purges Derived from Calcium Looping CO_2 Capture Systems", Energy & Fuels 28 (2014) 1325-1330.

Lista de Figuras

1 Introducción

Uno de los mayores retos a los que se enfrenta la humanidad en el siglo XXI es el cambio climático. Según el Panel Intergubernamental para el Cambio Climático (IPCC en sus siglas en inglés), [1], el calentamiento global es inequívoco y muchos de los cambios observados no tienen precedentes en decenas de milenios. De hecho, en el hemisferio norte, es probable que el periodo 1983-2012 haya sido el periodo de 30 años más cálido de los últimos 1400 años. Estos cambios se han producido principalmente por el aumento de las emisiones de gases de efecto invernadero (GEI) de origen antropogénico [1].

Las concentraciones atmosféricas de los GEI han aumentado a niveles sin precedentes en los últimos 800 000 años. Este aumento procede directamente de los sectores energético, industrial y del transporte [2]. De entre los GEI, se considera el CO_2 como el gas de mayor contribución debido a su volumen de emisión. El aumento de la concentración de CO_2 se debe principalmente al uso de combustibles fósiles, a procesos industriales, y a las emisiones netas derivadas del cambio de uso del suelo [2].

Es necesario tomar medidas inmediatamente para reducir el aumento de la concentración de CO_2 en la atmósfera puesto que el CO_2 tiene un tiempo de residencia alto en ella (hasta 200 años) y las emisiones acumuladas de CO_2 determinarán en gran medida el calentamiento medio global en la superficie a finales del siglo XXI y posteriormente. Por ello. La mayoría de los efectos

del cambio climático perdurarán durante varios siglos [1]. Retrasar los esfuerzos de mitigación previstos más allá de 2030 aumentará sustancialmente la dificultad para alcanzar los niveles de emisiones a largo plazo y estrechará el intervalo de opciones para mantener el aumento medio de la temperatura terrestre por debajo de 2 ºC con respecto a los niveles pre-industriales [2]. Por tanto, es fundamental abordar desde estos momentos una profunda transformación del sistema energético mundial.

1.1 Cambio climático, CO_2 y energía

A pesar del continuo debate sobre políticas de mitigación de cambio climático, las emisiones anuales de GEI aumentaron una media de 1 $GtCO_2eq$/año en el periodo 2000-2010 comparadas con las 0.4 $GtCO_2eq$/año del periodo 1970-2000. Las emisiones totales antropogénicas de GEI en el periodo 2000-2010 fueron las más elevadas en toda la historia de la humanidad, alcanzando un valor de 49 $GtCO_2eq$/año en 2010. La crisis económica mundial de 2007-2008 sólo redujo temporalmente las emisiones [2].

Tomando el año 2010 como base, de las 49 $GtCO_2eq$ de GEI emitidas, el 35 % fueron emitidas desde el sector de energía, el 24 % desde el sector agrícola, forestal y de otros usos del suelo, el 21 % del sector industrial, el 14% desde el sector del transporte y el 6.4 % en edificios. En la última década, las mayores contribuciones al aumento de las emisiones fueron debidas al crecimiento en la demanda energética y al aumento del uso de carbón en el mix energético global. La descarbonización en el sector de generación de energía eléctrica es un componente clave para alcanzar niveles bajos estables de GEI en la atmósfera (430-550 ppm CO_2eq) en las estrategias de mitigación de bajo coste [2].

De las 49 $GtCO_2$ eq/año de emisiones globales antropogénicas de GEI en 2010, el 76 % (37 $GtCO_2$eq/año) corresponden a las emisiones de CO_2, que se mantiene como el mayor GEI antropogénico. Las emisiones de CO_2 debidas al uso de combustibles fósiles alcanzaron las 32 $GtCO_2$/año en 2010, crecieron un 3% entre el 2010 y el 2011 y alrededor de 1-2 % entre el 2011 y 2012 [2]. En consecuencia, la concentración de CO_2 (junto con el CH_4 y el N_2O) no ha dejado de aumentar Figura 1.1 [1].

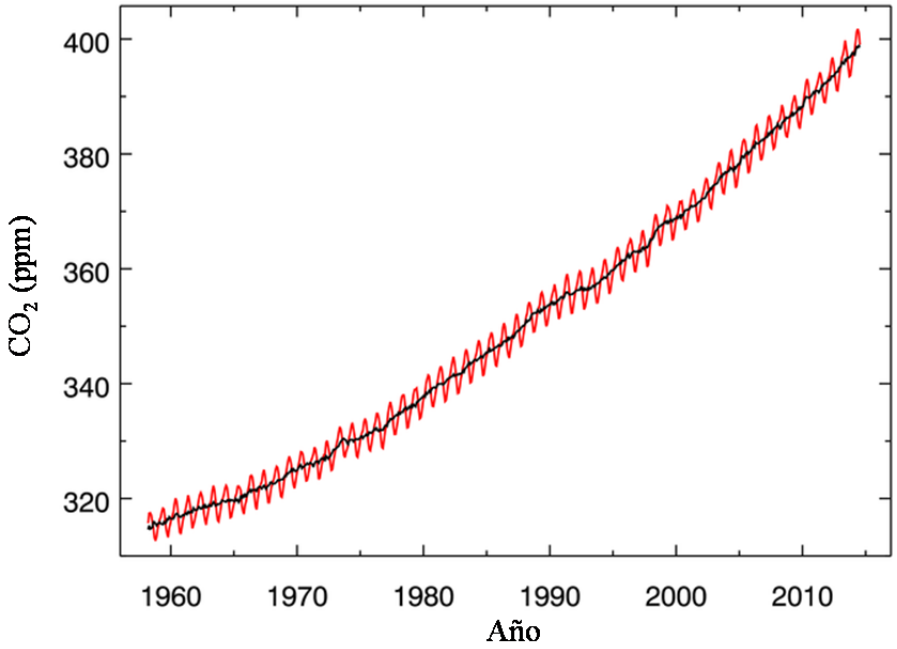

Figura 1.1. Evolución de la concentración de CO_2 atmosférico (ppmv) durante los últimos años en el observatorio de Mauna Loa (Hawai). La línea roja une puntos de media mensual, mientras que la línea negra corresponde a la media anual [3].

En la mayor parte de los escenarios de bajas emisiones estimados en el último Informe de Bases Físicas sobre el cambio climático del IPCC [1], la contribución del sector eléctrico de bajas emisiones (energía renovable,

nuclear, y captura y almacenamiento de CO_2) al mix global ha de aumentar desde el 30 % actual a más del 80 % en el año 2050. La generación eléctrica a partir de combustibles fósiles (sin captura y almacenamiento de CO_2) prácticamente ha de desaparecer [2].

1.2 Captura y almacenamiento de CO_2

La captura y el almacenamiento de CO_2 (CAC) se refiere a la captura de CO_2 emitido por grandes fuentes estacionarias industriales, su compresión para su transporte, y a continuación su inyección en una formación geológica segura donde puede ser almacenado permanentemente [4].

Sus principales etapas se describen a continuación.

La *captura de CO_2* sólo se puede aplicar a grandes a centrales térmicas basadas en combustibles fósiles o en biomasa, grandes industrias emisoras de CO_2, extracción de gas natural, plantas de combustibles sintéticos, y plantas de producción de hidrógeno basadas en combustibles fósiles. El principal objetivo de esta etapa es obtener una corriente pura o fácilmente purificable de CO_2 adecuada para transporte y almacenamiento. Esta etapa suele suponer ¾ partes del coste total de mitigación [4, 5].

Los sistemas de captura de CO_2 se suelen clasificar en función del lugar donde tenga lugar una etapa importante de separación de gases. Esta separación de gases no es necesariamente una separación de CO_2. Esquemáticamente, esta clasificación para el caso de centrales térmicas se muestra en la Figura 1.2 [5].

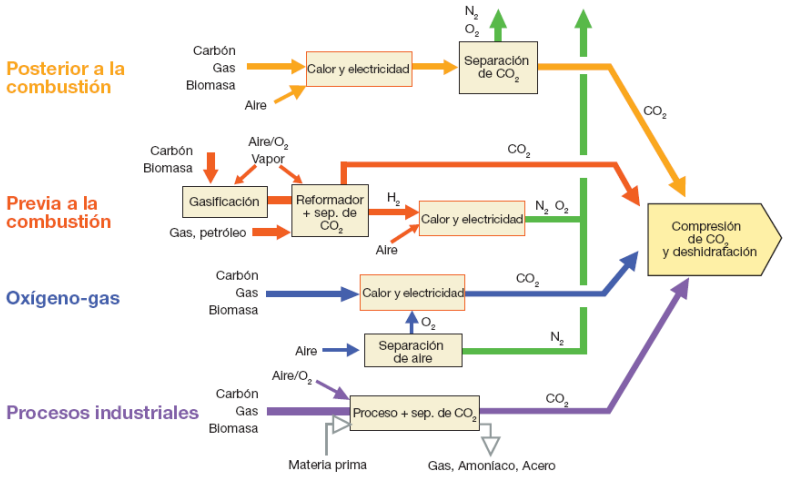

Figura 1.2. Esquema general de los sistemas de captura de CO_2 [5].

Por simplicidad, otras plantas de sectores no energéticos se clasifican aparte como "procesos industriales", si bien pueden normalmente clasificarse igualmente atendiendo al criterio del sector energético. A continuación se describe brevemente cada uno de ellos.

Post-combustión: En estos procesos se separa el CO_2 de una corriente de gases producida por la combustión de combustibles fósiles o biomasa en aire. El CO_2 diluido en los gases de combustión se haría pasar a través de un equipo capaz de separar el CO_2 con alta eficacia, en forma de corriente concentrada en CO_2, mientras que el resto de gases con un bajo contenido en CO_2 se descargaría a la atmósfera. La mayor parte de la infraestructura energética a nivel mundial se base en la combustión con aire, por lo que estas tecnologías serían las únicas viables para centrales existentes de reciente construcción.

Pre-combustión: se denomina así a los sistemas que presentan la etapa de separación de gases previamente a la combustión. Bajo este término se agrupan los procesos que producen combustibles bajos en carbono, como el

caso del H_2, que se quema en turbinas o en pilas de combustible. Las dos reacciones químicas fundamentales son la del combustible con vapor de agua u oxígeno, dando como resultado H_2 y CO, y la llamada reacción de desplazamiento de gas de agua, que convierte el CO en CO_2 y H_2. La etapa de separación consistiría en separar el CO_2 del H_2. La mezcla de estos gases suele estar a alta presión, facilitando el rendimiento energético de la separación de gases. A este proceso se le concede una alta importancia debido a que favorece la llamada economía del hidrógeno, o la producción de combustibles de automoción con bajo contenido en carbono, si se captura el CO_2 durante la producción de dichos combustibles.

Oxi-combustión: consiste en la combustión del combustible en una mezcla de O_2 y CO_2 en lugar de aire, lo que resulta en un gas de combustión muy rico en CO_2 y en consecuencia se facilita la etapa de purificación final antes del transporte y almacenamiento. La etapa característica de separación de gases en estos sistemas sería la de separación de O_2 del aire.

En la actualidad, existen varias tecnologías para la captura de CO_2 que son comerciales en algunas aplicaciones industriales aunque no a la escala requerida para su aplicación directa en centrales térmicas. Los procesos basados en absorción química y/o física se usan en la industria petroquímica y en la producción de gas natural o amoniaco. La adsorción también se emplea en procesos industriales como la purificación de hidrógeno y del gas natural. Los dispositivos que hacen uso de membranas se están desarrollando también para las aplicaciones de separación y purificación de CO_2 de corrientes gaseosas (actualmente las tecnologías comerciales de membranas para separación de CO_2 tienen aplicación en la purificación del gas natural [6]).

El *transporte de CO_2* es la etapa más desarrollada de los procesos CCS en la actualidad. Esto es gracias a la existencia de gaseoductos terrestres y

marinos que llevan funcionando desde los años 70 en EEUU, donde hoy en día se transportan entre 48-58 $MtCO_2$/año a través de 6500 km de gaseoductos [4]. Otra forma adecuada de transporte de CO_2, pero que en la actualidad sólo se hace en pequeñas cantidades, es como gas licuado en barcos. El transporte de gases licuados por medio marítimo es una tecnología conocida, pues es un medio típico de transporte para fracciones del petróleo como el gas natural, el butano y el propano.

El *almacenamiento de* CO_2 es la etapa final del proceso y supone el confinamiento permanente del CO_2. La opción más común y que ofrece mayores posibilidades es la que comprende la compresión del CO_2 a un estado supercrítico, y su inyección en formaciones geológicas adecuadas a más de 800 metros de profundidad tales como: formaciones con acuíferos salinos profundos, yacimientos agotados de petróleo y gas natural, y formaciones de carbón no disponible para extracción por minería (pudiendo además desplazar al CH_4 adsorbido, permitiendo su extracción). Aunque la inyección de CO_2 puede utilizarse en la extracción mejorada del petróleo, se prevé que la mayor parte de los futuros proyectos CAC utilicen formaciones salinas, porque son muy abundantes y tienen una gran capacidad de almacenamiento [4]. En España existen mayoritariamente este tipo de formaciones salinas.

La formación geológica que actúe como almacén de CO_2, ha de tener una cubierta geológica impermeable al CO_2 pues parte de él podría ascender por su menor densidad en comparación con la del agua salina subterránea, de esta forma el CO_2 almacenado se disolverá en estas aguas, rellenará los poros de las rocas, y finalmente reaccionará con las rocas dando lugar a minerales [4].

El almacenamiento en formaciones geológicas profundas supone el uso de muchas de las tecnologías que se han desarrollado para la prospección de

petróleo y gas. Por lo tanto es un proceso real a escala industrial, ejemplos: el proyecto *In Salah CO_2 Storage* en Argelia que lleva almacenados 3.8 $MtCO_2$ en formaciones salinas, el proyecto *Great Plains Synfuel Plant and Weyburn-Midale Project* en Canadá, que transporta y almacena 3 $MtCO_2$/año en recuperación mejorada del petróleo, el proyecto *Sleipner CO_2 Injection* en el Mar del Norte inyecta en formaciones salinas profundas sobre 0.9 $MtCO_2$/año [4].

A pesar de que todos los componentes integrantes de un sistema CAC existen por separado y se usan hoy en día a escala comercial, los sistemas CAC no se han aplicado todavía a la generación eléctrica a gran escala. Para que las tecnologías CAC se desplieguen en este sector, es necesario incentivar un marco de regulación y/o mejorar la competitividad con los procesos con CAC [2]. Es por ello, que en los últimos años se están desarrollando una serie de tecnologías de captura de CO_2 que reduzcan las penalizaciones energéticas y los costes de los procesos. De entre estas tecnologías emergentes, una de las más prometedoras es la tecnología basada en los ciclos de calcinación/carbonatación del CaO o Calcium Looping (CaL). Debido a la importancia de estas tecnologías, y al ser el objeto principal de trabajo de esta Tesis, se describirán a continuación los procesos más relevantes de este tipo.

1.3 Sistemas de captura de CO_2 mediante ciclos de calcinación-carbonatación a alta temperatura

La captura de CO_2 utilizando CaO como sorbente regenerable no es un concepto nuevo, dado que muchos procesos basados en esta reacción fueron propuestos en el siglo XIX. En los años 60 del siglo XX, Curran et al. [7] demostraron la posibilidad de un método (*Acceptor Coal Gasification*

Process) para separar el CO_2 durante la gasificación del carbón enriqueciendo la corriente de H_2 a la vez que se aprovechaba el calor de la reacción de carbonatación. Shimizu et al. [8] propusieron por vez primera la utilización de dos reactores de lecho fluidizado interconectados como sistema para la captura de CO_2 en post-combustión, utilizando CaO como sorbente regenerable. El CSIC ha trabajado en la demostración y desarrollo de esta tecnología y de otros procesos avanzados de captura de CO_2 desde el año 2002 [9-18].

Los sistemas de captura de CO_2 mediante ciclos de calcinación/carbonatación poseen importantes ventajas respecto a otros sistemas de captura. En primer lugar, son sistemas que trabajan a alta temperatura. Esta característica permite la integración energética con una planta de generación de energía, lo que reduce la penalización energética del sistema de captura. En segundo lugar, el sorbente empleado es CaO. El CaO necesario para la captura de CO_2 procede de la calcinación de caliza. La caliza es un material abundante, y ampliamente distribuido geográficamente, lo que lo convierte en uno de los materiales más baratos [19] como precursor de un sorbente de CO_2. El CaO tiene una cinética de reacción rápida con el CO_2 a temperaturas en torno a 650 ºC, lo que permite que los reactores sean compactos. Además y dado que la caliza tiene un uso habitual en las centrales térmicas para desulfuración y también se emplea en la fabricación del cemento, es un material conocido y se maneja a gran escala. Finalmente, los equipos utilizados son fundamentalmente reactores de lecho fluidizado circulante (CFB por sus siglas en inglés), que es una tecnología de combustión muy conocida y desarrollada a gran escala (CFBC). Muchas de las soluciones térmicas y mecánicas desarrolladas para centrales térmicas del tipo CFBC son aplicables al sistema de captura de CO_2, lo que puede facilitar su rápido escalado.

No obstante, los procesos de captura basados en CaO presentan una serie de inconvenientes. Uno de ellos es la rapidez con la que decae la capacidad máxima de captura de CO_2 del sorbente debido a un proceso de sinterización que tiene lugar a medida que el CaO sufre los ciclos de calcinación/carbonatación. Una forma de compensar esta pérdida de capacidad consiste simplemente en alimentar un flujo de sorbente fresco al sistema [10], aprovechando el bajo coste de la caliza natural. Esto hace que sea necesario purgar sólidos de éste. No obstante, la purga extraída puede tener utilización por ejemplo en cementeras, donde el CaO es una materia prima fundamental [20]. Otra posibilidad para esta purga, que también resulta atractiva, es su utilización como agente desulfurante en calderas de combustión [21], donde se llevan décadas empleando calizas para tal propósito. Por otra parte, debe tenerse en cuenta que esta capacidad del CaO para absorber también el SO_2 produce una desactivación adicional del sorbente:

$$CaO + SO_2 + 1/2\ O_2 \rightarrow CaSO_4$$

, ya que la formación de $CaSO_4$ es irreversible a diferencia de la formación de $CaCO_3$ durante el proceso de calcinación/carbonatación. Sin embargo, puesto que el SO_2 es siempre un contaminante minoritario respecto al CO_2, la reacción de sulfatación de CaO abre la posibilidad de la captura de ambos contaminantes, CO_2 y SO_2, en el mismo equipo, lo que puede aportar grandes ventajas competitivas al proceso en su conjunto (las centrales térmicas con captura de CO_2 por calcinación/carbonatación no necesitarían de costosas unidades de desulfuración (FGD o similar)). .

A continuación, se exponen brevemente diferentes configuraciones de sistemas de captura de CO_2 basados en CaO como sorbente regenerable, resaltando el esquema básico de los procesos y las diferentes condiciones de operación donde se produce el contacto entre las partículas de CaO y los

gases conteniendo CO_2, SO_2 que reaccionan con dichas partículas y que son el objeto de investigación de esta Tesis.

1.3.1 Sistema de captura de CO_2 en régimen de post-combustión para centrales existentes.

Este proceso de captura de CO_2 se esquematiza en la Figura 1.3. Tiene como objetivo el tratamiento de los gases de combustión procedentes de una central de carbón convencional. Consiste en dos lechos fluidizados circulantes interconectados: un carbonatador y un calcinador. Si atendemos únicamente a los flujos de CO_2, los gases de combustión procedentes de la caldera y que contienen el CO_2 (F_{CO2}) entran al carbonatador, donde la reacción de carbonatación del CaO (F_{CaO}) tiene lugar a temperaturas entre 600 y 700 ºC. La eficacia de captura dependerá por tanto de las propiedades (capacidad de captura y velocidad de reacción) del sorbente y del diseño del reactor. Los gases prácticamente libres de CO_2 saldrían del carbonatador. El flujo de sólidos que sale del carbonatador contiene mayoritariamente CaO no reaccionado y $CaCO_3$ (además de $CaSO_4$ y cenizas) que se circulan desde el carbonatador hacia el calcinador donde se regenerará como CaO el $CaCO_3$ formado en el carbonatador. Para aportar el calor necesario para llevar a cabo la reacción de calcinación, se emplea carbón como combustible y el calcinador trabajará en régimen de oxi-combustión, siendo necesaria una unidad de separación de aire (ASU por sus siglas en inglés) para proporcionar el O_2 necesario para la combustión. Será necesaria una temperatura >900 ºC (aunque puede rebajarse disminuyendo la presión parcial de CO_2) para la reacción de calcinación. Debido a las condiciones de combustión en el calcinador, a la salida de este reactor, la concentración de CO_2 en los gases es muy elevada y es fácilmente purificable posibilitando su posterior compresión y transporte. El CaO regenerado volverá al carbonatador.

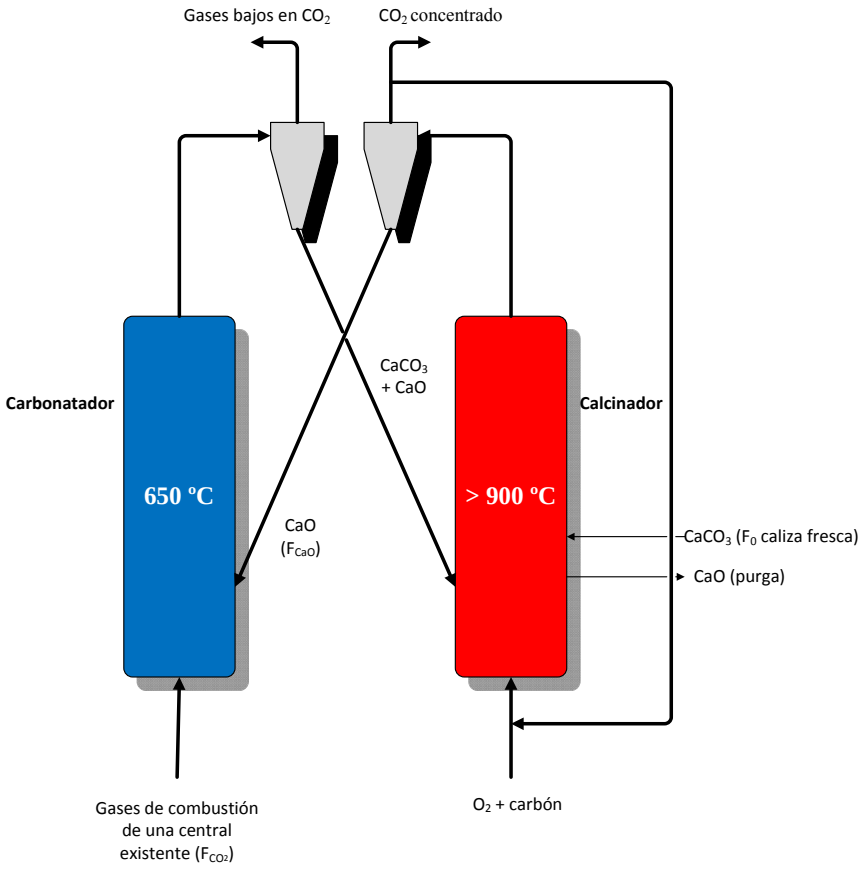

Figura 1.3. Esquema de un sistema de dos reactores interconectados de calcinación/carbonatación aplicado a la captura de CO_2 de gases de post-combustión.

Tal y como ya se ha mencionado, todos los sistemas de captura de CO_2 imponen una penalización energética sobre el sistema al que se les acopla. En los esquemas de separación basados en ciclos sorción-desorción, esta penalización energética es en gran parte debida a la energía necesaria que hay que aportar en la etapa de desorción (en este caso en el calcinador). Sin embargo la energía invertida en el calcinador abandona el reactor en corrientes de materia a alta temperatura, y se podría recuperar por ejemplo mediante un ciclo de vapor. El propio calcinador podría considerarse como

un oxi-combustor en lecho fluidizado circulante que aporta más energía a la central ya existente [22].

La energía que es necesario aportar al calcinador depende además de la actividad del sorbente: la actividad decae con los ciclos de calcinación/carbonatación, además de la desactivación producida debido al SO_2 (proporcional a la concentración de S del carbón). Más aún, las cenizas generadas en la combustión en el calcinador van acumulándose en el sistema CaL. La actividad se puede controlar mediante la purga de sorbente y la alimentación de caliza fresca, aunque si bien la renovación del sorbente trae consigo un aumento de actividad y por tanto un descenso en la energía requerida en el calcinador, la excesiva introducción de caliza fresca aumentará la energía requerida para la calcinación de tal manera que superaría el efecto positivo que conlleva el aumento de actividad. Habrá pues un óptimo de alimentación de sorbente fresco y purga [23].

La viabilidad de esta tecnología ha sido probada ya a escala de planta piloto. La planta localizada en la central térmica de La Pereda (Mieres) está diseñada con un carbonatador que puede tratar gases de combustión procedentes de la combustión de 1.7 MWt. Es la mayor planta en operación [16] en el mundo con esta tecnología y fue concebida y diseñada a partir de los resultados de una prototipo de 0.03MWth diseñada, construida y operada en el INCAR [15, 24]. Otras plantas piloto con resultados prometedores son: la planta de 1MWt en Darmstadt (Alemania) [25], la planta de 0.3 MWt en La Robla [26], la planta de 0.2 MWt de la Universidad de Stuttgart (Alemania) [27] y la planta de 1.9 MWt de Taiwán [28]. Existen además otras plantas más pequeñas que también han obtenido resultados positivos [24, 29, 30] sobre la viabilidad de la tecnología de calcinación/carbonatación.

1.3.2 Sistema de captura de CO_2 basado en tres lechos

El objetivo en esta variante de proceso es evitar la necesidad de una planta de separación de aire para alimentar O_2 puro al calcinador. En este proceso, para aportar el calor necesario para la calcinación de $CaCO_3$ se emplea una corriente de sólidos que transporta calor desde la caldera de combustión al propio calcinador, lo que hace innecesaria la oxi-combustión de combustible en el calcinador. Parte del CO_2 a la salida se recircula y se utiliza para la fluidización del propio calcinador.

La caldera de combustión es del tipo CFBC, trabajando a elevada temperatura (mayor de 1000 ºC). Una corriente de CaO se circula desde el calcinador hacia este reactor, se sobrecalienta y se recircula al calcinador, de modo que es posible aprovechar el calor de esta corriente para la calcinación del $CaCO_3$ producido en el carbonatador.

El carbonatador trabaja a 650 ºC, trata los gases producidos en el combustor y de él se obtendría una corriente con bajo contenido en CO_2 así como una corriente de sólidos (CaO más $CaCO_3$) que se circulan al calcinador.

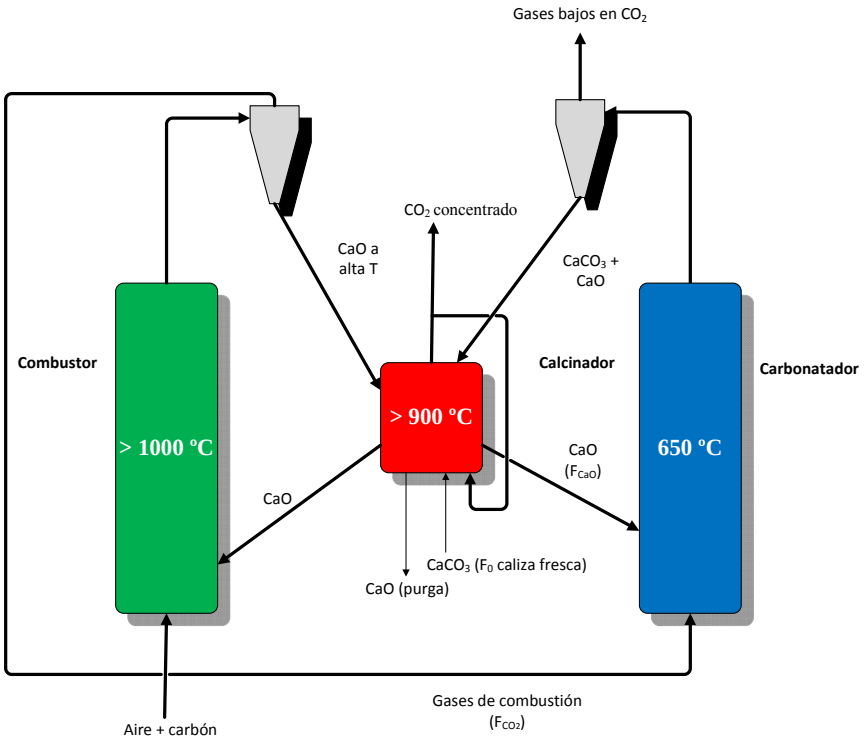

Figura 1.4. Esquema de un sistema de tres reactores interconectados.

Hasta la fecha este sistema, patentado por el CSIC, está en fase conceptual [31]. El estudio realizado demuestra que es posible alcanzar eficiencias de generación de energía de alrededor del 38% con la etapa de compresión de CO_2 incluida y una eficacia de captura de CO_2 del 90%.

Otra posible variante de aplicación del concepto anterior es la utilización de una corriente de CaO sobrecalentada proveniente de un combustor para aportar el calor para la calcinación del $CaCO_3$ alimentado a una cementera. [32],

1.3.3 Combustión de biomasa con captura in situ de CO_2. Emisiones negativas.

Otra posible configuración de un proceso de CaL es la captura de CO_2 de los gases generados durante la combustión a baja temperatura (650-700 ºC) de biomasa [33]. El sistema se describe en la Figura 1.5. El sorbente sería regenerado en un calcinador oxi-CFB obteniendo una corriente de CO_2 fácilmente purificable y adecuada para su compresión, transporte y almacenamiento. El CaO que entra al combustor/carbonatador capturaría el CO_2 desprendido durante la combustión de la biomasa "in situ".

Puesto que se considera que la combustión de biomasa renovable tiene emisiones cero, la captura del CO_2 procedente de la combustión de esta biomasa conduce al concepto de emisiones negativas. Este tipo de procesos (BECCS por sus siglas en inglés) son los únicos que permiten una descarbonización de la atmósfera y juegan un papel importante en algunos de los escenarios de estabilización de bajas emisiones [2].

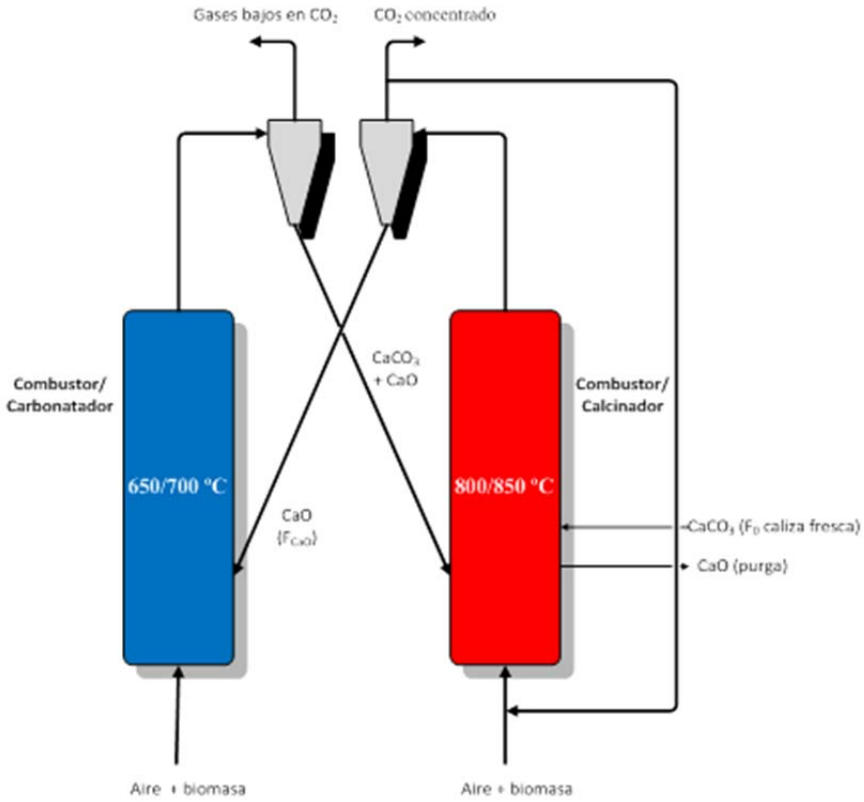

Figura 1.5. Esquema de un sistema de dos reactores interconectados con captura in situ de CO_2.

Se ha demostrado la viabilidad técnica de este proceso a escalas de 30 kWt y 300 kWt [13, 14, 18].

1.4 Comportamiento de CaO como sorbente de CO_2 y SO_2.

Puesto que el principal objetivo de esta Tesis ha sido investigar las reacciones de captura de CO_2 y SO_2 en sistemas de post-combustión de CaL, se revisan a continuación las principales características conocidas del comportamiento de CaO en reactores de este tipo.

1.4.1 El CaO como sorbente de CO_2

Como ya se ha descrito anteriormente, una de las principales ventajas del CaO es la enorme disponibilidad y bajo coste de su fuente natural, la caliza. [19]. La segunda gran ventaja es su elevada capacidad de captura de CO_2 cuando se compara este sorbente con otros óxidos metálicos u otras moléculas que capturan CO_2, siendo la capacidad de absorción teórica máxima (masa de CO_2/masa de sorbente) para CaO puro del 78.6 % en peso. Incluso con una conversión molar modesta (baja actividad) el CaO mantiene una capacidad de captura comparable a la de otros sorbentes sintéticos basados en CaO.

No obstante, y a pesar de las ventajas, existen una serie de limitaciones cuando se emplea CaO como sorbente de CO_2 que se enumeran a continuación:

La primera limitación está determinada por la termodinámica y las cinéticas a escala de partícula.

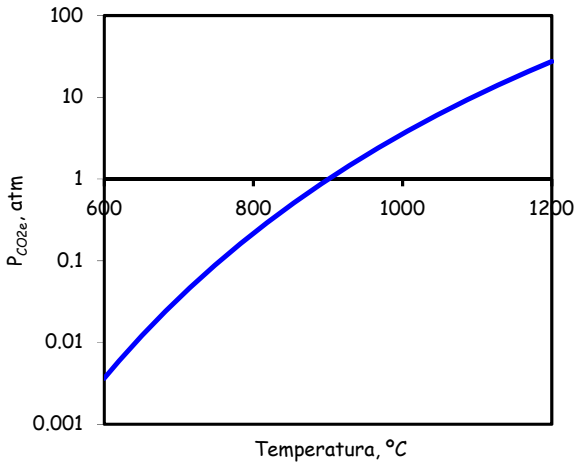

Figura 1.6. Presión parcial de equilibrio de CO_2 sobre el CaO

La Figura 1.6 representa la curva de este equilibrio en el intervalo de temperaturas 600-1200 ºC [34] que es un intervalo de temperaturas de interés para un sistema CaL. La reacción de carbonatación se ve favorecida a bajas temperaturas, aunque por debajo de 600 ºC la velocidad de reacción es lo suficientemente baja como para descartar esas temperaturas. Una temperatura idónea es 650 ºC, puesto que a presión atmosférica el equilibrio se establece con una concentración del 0.9 % vol. permitiendo eficacias máximas de captura superiores al 90% para un gas de combustión típico, manteniendo a su vez elevadas velocidades de reacción. A presión atmosférica, se necesitan temperaturas superiores a 900 ºC para tener una concentración de CO_2 en fase gas del 100 %vol. Esto hace que para la calcinación se establezcan temperaturas ligeramente por encima de 900 ºC, dado que la velocidad de reacción de calcinación es muy elevada incluso a temperaturas cercanas al equilibrio [35]. Para llevar a cabo la calcinación de forma efectiva y a temperaturas inferiores a 900 ºC, es necesario que la presión parcial de CO_2 sea inferior a 1 atm (haciendo uso de vapor de agua).

La segunda limitación bien conocida es la pérdida de la capacidad de captura de CO_2 del CaO con el número de ciclos de calcinación/carbonatación. Barker [36] ya demostró que el CaO pierde capacidad de captura al aumentar el número de ciclos de calcinación/carbonatación. Esta pérdida de capacidad depende de las condiciones en las que tengan lugar tanto la carbonatación como la calcinación, así como de la naturaleza de la caliza original, y tiene que ver con la sinterización del sorbente.

En las condiciones esperables de operación de un CaL con CFBs interconectados, esto es, concentraciones de CO_2 a la entrada del carbonatador en torno a 15 % v, tiempos de residencia de sólidos bajos, en torno a 5 min, y concentraciones de CO_2 en torno a 70 % en el calcinador, la pérdida de capacidad de CaO con el número de ciclos se muestra en la Figura 1.7 [37].

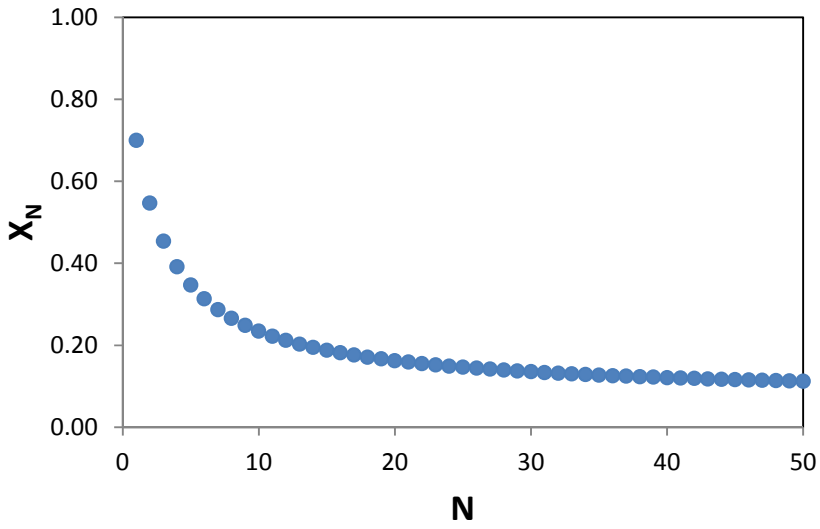

Figura 1.7. Curva típica de desactivación del sorbente con los ciclos de calcinación/carbonatación (X_N vs. N).

Incluso para un elevado número de ciclos, el CaO es capaz de mantener una cierta capacidad de captura, llamada habitualmente conversión residual, que se sitúa entre el 7-10 % [37]. No existen grandes diferencias entre calizas, si bien existe alguna que se desactiva más rápido y su conversión residual es menor [37]. La conversión máxima molar a $CaCO_3$ (X_N) en cada ciclo se puede obtener mediante la ecuación propuesta por Grasa et al. [37]:

$$X_N = \frac{1}{\frac{1}{1 - X_r} + kN} + X_r$$

donde la constante de desactivación k y la conversión residual Xr (la mínima X_N que se obtiene por el efecto de la sinterización por ciclos de calcinación/carbonatación) presentan valores medios de, respectivamente, 0.52 y 0.075, datos medios ajustados para sorbentes obtenidos de numerosas calizas [37].

Si las condiciones en las que se realiza la carbonatación y/o calcinación son diferentes, la velocidad con la que se desactiva el CaO con el número de ciclos cambia, si bien las curvas son cualitativamente similares. Al aumentar el tiempo de carbonatación y/o la concentración de CO_2, la pérdida de capacidad de captura es menor para el mismo número de ciclos [38, 39]. De hecho, uno de los métodos de reactivación del sorbente se basa en aumentar su conversión mediante el uso de un recarbonatador [38]. Por otra parte, si se aumenta la temperatura y/o el tiempo de calcinación, la conversión máxima del CaO disminuye para el mismo número de ciclos, pudiendo incluso desactivarse completamente [40].

La causa principal de esta pérdida de capacidad es la reducción de superficie de reacción debido a la sinterización del CaO [41]. La Figura 1.8 muestra un ejemplo de curva de conversión en función del tiempo para CaO sometido a distinto número de ciclos de calcinación/carbonatación [42].

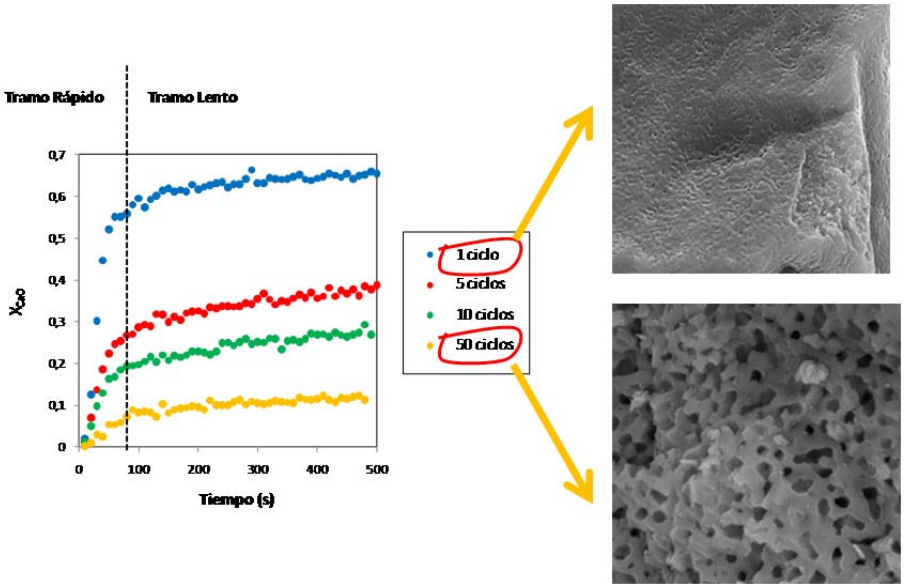

Figura 1.8. Desactivación que producen los ciclos de calcinación/carbonatación. Se muestra además fotografías SEM de las muestras carbonatadas, donde se observa el cambio textural sobre el sorbente a medida que avanzan los ciclos.

A la vista de la figura se observa que la reacción de carbonatación del CaO transcurre en dos etapas: una rápida y una lenta [36]. La etapa rápida está controlada por la cinética intrínseca de carbonatación, mientras que la lenta está controlada por la difusión a través de una capa producto de $CaCO_3$. El espesor de la capa de producto en el que se produce el cambio de un régimen a otro se ha determinado en torno a los 50 nm [43]. La formación de esta capa de producto sobre la superficie interna de las partículas de CaO constituye el tercer límite al progreso de la carbonatación del CaO. Hay que destacar, que bajo las condiciones típicas de sistemas CaL no existe bloqueo externo de poros, lo que apunta a un patrón de carbonatación homogéneo. Sin embargo, a medida que el CaO sufre ciclos de calcinación/carbonatación el diámetro de poro medio va aumentando de forma que se pierde superficie

específica de reacción [44], tal y como muestran las fotografías SEM de la Figura 1.8. Por tanto, la desactivación del CaO debido a los ciclos de calcinación/carbonatación se debe principalmente a la pérdida de superficie específica por sinterización y al modesto grosor de la capa de producto de carbonato que se forma sobre dicha superficie específica.

Finalmente, las cinéticas de la reacción de carbonatación se han ajustado con éxito empleando el modelo de poro de Bathia y Permultter [45-47] en las condiciones típicas de operación de un CaL [48].

1.4.2. El CaO como sorbente de SO_2

En esta sección se comenzará repasando el estado del arte sobre el comportamiento del CaO como sorbente de SO_2 en sistemas diferentes al CaL. Se finalizará resumiendo las conclusiones encontradas por otros autores sobre la sulfatación del CaO en sistemas de CaL, a modo de introducción a los trabajos que constituyen esta Tesis.

1.4.2.1 Sulfatación de CaO en gases de combustión

La sulfatación de CaO es una de las reacciones más estudiadas debido a su interés industrial en sistemas de desulfuración de gases de calderas de combustión. En calderas de lecho fluido circulante, es posible la desulfuración de los gases "in situ", durante el propio proceso de combustión. Para ello, se inyecta caliza a la caldera, que en las condiciones de operación de la misma se calcina y posteriormente se produce la reacción de sulfatación.

En las calderas de combustión en lecho fluidizado circulante la temperatura está en torno a 850 ºC, la concentración de CO_2 está en torno a 15 %v y la atmósfera es oxidante, por lo que el producto de reacción de sulfatación más

favorecido es $CaSO_4$ [49]. La reacción de sulfatación se trata de una reacción irreversible en las condiciones analizadas en la literatura, desviada hacia la formación de $CaSO_4$ estable [50] hasta una temperatura de 1230 ºC a presión atmosférica [51]. Por tanto, la sulfatación no estará limitada por la termodinámica dentro de las temperaturas utilizadas en todos los reactores descritos en la sección 1.3 y sólo las limitaciones cinéticas son las que introducen ineficacias en la captura de SO_2.

La primera limitación para la sulfatación de CaO procedente de caliza es debida a que el volumen molar del $CaSO_4$, 52.2 cm^3/mol, es mayor que el volumen molar del $CaCO_3$, 46 cm^3/mol. Como consecuencia, no es posible que una partícula de CaO procedente de caliza se convierta totalmente a $CaSO_4$ sin expandirse, aunque toda la porosidad inicial se rellene de producto [50, 52, 53]. Además de esta limitación, es conocida la dependencia de esta reacción con la naturaleza de la caliza de la que procede el CaO. Así, una regla general que se aplica normalmente, es que cuanto más joven sea la edad geológica de la caliza, mayor es su porosidad y mayor capacidad de captura de SO_2 tiene [52]. La capacidad de sulfatación del CaO va a depender tanto de la porosidad como del tamaño de poro que se genera durante la calcinación de la caliza.

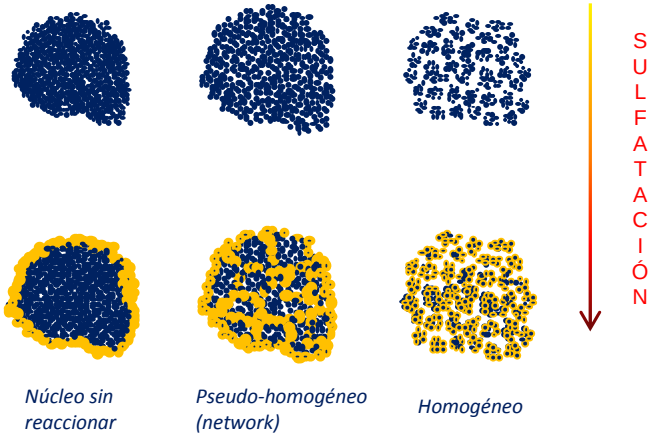

Figura 1.9. Tres diferentes patrones de sulfatación del CaO.

Se han identificado tres tipos básicos de patrones de sulfatación, cuyo esquema se muestra en la Figura 1.9 [54]. El patrón de núcleo sin reaccionar es típico de sorbentes con microporos y carentes de fracturas que faciliten la difusión del SO_2 hacia el interior de las partículas. La sulfatación da lugar a una partícula con un caparazón externo de sulfato que restringe la reacción hacia el interior, que permanece nada o poco sulfatado. El patrón pseudo-homogéneo o *network* es típico de partículas de sorbente con una red de micro-fracturas que permite la difusión del SO_2 hacia las superficies internas reaccionando para dar $CaSO_4$ en la proximidad de tales fracturas. La partícula queda entonces dividida en bloques separados por las fracturas. Cada bloque se comporta como si su patrón fuera de núcleo sin reaccionar ya que, sólo la superficie próxima a las fracturas alcanza un alto grado de sulfatación. Por último, el patrón homogéneo es característico de pequeñas partículas con amplios poros interconectados mediante fracturas. Por lo tanto, el reactivo SO_2 puede alcanzar toda la superficie interna de la partícula, y el $CaSO_4$ se formará homogéneamente en toda ella. Todos los patrones descritos se han encontrado en diferentes fuentes bibliográficas [50, 54].

En ausencia de efectos difusionales en fase gas, se ha demostrado [51, 55, 56] que la sulfatación del CaO transcurre habitualmente en dos etapas: una rápida, controlada por la cinética intrínseca, y una lenta, controlada por la difusión a través de la capa producto de $CaSO_4$. En caso de existir, habría que tenerse en cuenta además la difusión externa y/o la difusión de reactivo a través de los poros abiertos de la partícula.

La velocidad de sulfatación aumenta al aumentar la temperatura [51, 53]. No obstante, se ha encontrado en varias ocasiones [50] que se da un óptimo en la capacidad de sulfatación del CaO en FBCs en torno a los 850 ºC. A medida que aumenta la temperatura, la velocidad de reacción inicial aumenta pero se produce antes la transición entre la etapa de control cinético a control difusional en capa producto [57, 58]. Los autores explican que si bien es cierto que un aumento de la temperatura conduce a mayor velocidad inicial, también conlleva un aumento de las resistencias difusionales de SO_2 en los poros. Esto explicaría el sellado de los poros cercanos a la superficie, mientras que a más bajas temperaturas, la reducida cinética permite una sulfatación de la partícula de CaO más uniforme radialmente. Es evidente que aquellos factores, como por ejemplo el aumento del tamaño de partícula, que aumenten la resistencia difusional en poro favorecerán el patrón de sulfatación de núcleo sin reaccionar.

La reacción inicial de sulfatación de CaO, al ser una reacción superficial, dependerá de la superficie específica de reacción. Cuanto menor es la superficie específica, menor es la velocidad inicial de sulfatación y la conversión final a $CaSO_4$ para un tiempo determinado [57]. Entonces, tanto la velocidad de reacción como la capacidad de sulfatación dependerán de las condiciones en las que se haya llevado a cabo la calcinación de la caliza puesto que la textura del sorbente se ve drásticamente modificada dependiendo de las condiciones de calcinación.

El orden de reacción de la reacción de sulfatación del CaO con respecto al SO_2 según numerosos autores y condiciones está comprendido entre 0.6-1 [51, 53, 57, 59, 60].

Un área de interés reciente para la reacción de sulfatación, con problemas comunes a los esperados en los sistemas de captura CaL descritos en el apartado 1.3, es la sulfactación de CaO en calderas de lecho fluidizado circulante operando en modo oxy-combustion. Se ha demostrado que en las condiciones de un oxi-combustor, las altas concentraciones de CO_2 no tienen influencia sobre la reacción de sulfatación [61]. El efecto del vapor de agua en las condiciones de un combustor ha sido estudiado por algunos autores [62, 63] que concluyeron que la presencia de vapor de agua afecta a la etapa de difusión en capa producto y no a la etapa inicial, debido a la mejora en la difusividad del SO_2 a través de la capa producto o a la aparición de $Ca(OH)_2$ como intermedio de reacción, aunque esto no ha sido demostrado de forma concluyente.

Al ser la sulfatación del CaO en lecho fluidizado una reacción muy estudiada en los últimos 40 años, se han propuesto diversos modelos se sulfatación con el objetivo de ser integrados dentro de modelos de reactor [64, 65]. Esencialmente, hay dos tipos de modelos útiles para esta reacción gas-sólido: los de grano y los de poro. Los primeros modelos de grano adoptan la suposición de que las partículas están formadas por bloques más pequeños denominados granos (a veces micro-granos). Se supuso que dichos granos son esféricos, no porosos y que presentaban una distribución de tamaños uniforme. La reacción seguiría un patrón de núcleo sin reaccionar en cada grano. Los cambios estructurales producidos al irse formando la capa de $CaSO_4$ no fueron considerados en estos primeros modelos. Los regímenes que normalmente controlaban la reacción eran el difusional en fase gas (poros), combinado o no con la cinética, y la difusión de los reactivos a

través de la capa producto de $CaSO_4$ formada sobre los granos [57, 64, 66, 67]. Más tarde, los modelos de grano evolucionaron, teniendo en cuenta otras geometrías para los granos (o micro-granos): plato y cilíndrica [65, 68]. Además comenzó a estudiarse el cambio en la estructura de los granos según la reacción transcurría [69-73], y la distribución de tamaños de grano [68, 73].

Por otra parte, los modelos de poro adoptaron los supuestos de que las partículas estaban atravesadas por poros normalmente cilíndricos, de que poseían un diámetro uniforme y que estaban aleatoriamente intersectados [74, 75]. Este tipo de modelo continuó su desarrollo modelando no sólo la estructura porosa inicial sino su posterior transformación según la reacción avanzaba. La estructura porosa fue descrita en términos de la evolución de la distribución de diámetros de poro. Por ejemplo, Simons et al. [76], describieron la estructura porosa como un complejo árbol donde los tamaños de poro disminuían hacia el interior de las partículas. Uno de los modelos de poro más utilizado es el RPM (Random Pore Model, del inglés) desarrollado por Bhatia y Perlmutter [45, 46]: este modelo supone que la partícula está atravesada por poros cilíndricos aleatoriamente distribuidos con superficies que se intersectan y solapan con el transcurso de la reacción. Fue aplicado con éxito a reacciones gas-sólido [48] incluyendo la carbonatación y la sulfatación del CaO generado tras una única calcinación de caliza fresca [47, 48, 53, 77].

1.4.2.2 Sulfatación de CaO en sistemas de calcinación/carbonatación

Puesto que los sistemas de calcinación/carbonatación para la captura de CO_2 se han desarrollado recientemente, sólo algunos estudios publicados se han dedicado a investigar la sulfatación del CaO en condiciones adecuadas a los reactores de estos sistemas [78-82]. El principal objetivo de estos estudios

fue estudiar el efecto de la sulfatación sobre la desactivación del CaO respecto a CO_2 con el avance del número de ciclos de calcinación/carbonatación. En todos los trabajos se concluye que la presencia de SO_2 en el CaL desactiva más rápidamente el CaO para la captura de CO_2. Esta desactivación aumenta con el aumento de la concentración de SO_2. El SO_2 competirá con el CO_2 por el CaO en las condiciones de operación del carbonatador y reaccionará con el CaO en el calcinador reduciendo la cantidad de CaO para la carbonatación.

La fracción total de CaO activo disminuye durante los primeros ciclos debido a la suma de la fuerte sinterización inicial debida a los ciclos de calcinación/carbonatación sumada a la desactivación irreversible por reacción con SO_2. Sin embargo, al ir aumentando el número de ciclos de calcinación/carbonatación, el uso total de Ca va en aumento debido a que el grado de sulfatación acumulada aumenta [81] muy por encima de la conversión residual a carbonato (parte de la cual se mantiene incluso con contenidos relativamente altos de $CaSO_4$). Además, el tipo de caliza tiene un efecto importante sobre las curvas de desactivación en presencia de SO_2, sobre todo en los primeros ciclos, de forma que un sorbente que sea muy activo respecto a SO_2 tiende a sufrir una desactivación más pronunciada por su mayor reactividad.

Los estudios anteriores sobre la reacción de sulfatación de CaO para sistemas de captura de CO_2 con CaO son semicuantitavos, poco centrados en la determinación y modelado de velocidades de reacción a las condiciones presentes en los reactores del sistema de captura (alto número de ciclos de calcinación/carbonatación, temperaturas y atmósferas de reacción muy variadas dependiendo del reactor, etc). Puesto que el futuro escalado de estos sistemas de captura de CO_2 requiere de un conocimiento detallado del comportamiento del SO_2 en los principales reactores del sistema, se hace

necesaria una investigación específica sobre estas reacciones de sulfatación en sistemas CaL y su impacto en los procesos de captura de CO_2.

2. Objetivos

Esta Tesis se enmarca en el contexto de los procesos de captura de CO_2 por calcinación /carbonatación de CaO en la ruta de post-combustión. Este tipo de procesos de captura ofrece la posibilidad de evitar la etapa de desulfuración y eliminar el SO_2 durante el proceso de captura de CO_2.

El principal objetivo de esta Tesis es el estudio de las velocidades de reacción y de capacidad de sulfatación de CaO en el entorno de las condiciones de operación de los reactores característicos de un CaL, incluyendo el efecto de la co-captura de CO_2. Esta meta se completa con un modelo de reacción generalizado aplicable a todo el intervalo de condiciones de operación posibles en estos reactores.

El segundo objetivo ha sido el estudio del aprovechamiento de la purga de un calcinador de un CaL para su aplicación en la desulfuración en el entorno del propio combustor para reducir el impacto de la sulfatación del CaO en la captura de CO_2 en el carbonatador.

Los estudios realizados para la consecución de estos objetivos generales han sido objeto de cinco publicaciones en revistas internacionales de prestigio en el campo de la Ingeniería Química y de la Energía, a lo largo del desarrollo de esta Tesis. Por ello, se ha decidido presentar esta memoria como un compendio de las publicaciones realizadas.

3. Equipos y metodología experimental

En este apartado se describen los diferentes equipos utilizados así como la metodología de trabajo empleada durante los trabajos de investigación realizados con los mismos.

3.1 Equipo termogravimétrico TGA

Los ciclos de calcinación/carbonatación así como los ensayos de sulfatación del CaO se llevaron a cabo en una termobalanza (TGA) especialmente diseñada para llevar a cabo numerosos ciclos de dichas reacciones reversibles. Este equipo permite también el análisis de la reacción de sulfatación a nivel de partícula en condiciones controladas.

3.1.1 Descripción del equipo TGA

La Figura 3.1 muestra un diagrama de flujo del equipo TGA. Puede dividirse en tres secciones principalmente:

a. Sección de alimentación de gases

La sección de alimentación de gases está constituida por cuatro líneas independientes por las que se alimentan CO_2, aire, SO_2/N_2 (0.4 %v) y vapor de agua. El flujo de los gases está regulado por medidores-controladores de flujo másico BRONKHORST, con intervalos de medida de 0-30 LN/h en el

caso del aire y de SO_2/N_2, 0-10 LN/h en el del CO_2, y de 5-100 g/h en el caso del agua líquida.

Además, las líneas de gases constan de válvulas de bola, válvulas antirretorno y filtros. Existe una quinta línea que alimenta aire continuamente a la cabeza de la TGA como gas inerte de purga, y que se controla mediante un rotámetro.

El vapor de agua proviene de una línea de producción de vapor, que consta de dos reservorios de agua, un medidor-controlador para agua líquida, seguido por un conducto de acero envuelto en cintas calefactoras cuya temperatura se fijó en 400 ºC para la producción de vapor. Una válvula regulable de aguja consigue aumentar la presión a su entrada, de manera que a la salida se obtiene un flujo continuo de vapor libre de oscilaciones. Una electroválvula regula la entrada o no de vapor a la termobalanza.

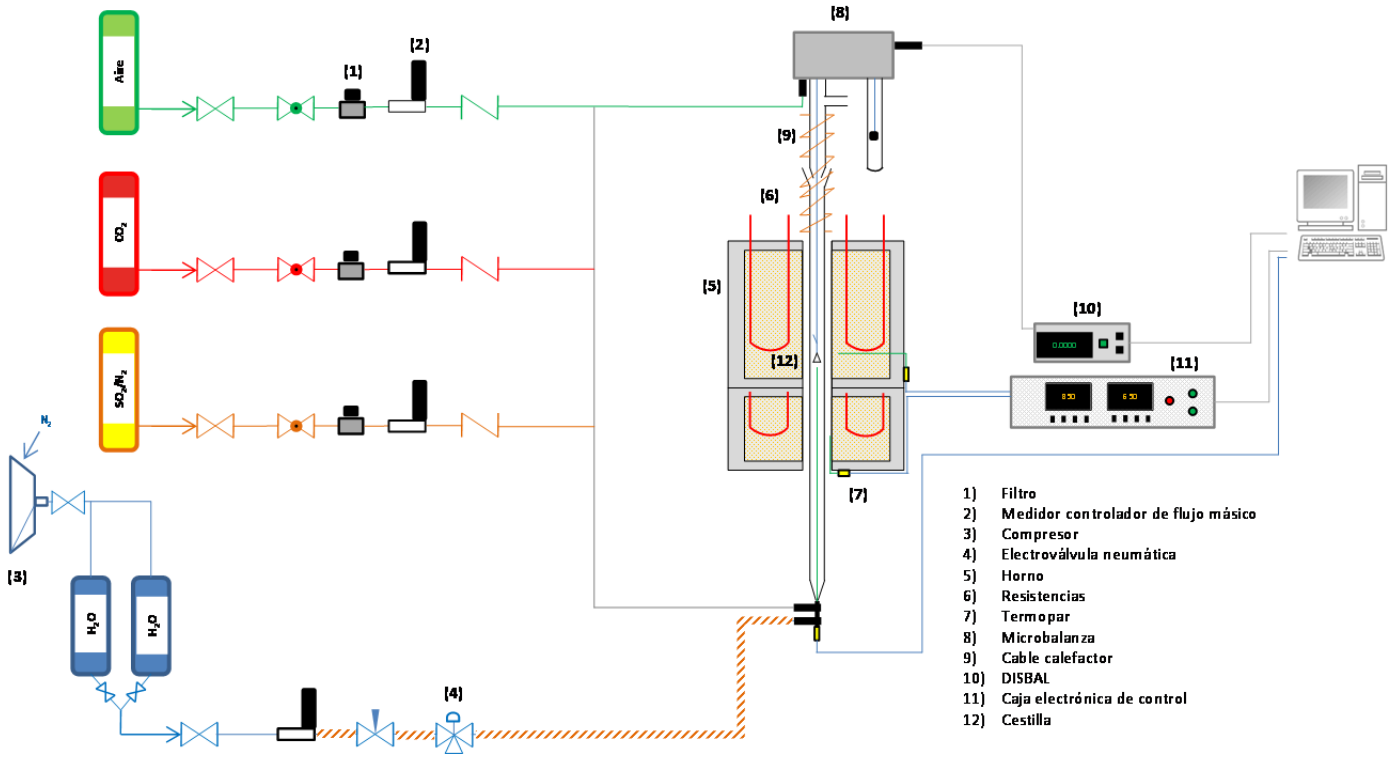

Figura 3.1. Esquema del principal equipo termogravimétrico utilizado en los ensayos de esta Tesis.

b. Sección de reacción

La sección de reacción constituye el núcleo principal del equipo y está formada fundamentalmente por un reactor de cuarzo, un horno y una microbalanza situada en la parte superior (cabeza).

Los gases se introducen por la parte inferior del reactor cilíndrico de cuarzo de 24 mm de diámetro interno y 1.55 m de altura.

La muestra objeto de estudio se sitúa en el interior del reactor de cuarzo dentro de una cestilla de platino, suspendida de la microbalanza mediante varillas de cuarzo. Este reactor se encuentra en el interior de dos hornos montados coaxialmente sobre un pistón neumático. El diámetro de los hornos es de 33 cm. El horno superior tiene una longitud de 35 cm, y es capaz de alcanzar temperaturas de hasta 1250 ºC, mientras que el horno inferior tiene una altura de 15 cm y alcanza temperaturas de hasta 900 ºC. La temperatura de cada uno de los hornos se controla de manera independiente por medio de dos controladores de temperatura.

Una característica especial de este diseño es que mediante el pistón neumático es posible un cambio rápido de las condiciones de temperatura en los alrededores de la muestra, lo que resulta muy útil durante los ciclos de calcinación-carbonatación. La temperatura de la muestra se mide mediante un termopar tipo K que se sitúa a 5 mm por debajo de la cestilla de platino.

La masa de la muestra se mide con una microbalanza CI MK2-M5 de CI electronics situada sobre un bloque de aluminio rígido cerrado herméticamente por una caja del mismo material (cabeza). Esta microbalanza permite obtener medidas precisas y sensibles de los cambios de peso que experimenta la muestra. Tiene una capacidad de hasta 5 gramos y una sensibilidad de 0.1 μm.

c. Control y medición informáticos

La microbalanza se controla mediante una unidad autosuficiente DISBAL Dicha unidad está integrada junto con los controladores de temperatura y los controladores de gases en un programa informático basado en LabVIEW para el control, medición y almacenamiento de datos.

3.1.2 Metodología experimental utilizada en la TGA

El procedimiento durante los ensayos realizados en TGA se detalla a continuación.

En primer lugar, se somete la caliza inicial a un determinado número de ciclos de calcinación/carbonatación. Para ello se toman alrededor de 10 mg de caliza que se depositan en la cestilla de platino en el interior de la TGA. Se arranca el programa correspondiente, que controla las temperaturas, posiciones del horno y los flujos de las diversas especies de la atmósfera reaccionante. En condiciones de experimentación estándar, la carbonatación se realiza con 10% vol. CO_2 en aire a 650 ºC durante 10 minutos, mientras que la calcinación tiene lugar a 930 ºC en aire durante 10 minutos.

A continuación se retiran los 10 mg de muestra ya sometida a ciclos de calcinación/carbonatación, y se toman alrededor de 2 y 3 mg para realizar los ensayos de sulfatación. En ensayos variando la masa inicial de muestra se observó que masas superiores a 3 mg provocaban resistencias difusionales externas (a escala de plato o cestilla de la termobalanza) que debían ser eliminadas. Esta muestra se dispersa homogéneamente sobre la cestilla de platino, que es colgada del hilo de suspensión. Acto seguido se coloca el reactor cilíndrico de cuarzo. Entonces se espera a que el peso de la muestra se mantenga estable, se mide, y se arranca el programa previamente

desarrollado, que indica los flujos de las diversas especies reaccionantes, así como las temperaturas y posiciones del horno. Previamente, un flujo total de 26.2 LN/h fue seleccionado al no provocar resistencias difusionales, hecho que fue comprobado al observar que cuando este flujo se reducía a la mitad, no variaban las curvas X_{CaO} vs t obtenidas.

Además, para cada diferente ensayo se hicieron experimentos cargando material inerte (mullita) para comprobar el efecto sobre el peso del empuje de los gases y de la temperatura, entre otros calibrados con blancos.

3.2 Planta piloto de 30 kW de lechos fluidizados circulantes interconectados del sistema de captura de CO_2 del INCAR-CSIC

Además, para la consecución de esta Tesis, se han realizado estudios de sulfatación en la planta piloto CaL de 30 kWth situada en el INCAR (CSIC), que permiten el análisis del comportamiento del sorbente en régimen de lecho fluidizado circulante. La descripción y metodología empleada en este equipo se presentan a continuación.

3.2.1 Descripción de la planta piloto de lechos fluidizados circulantes interconectados del INCAR-CSIC

El sistema CaL de 30 kW del INCAR-CSIC se muestra en la Figura 3.2.

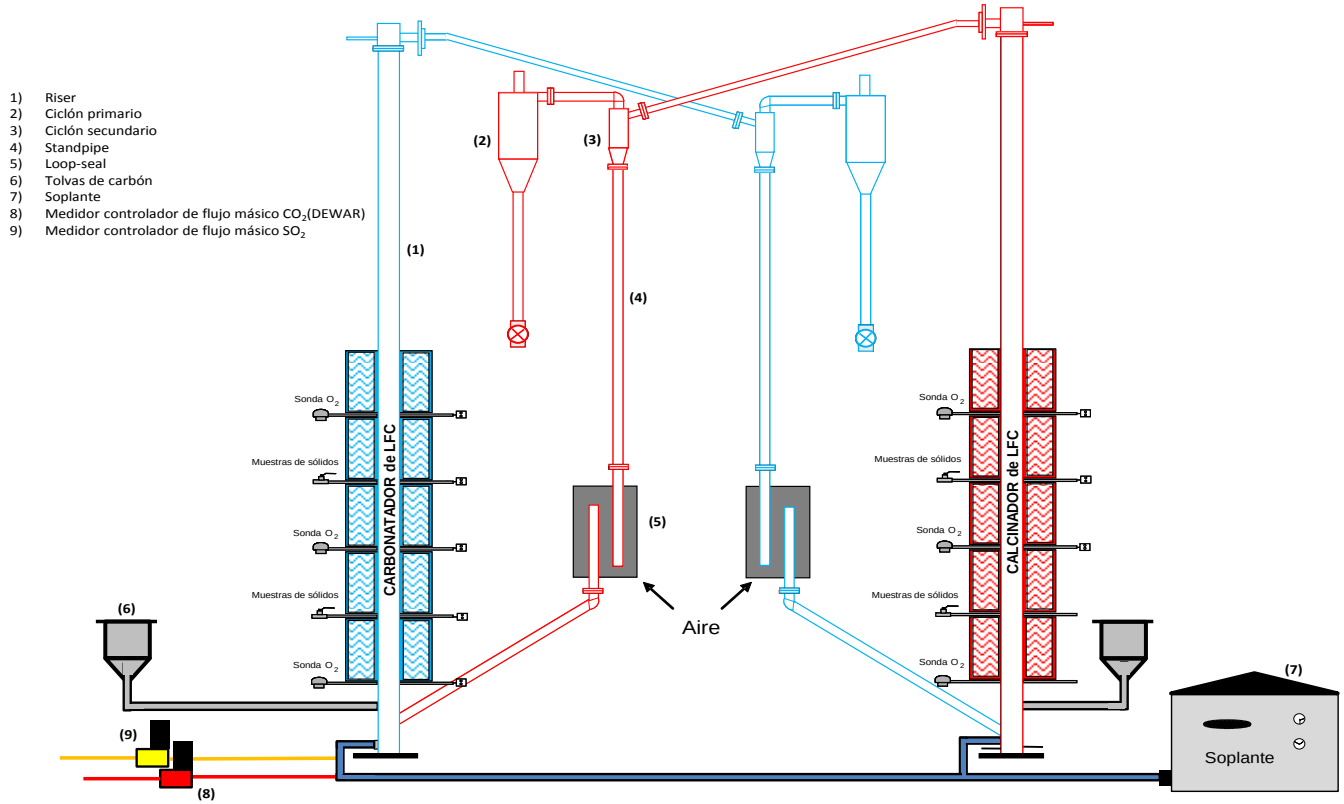

Figura 3.2. Planta piloto de 30 kW del INCAR-CSIC.

La planta piloto de 30 kW térmicos (se considera que el carbonatador está diseñado para tratar gases de combustión generados al quemar 30 kW de carbón) tiene una altura de 6.5 m. El sistema de reactores de carbonatación y calcinación está formado por dos *risers* de acero inoxidable refractario (AISI30) de 0.1 m de diámetro interior. Las tuberías de reciclo de sólidos conducen los sólidos de un reactor a otro gracias a las válvulas no mecánicas de tipo *loop-seal*. Su tamaño es de 200x100x400 mm, y funcionan fluidizando los sólidos con aire de modo que los descargan a través de una tubería hacia el reactor.

La instalación dispone de seis hornos eléctricos en cada *riser*, además de un horno eléctrico en cada *loop-seal*. El calentamiento de las cámaras de reacción hasta el entorno de los 500 ºC se hace con ayuda de los hornos eléctricos. Para llevar la temperatura hasta las condiciones de calcinación (en torno a 800-900 ºC) se alimenta carbón a ambos reactores una vez que se han alcanzado los 500 ºC con los hornos.

Además se dispone de un sistema discontinuo de alimentación de sólidos al sistema mediante el cual se pueden hacer inyecciones de caliza durante el transcurso de un ensayo. La alimentación de sólidos se hace a través de la *loop-seal* del calcinador. El objeto de hacer inyecciones de sólidos durante el experimento es aumentar el inventario y la circulación de sólidos del sistema. De este modo, y para hacer diferentes pruebas, se puede inyectar caliza fresca o parcialmente calcinada en cualquier momento.

Referente a la instrumentación y control, en la planta piloto se miden de forma continua las siguientes variables:

1) La temperatura en diferentes puntos de la instalación (40 puntos de medida) mediante termopares tipo K.

2) La presión diferencial (40 puntos de medida) mediante transductores de presión.

3) La concentración de O_2 en el lecho (tres sondas de zirconio en el reactor de carbonatación y una en el calcinador).

4) Los flujos de aire, CO_2 y SO_2 a suministrar a los diferentes equipos y dispositivos mediante medidores de flujo másico.

5) La composición de los gases en continuo mediante dos analizadores de gases TESTO 360. En la instalación se pueden tomar medidas de concentración de gases en cinco puntos diferentes: a la entrada del carbonatador, a la salida del carbonatador (antes y después del ciclón secundario) y a la salida del calcinador (antes y después del ciclón secundario).

Todos los datos medidos de forma continua quedan registrados en un sistema de adquisición de datos a través de un multímetro conectado a un ordenador.

Además, el sistema dispone de varios puntos de extracción de muestras sólidas: se pueden extraer muestras sólidas en cualquier momento del carbonatador, del calcinador y de la tubería de reciclo de sólidos desde la *loop-seal* al carbonatador. Las muestras de sólidos son analizadas en la TGA descrita en la sección 3.1 para obtener información acerca de los grados iniciales de carbonatación, de las capacidades máximas de captura de CO_2 y de las velocidades de carbonatación de los sólidos obtenidos en la planta piloto.

3.2.2 Metodología experimental utilizada en la planta piloto de 30 kW

La metodología experimental utilizada en la planta piloto de 30 kW consta de varias etapas. Primeramente se realiza la calcinación de la caliza fresca o

de la caliza parcialmente calcinada. El inventario total de sólidos suele situarse en torno a los 20 kg. Para llevar a cabo la calcinación, se encienden los hornos eléctricos y se espera a que alcancen una temperatura de alrededor de 400 ºC. En ese momento se introduce un flujo de aire para provocar la circulación de los sólidos entre reactores. Mientras los hornos se precalientan, se calibran los analizadores de gases con botellas de gases patrón. Una vez los hornos superan los 500 ºC, comienza a inyectarse carbón a ambos reactores, con lo que la temperatura alcanza fácilmente los 850 ºC. Estas condiciones favorecen la calcinación de la caliza, que tiene lugar durante aproximadamente 8 horas. Se busca calcinar el inventario de sólidos hasta un grado lo más cercano posible a la calcinación completa. Se extraen muestras sólidas durante esta etapa que son analizadas inmediatamente para medir la conversión media molar a carbonato cálcico, mediante un analizador carbono/azufre LECO CS 230.

En la siguiente etapa se deja que la temperatura del carbonatador baje hasta 600 ºC parando la alimentación de carbón a este reactor. Entonces pasa a alimentar al carbonatador un gas sintético que simula el gas de combustión de una caldera. Este gas contendrá en torno a un 12% vol. de CO_2 y concentraciones variables de SO_2. Al ser la carbonatación (y la sulfatación) del CaO una reacción exotérmica, la temperatura del carbonatador aumenta hasta situarse entre los 650-700 ºC. Mientras tanto, la alimentación de carbón al calcinador continúa para hacer posible la calcinación del $CaCO_3$ formado en el carbonatador.

La información que se puede obtener durante un ensayo de la instalación experimental con la instrumentación antes detallada es la siguiente:

Mediante los analizadores de gases se puede seguir la concentración de los gases a la entrada y a la salida del carbonatador, y a la salida del calcinador.

Así se puede comprobar en todo instante cómo se desarrollan las reacciones de carbonatación, sulfatación, calcinación y la combustión en el calcinador.

Las sondas de zirconio se utilizan para medir la concentración de oxígeno dentro de los reactores. Los datos que miden se contrastan con la señal del analizador, y así se conoce la distribución del aire de las válvulas *loop-seal* en el sistema. La corriente de gas de entrada al carbonatador puede verse diluida por la corriente de aire que fluidiza la válvula *loop-seal* si este gas se dirige desde la *loop-seal* (que recoge sólidos del ciclón primario del calcinador) al propio carbonatador. Dependiendo de la fluidodinámica del sistema, este gas de aireación de la *loop-seal* puede también dirigirse hacia el ciclón primario.

Las sondas de presión se utilizan para conocer el inventario total de sólidos en el sistema y su distribución en él.

Los termopares instalados por toda la instalación dan la medida de la temperatura en numerosos puntos. Como los sólidos transportan calor, la distribución de temperatura a lo largo de los *risers* ofrece una visión de la circulación de éstos en su interior. Se considera que la circulación es buena cuando se observa igualdad de temperaturas en los cinco termopares del carbonatador.

La circulación de sólidos en el equipo se puede calcular cuantitativamente gracias a la instalación de una tubería con dos válvulas en la tubería de recirculación de los sólidos entre la válvula *loop-seal* y el calcinador. Con este sistema se pueden extraer sólidos circulantes de la instalación. Si se mide el tiempo en que se obtuvo una masa determinada, se puede calcular la circulación.

Para obtener información de la fase sólida, se pueden extraer muestras del calcinador y del carbonatador. También se obtienen muestras sólidas de la

tubería entre la válvula *loop-seal* y el carbonatador. Estas muestras también se estudian en TGA (además de en el analizador LECO CS 230), obteniendo las capacidades máximas de captura de CO_2 así como las velocidades de carbonatación y sulfatación.

Un ensayo de este tipo puede llegar a durar más de 18 horas, por lo que requiere la intervención, por turnos de diversos miembros del grupo de investigación.

4 Resultados

Para llevar a cabo el principal objetivo de esta Tesis se ha comenzado por el estudio de la velocidad de reacción y la capacidad de sulfatación del CaO en las condiciones del reactor de carbonatación en una termobalanza (TGA). Este trabajo se recoge en la publicación I. Posteriormente se estudió la co-captura de CO_2 y SO_2 en un reactor de carbonatación y los resultados experimentales se presentan en la publicación II. El estudio de la velocidad de reacción y capacidad de sulfatación del CaO en las condiciones del reactor de calcinación se presentan en la publicación III. El estudio de la velocidad de reacción y capacidad de captura en las condiciones de un combustor y la generalización del modelo de reacción para los reactores principales de un CaL se presentan en la publicación IV. Finalmente, y tal y como se mencionó en la Introducción de esta Tesis, la purga procedente del calcinador podría aprovecharse para la desulfuración del gas de combustión en el propio combustor. El estudio de la velocidad de reacción y capacidad de sulfatación de estas purgas se presenta en la publicación V.

4.1 Investigación de la velocidad y capacidad de sulfatación del CaO en las condiciones del carbonatador de un CaL para captura de CO_2

Tal y como se ha mencionado en la Introducción, la reacción de sulfatación de CaO es una de las reacciones más estudiadas en calderas de lecho fluidizado circulante, pero es necesario adaptar la información a los reactores

de carbonatación en un sistema CaL. Las principales diferencias entre estos estudios anteriores y las condiciones de un reactor de carbonatación son tres: la relación Ca/S es muy superior en un CaL, el número medio de ciclos de carbonatación/calcinación en un CaL es muy superior a 1 y en consecuencia el diámetro de poro es mayor que para una caliza que sólo haya sufrido una calcinación (ciclo 1, típico de estudios de sulfatación en combustores) y además la temperatura de reacción es menor que en el caso de un combustor. A estas temperaturas y en presencia de CO_2 tendrá lugar la competencia entre las reacciones de carbonatación y sulfatación.

En el primer trabajo recopilado en esta Tesis (Publicación I) se ha estudiado el efecto de la concentración de SO_2 sobre las velocidades de sulfatación en el carbonatador, puesto que la concentración media en el reactor dependerá de la concentración de S del combustible empleado en el combustor y del grado de desulfuración con el que llegan los gases al carbonatador. De esta forma se determinó el orden de reacción en las condiciones del carbonatador. Se ha estudiado también el efecto del número de ciclos de calcinación/carbonatación sobre dichas cinéticas de sulfatación. Se confirmó que al aumentar el número de ciclos de calcinación/carbonatación (el diámetro medio de poro aumenta) los fenómenos de bloqueo de poros descritos en la Introducción de esta Tesis son menores o incluso desaparecen tras un alto número de ciclos para algunas calizas. Esto puede favorecer el aumento de la capacidad de sulfatación del sorbente respecto a una aplicación similar en calderas de combustión. No obstante, este aumento del diámetro de poro lleva asociada una disminución de la superficie de reacción, con lo que, para un número de ciclos elevado, la capacidad de sulfatación vuelve a disminuir para los mismos tiempos de reacción. Puesto que el número de ciclos de calcinación/carbonatación altera drásticamente las características texturales iniciales del sorbente, se observa en los datos experimentales que el patrón de sulfatación del sorbente también cambia con

el número de ciclos. Además, este patrón depende de las características de la propia caliza. Por tanto, todo el estudio se ha llevado a cabo con tres calizas diferentes utilizando distintos diámetros de partícula.

Finalmente se han ajustado los datos experimentales a un modelo de poro que incluye la evolución de la estructura porosa según transcurre la reacción (RPM) teniendo en cuenta que la reacción de sulfatación del CaO transcurre siguiendo las etapas cinética y de control de difusión en capa producto.

4.2 Investigación de la captura de SO_2 en el carbonatador de lecho fluido circulante de un sistema CaL

En el trabajo anterior se ha estudiado la sulfatación del CaO a escala de partícula y en ausencia de CO_2. La Publicación II supone un salto importante de validación de los resultados de la publicación I, al recoger el estudio de la co-captura de CO_2 y SO_2 en un reactor de carbonatación piloto (el CFB de la instalación de CaL de 30 kW del INCAR descrita en la sección 3.2). Para el ajuste de los datos experimentales, se ha empleado un modelo sencillo de reactor que ha demostrado su validez en ensayos de captura de CO_2. En dicho modelo, se han integrado las ecuaciones del modelo de reacción de sulfatación a nivel de partícula desarrollado en el artículo anterior, obteniéndose la validación del modelo para predecir la sulfatación del CaO en el carbonatador de un proceso de CaL.

Se ha obtenido un factor de contacto gas-sólido muy próximo a 1, indicando que la sulfatación del CaO en el carbonatador CFB está controlada por la cinética de la propia reacción de sulfatación. Por otro lado, en las condiciones habituales de operación de los carbonatadores de sistemas CaL (inventario de sólidos, velocidades de circulación) que permiten obtener una

eficacia elevada de captura de CO_2, se ha demostrado que la eficacia desulfuradora de estos equipos es prácticamente del 100%. Se ha encontrado que sólo cuando se trabaja forzando el equipo con condiciones poco prácticas (bajo inventario de sólidos, bajos tiempos espaciales) se consiguen obtener eficacias de captura de SO_2 por debajo del 90%. Por tanto, en sistemas CaL operando con eficacias de captura de CO_2 elevadas, está prácticamente garantizada una altísima eficacia de captura de SO_2 , con emisiones cercanas al límite de detección (5 ppmv).

4.3 Sulfatación de partículas de CaO en las condiciones del calcinador de lecho fluidizado circulante de un sistema CaL

El trabajado desarrollado en la Publicación III se centró en el estudio de la reacción de sulfatación del CaO en las condiciones de operación de un reactor de calcinación en un sistema CaL. Este reactor se caracteriza por operar a temperaturas superiores a 870 ºC y concentraciones de CO_2 superiores al 70 %v. Tal y como ya se ha mencionado en la Introducción de esta Tesis, al aumentar la temperatura de reacción en la sulfatación, la velocidad de reacción aumenta, pero la etapa en que la reacción está controlada por la cinética posiblemente se acorte (al colmatarse más rápidamente con sulfato los poros más externos) , pudiendo darse el control difusional en el poro cuando el número de ciclos de calcinación/carbonatación es bajo.

El estudio experimental llevado a cabo ha tenido un desarrollo similar al realizado en la Publicación I, pero centrado en los nuevos ambientes posibles de reacción en el calcinador. Se ha estudiado el efecto de la concentración de SO_2 ya que ésta depende del contenido en S del combustible que esté siendo alimentado al calcinador CFB. Así, se obtuvo un orden de reacción idéntico

al obtenido en las condiciones del carbonatador de un sistema CaL, indicando que la temperatura no le afecta en el intervalo de interés (650-930 ºC) en este tipo de procesos. Igualmente se estudió el efecto del número de ciclos de calcinación/carbonatación, puesto que ha demostrado tener una importancia clave en la evolución de los patrones de sulfatación (Publicación I). Los resultados indican que para partículas típicas de sistemas CaL sometidas a un número determinado de ciclos de calcinación/carbonatación, el patrón tenderá a volverse homogéneo previniendo el bloqueo de poros. Estos análisis se han realizado con diferentes calizas y con diferentes tamaños de partículas. Además se ha estudiado el efecto de la elevada concentración de CO_2 característica de este reactor, ya que como ya se ha mencionado en la Introducción, es conocido el efecto sinterizante que tiene sobre la estructura del CaO. Sin embargo, no se ha hallado una apreciable contribución de la presencia de altas concentraciones de CO_2 al cambio en las velocidades de sulfatación en sorbente sometido a ciclos de calcinación/carbonatación.

De igual manera que lo concluido en las Publicaciones I y II, las elevadas velocidades y capacidades de sulfatación en los calcinadores de sistemas CaL los señalan como eficaces equipos desulfurantes.

4.4 Modelización de la cinética de sulfatación de partículas de CaO en las condiciones de reactores de CaL

El principal objetivo de la Publicación IV fue el ajuste de un modelo general de poro (RPM) a los datos experimentales de sulfatación del CaO obtenidos en TGA para la obtención de ecuaciones que predigan la velocidad de la reacción de sulfatación del CaO en las condiciones de operación típicas de cualquiera de los reactores que conforman un sistema de post-combustión de

CaL. Este trabajo supone una generalización de los trabajos anteriores, complementando con una base de datos experimental mucho más amplia la información presentada en las Publicaciones I y III. Para ello, se han extendido los estudios experimentales anteriores en lo que respecta a la influencia del número de ciclos de calcinación/carbonatación sobre el patrón de sulfatación. Los resultados obtenidos muestran que cuanto más elevada es la temperatura de sulfatación del CaO, mayor tendencia tiene el patrón de sulfatación a ser del tipo de núcleo sin reaccionar. Este hecho es debido al incremento de las resistencias difusionales en los poros que provocan su bloqueo. Además, un mayor tamaño de partículas da lugar más fácilmente a patrones no homogéneos, puesto que mayor longitud de poro conlleva mayor resistencia a la difusión en él. Sin embargo, para un sorbente típicamente sometido a ciclos de calcinación/carbonatación, y tamaños de partícula habituales (entorno a 100 micras), el patrón es homogéneo para cualesquiera condiciones de operación dentro de los reactores de un sistema CaL en régimen post-combustión, si bien el número de ciclos de calcinación/carbonatación para obtener este patrón es mayor con el aumento de temperatura (se requiere mayor grado de sinterización, poros de mayor diámetro, para contrarrestar el incremento de resistencia difusional). Además, se han validado las deducciones acerca de los patrones de sulfatación mediante observaciones directas mediante SEM-EDX.

La presencia de CO_2 en el combustor y en el calcinador no afectó a las velocidades de sulfatación de sorbentes ciclados. Mientras que la presencia de vapor de agua en ambos reactores mejoró las velocidades de sulfatación en el tramo lento controlado por la difusión a través de capa producto, pero no afectó al tramo rápido cinético.

Además y teniendo en cuenta el posible uso de la purga de un CaL como sorbente de SO_2 en la propia caldera, se ha realizado un estudio experimental

de la velocidad de reacción y capacidad de sulfatación del CaO en las condiciones de operación de la propia caldera que genera los gases de combustión que entran al carbonatador. Las elevadas capacidades de sulfatación de un sorbente ciclado, debidas a su patrón homogéneo, son mayores que las obtenidas para el mismo sorbente fresco calcinado, lo que apunta a que el sorbente extraído mediante purgas de un sistema CaL es un buen agente desulfurante en calderas comerciales CFBC.

Los datos experimentales obtenidos para el desarrollo de los trabajos de las Publicaciones I, III y IV han sido ajustados al modelo de poro (RPM), empleando una metodología validada para los estudios de carbonatación del CaO en otros trabajos. De esta forma se ha obtenido un modelo generalizado de sulfatación del CaO a nivel de partícula válido para su integración en los reactores que conforman un sistema CaL en post-combustión.

4.5 Sulfatación del CaO de purgas de sistemas CaL de captura de CO_2

Tal y como se ha mencionado en secciones anteriores, el aprovechamiento de la purga de un sistema de post-combustión de CaL para la desulfuración "in situ" (en la propia caldera donde se generan los gases de combustión) supone una ventaja competitiva importante para estos sistemas de captura de CO_2, puesto que se reduce el consumo de sorbente fresco en ellos. Por tanto, el estudio de la velocidad de reacción así como la capacidad de sulfatación de muestras de purga de ensayos estables [16] en la planta piloto de captura de CO_2 de 1.7 MWt de La Pereda es el objeto principal de la Publicación V.

A diferencia de los sólidos empleados en los estudios anteriores, las muestras que proceden de esta purga se caracterizan por una distribución de

números de ciclo de calcinación/carbonatación representados por un valor medio. Contienen además cenizas y una conversión inicial a $CaSO_4$, debido a la presencia de S y cenizas en la composición del combustible empleado tanto en la caldera de la CT de la Pereda como en el combustible del calcinador.

Los ensayos de sulfatación se realizaron en el equipo TGA de la Figura 3.1. Para determinar la viabilidad del uso de estas purgas como agente desulfurante en la caldera, se comparó su velocidad y capacidad de sulfatación respecto al sorbente fresco. Los resultados muestran que la eficacia de sulfatación de las purgas ricas en CaO provenientes de la planta piloto es mayor que la del correspondiente sorbente fresco calcinado. Este hecho se comprobó mediante análisis SEM-EDX, observándose un patrón homogéneo para las partículas de purgas de planta piloto. Un estudio de porosimetría de Hg mostró la variación de la distribución de diámetros de poro entre el sorbente fresco calcinado y una muestra sometida a ciclos de calcinación/carbonatación de la purga de planta piloto, encontrándose una distribución de diámetros de poro más amplia con un diámetro medio de poro un orden de magnitud superior al correspondiente al sorbente fresco calcinado. Por tanto, la justificación de la mayor eficacia obtenida para una muestra de purga sometida a ciclos de calcinación/carbonatación radica en el cambio de patrón de sulfatación: desde núcleo sin reaccionar a homogéneo, evitando el sellado de poros que normalmente se observa en calderas de combustión cuando se alimenta sorbente fresco.

Finalmente, los resultados experimentales de velocidades de sulfatación se ajustaron por el modelo RPM descrito en la Publicación IV.

4.6 Publicaciones

4.6.1 Publicación I

Sulfation Rates of Cycled CaO Particles in the Carbonator of a Ca-Looping Cycle for Postcombustion CO_2 Capture

Publicado en:

AIChE

Volumen 58

Año 2012

Índice de Impacto: 2.581

AIChE

Sulfation Rates of Cycled CaO Particles in the Carbonator of a Ca-Looping Cycle for Postcombustion CO_2 Capture

B. Arias, J. M. Cordero, M. Alonso, and J. C. Abanades
Instituto Nacional del Carbón, CSIC, C/Francisco Pintado Fe, No. 26, 33011 Oviedo, Spain

DOI 10.1002/aic.12745
Published online August 30, 2011 in Wiley Online Library (wileyonlinelibrary.com).

Calcium looping is an energy-efficient CO_2 capture technology that uses CaO as a regenerable sorbent. One of the advantages of Ca-looping compared with other postcombustion technologies is the possibility of operating with flue gases that have a high SO_2 content. However, experimental information on sulfation reaction rates of cycled particles in the conditions typical of a carbonator reactor is scarce. This work aims to define a semiempirical sulfation reaction model at particle level suitable for such reaction conditions. The pore blocking mechanism typically observed during the sulfation reaction of fresh calcined limestones is not observed in the case of highly cycled sorbents ($N > 20$) and the low values of sulfation conversion characteristic of the sorbent in the Ca-looping system. The random pore model is able to predict reasonably well, the CaO conversion to $CaSO_4$ taking into account the evolution of the pore structure during the calcination/carbonation cycles. The intrinsic reaction parameters derived for chemical and diffusion controlled regimes are in agreement with those found in the literature for sulfation in other systems. *AIChE J,* 58: 2262–2269, 2012
Keywords: sulfation kinetics, SO_2 capture, carbonation, Ca-looping, CO_2 capture

Introduction

Postcombustion CO_2 capture using CaO as a regenerable solid sorbent (or calcium looping, CaL) is a rapidly developing technology because of its potential to achieve a substantial reduction in capture cost and because of the energy penalties associated with more mature CO_2 capture systems.[1,2] In a postcombustion CaL system, CO_2 from the combustion flue gas of a power plant is captured using CaO as sorbent in a circulating fluidized bed (CFB) carbonator operating between 600 and 700°C. The stream of partially carbonated solids leaving the carbonator is directed to the CFB calciner, where the solids are calcined, thereby regenerating the sorbent (CaO) and releasing the CO_2 captured in the carbonator. To calcine the $CaCO_3$ formed in the carbonator and to produce a highly concentrated stream of CO_2, coal is burned under oxy-fuel conditions at temperatures above 900°C in the calciner. One of the main distinctive characteristics of this process is its lower energy penalty, as operation at high temperatures allows for efficient heat integration of the full system in the power plant.[3–8]

Another known benefit of CaL systems compared with other postcombustion technologies, such as amines, is the theoretical capability of operating with flue gases that have a high SO_2 content. This is because the calcined limestones present in carbonator and calciner reactors are known to be excellent desulfurization agents, and they are routinely used in many commercial scale power plants, including CFB combustors (CFBC) (see review in Ref. 9). Although several recent works have investigated sulfation phenomena in CaL systems,[10–17] there is a very little quantitative information on the sulfation rates of CaO in the carbonator and calciner reactor environments.

An important difference between sulfation studies with CFB combustors and sulfation studies with CaL systems concerns the typical range of conversion to $CaSO_4$ that can be expected of each of these systems. An obvious design target of any commercial flue gas desulfurization process is to make the most use of Ca and to achieve maximum conversion to $CaSO_4$. However, in a CaL system, there is generally a need for a large makeup flow of low-cost limestone to compensate for the decay in the sorbent's CO_2 carrying capacity along cycling. A mass balance for the recycling of Ca solids has shown[18] that this leads to $CaSO_4$ contents well below 5 mol % in a CaL system, even when high sulfur content fuels are used. This has important implications for the debate of the effect of sulfur on CaL systems, because this low conversion of the Ca sorbent to $CaSO_4$ is well below the limit of conversion required to achieve the extensive pore plugging that is characteristic of highly sulfated particles (see review in Ref. 9). The purpose of this work, therefore, is to fully examine the sulfation phenomena associated with these low levels of conversion to $CaSO_4$.

Several models have been proposed for studying and describing heterogeneous sulfation reactions and pore plugging processes under different reaction controlled regimes and for different sorbents.[19–25] The models increase in complexity when they need to quantify the diffusion phenomena of the reactants passing through plugged pores. However,

Correspondence concerning this article should be addressed to B. Arias at borja@incar.csic.es.

there is a general consensus concerning what happens in the initial stages of the reaction (low sulfation conversions). The first quantitative descriptions of the rate of reaction of SO_2 with CaO[26,27] established that, in the absence of diffusion through the pores of the particles, the reactivity of the sorbent toward SO_2 increases with the internal surface area. The overall reaction rate in these conditions is controlled by the chemical reaction at low values of sulfate conversion and by gas diffusion through a layer of $CaSO_4$ formed over the CaO sorbent that increases as the sulfation conversion increases. Regarding the effect of SO_2 concentration in gas phase, there is a general agreement that the reaction order ranges from 0.6 to 1.[28,20,22,29] This background information should be valuable in modeling the sulfation rates of CaO particles in the typical conditions of CaL systems.

Another important difference between early works on the sulfation reaction of CaO in combustion environments and this study is to do with the range of temperatures. The most suitable mathematical models for describing the rate of sulfation of individual particles are usually fitted to the data obtained at temperatures characteristic of CFBC (around 850°C). However, these conditions differ considerably from those of a carbonator reactor working with a flue gas at lower temperatures (650°C).

Finally, it is necessary to take into account the special characteristics of the CaO particles cycling in a CaL capture system, where the reversible carbonation reaction of CO_2 with CaO has a strong impact on the textural properties of the material. It is well-known that CO_2 carrying capacity of CaO sorbents decays with number of calcinations/carbonations[30,31] due to a sintering mechanism that drastically reduces the surface with the increasing number of cycles. In a scenario, where SO_2 is present in the flue gas entering the carbonator reactor, there is an additional deactivation of the CaO sorbent due to the formation of $CaSO_4$. Several works have shown[11–13,17] that SO_2 accelerates the decrease in CO_2 carrying capacity of a sorbent during cycling even when a low ratio of SO_2/CO_2 is used. One of the important conclusions of these cyclic tests is that the performance of limestones may differ considerably during sulfation in contrast to their similar behavior during carbonation.[13] In their studies of the performance of calcium aluminate pellets during cocapture tests of CO_2 and SO_2 Manovic et al.[17] showed that the deactivation of synthetic sorbents (calcium aluminate pellets) is greater than that of the natural limestone sorbent due to their higher reactivity toward SO_2.

On the other hand, the sintering process of CaO under cyclic carbonation/calcination cycles can have a positive impact on sorbent use during sulfation. Some researchers have found that the sulfation behavior of CaO is enhanced (higher maximum sulfation conversions are achieved) during the calcination/carbonation cycles.[10,13,14] This is because, the sintering of the particles during carbonation/calcination is accompanied by a widening of the pores to diameters of several 100 s nm after extended (100) cycles.[32] The opened structures formed during the calcination/carbonation cycles are then able to accommodate the bulky product layer of $CaSO_4$, thus reducing the pore blocking mechanism which limits CaO conversion during sulfation. On the basis of this sorbent behavior, some researchers have suggested the idea of using the spent sorbent from carbonate looping as feedstock material for SO_2 retention in CFB boilers during coal combustion.[13,15,16] This may be one of the reasons why most of the published data on the sulfation of spent sorbents is related with high temperatures typical of combustion temperatures (850–900°C) and there is a lack of experimental information on sulfation rates under carbonation temperatures (650°C).

Table 1. Chemical Composition (wt %) of Limestones Used in this Work

	Al_2O_3	CaO	Fe_2O_3	K_2O	MgO	Na_2O	SiO_2	TiO_2
Compostilla	0.16	89.7	2.5	0.46	0.76	<0.01	0.07	0.37
Imeco	0.10	96.1	0.21	0.05	1.19	0.01	1.11	<0.05
Enguera	0.18	98.9	<0.01	0.03	0.62	0.00	0.43	0.02

The focus in this work is on the capture of SO_2 from the flue gas fed into the carbonator reactor, as this operates in conditions that may need to reconsider and reformulate the application of existing models at particle level to describe the sulfation reaction rates of CaO. Indeed, despite the large body of literature on the reaction of CaO with SO_2 in a wide range of conditions relevant to the operation of CFBCs, there is insufficient experimental information on sulfation reaction rates in the conditions characteristic of a carbonator reactor (i.e., particles that have undergone very different numbers of carbonation/calcination cycles, having substantially different textural properties and with expected conversions to $CaSO_4$ compared to that of CFBC systems). This work addresses this knowledge gap and presents what we believe to be the first results of an investigation to define a semiempirical sulfation reaction model at particle level suitable for the conditions characteristic of a carbonator reactor in a Ca-looping postcombustion system.

Experimental

Three different limestones with particle sizes in the range of 63–100 μm were used for this study. Their chemical composition is shown in Table 1. The calcination/carbonation cycling and the sulfation of the sorbents were experimentally studied using a thermo-gravimetric analyser (TGA) especially designed for carrying out long carbonation/calcination cycles, as described elsewhere.[33] This TG consists of a quartz tube installed in a two-zone furnace which is able to work at two different temperatures. The furnace can be moved up or down by means of a pneumatic piston and its position with respect to the sample allows a rapid change from calcination (950°C) to carbonation temperatures (650°C) and vice versa. The system is equipped with a microbalance that continuously measures the weight of the sample which is held in a platinum basket. The gas mixture ($air/CO_2/SO_2$) was prepared using mass flow controllers and was fed into the bottom of the quartz tube. The weight and temperature of the sample were continuously recorded on a computer.

The experimental procedure starts with the calcination carbonation cycling of the limestone for a certain number of cycles. During these tests, calcination was performed in air at 950°C and carbonation under 10% CO_2 in air at 650°C. After cycling, the sample temperature was allowed to stabilize for 10 min until a temperature of 650°C was reached. A mixture of SO_2 with air was then introduced into the quartz tube to begin sulfation. Tests were performed to establish the experimental conditions (sample mass and total gas flow) needed to avoid external diffusion effects. In the light of the results, the total volumetric flux was finally set to 2.25×10^{-5} m^3/s, (corresponding to 0.05 m/s at 650°C). It was also

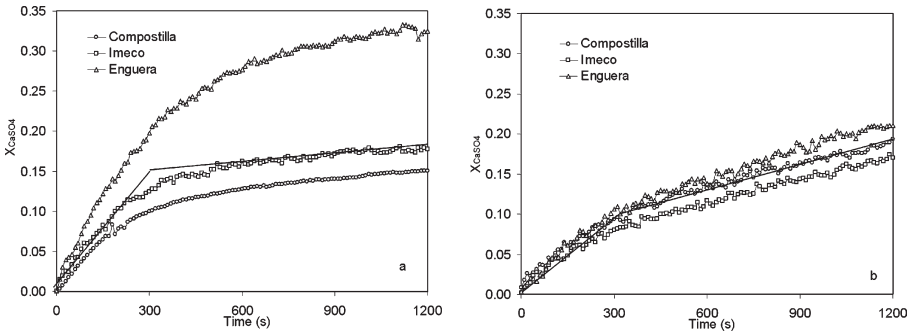

Figure 1. X_{CaSO_4} vs. time for limestones used in this work after the first calcination (a) and 50 calcination/carbonation cycles (b); T = 650°C, SO_2 concentration = 500 ppmv.

established that a sample mass below 3 mg was necessary to eliminate external mass diffusion effects (i.e., at T = 650°C and 500 ppmv of SO_2). CaO conversion of the sorbent was calculated from the weight gain assuming that $CaSO_4$ would be the main product of the reaction between CaO and SO_2 under the experimental conditions of this work. After the end of each run, the samples were weighed using a different balance to check the accuracy of the TGA. A good agreement between both series of measurements was obtained in all cases.

Results and Discussion

Figure 1a shows the evolution of CaO conversion to $CaSO_4$ with time for limestones tested after a first calcination at a temperature of 650°C using 500 ppmv of SO_2. As can be seen, the three sorbents exhibit an initial fast period followed by a second period with a lower reaction rate during which X_{CaSO_4} tends to stabilize to an almost constant value. In the case of the Compostilla and Imeco limestones, the sulfation rate of CaO fell sharply after 10 min of reaction, to a X_{CaSO_4} of 0.16 and 0.19, respectively. The reactivity of the Enguera limestone toward sulfation was much higher, yielding a X_{CaSO_4} of 0.35 at the end of the sulfation period. The drastic slowing down of the sulfation process has been reported widely in the literature and is attributed to pore blockage due to the different molar volumes of CaO and $CaSO_4$ (16.9 and 46.0 cm^3/g, respectively).[9]

Figure 1b shows the CaO conversions to $CaSO_4$ after 50 calcination/carbonation cycles. As can be seen, the evolution of X_{CaSO_4} is quite similar for the three sorbents after cycling, despite the different behaviors of the freshly calcined limestones (Figure 1a). This is a clear indication of the strong effect of a large number carbonation/calcination cycles on the pore structure of CaO particles, irrespective of their origin, as revealed in previous studies on carbonation.[34]

Certain similarities between Figures 1a and b are worth highlighting. On the one hand, the sulfation of the CaO cycled particles seems to maintain a certain transition (at about 300 s in these figures) between two stages in the rate of reaction. The fast reaction stage has a less inclined slope compared with the equivalent period in the fresh sorbent (Figure 1a), and this can be attributed to the smaller surface area of CaO particles after 50 carbonation/calcination cycles. Furthermore, the reduction in the reaction rate during the second stage is less pronounced in the case of the cycled sorbents (as the solid lines show). Even more interesting is the fact that in Figure 1b, the reaction rate remains almost constant until the very end of the sulfation experiment, in contrast to what one would expect when the pore blockage mechanism takes place (as in Figure 1a). This behavior might be expected in view of the evolution of the sorbent surface, with cycling, toward one with a more opened texture and wider pores.[13,17,32,35] A comparison of the experimental data in Figures 1a, b shows the importance of taking into account the evolution of sorbent texture during the calcination/carbonation cycles when modeling the sulfation process and determining the rate constants, as will be discussed later on.

Experiments with different particle sizes were performed to evaluate radial diffusion resistances throughout the pore network of the particles, focusing on the low level of sulfate conversion (fast reaction regions in Figure 1). Figure 2 shows the CaO conversion to $CaSO_4$ for the freshly calcined and cycled (N = 20) Compostilla limestone of two particle sizes, 63–100 and 400–600 μm, respectively. As can be seen, the reaction rates are similar for both sizes. This indicates that the SO_2 concentration is constant throughout the particle and that the sulfation rate can be described by means of a

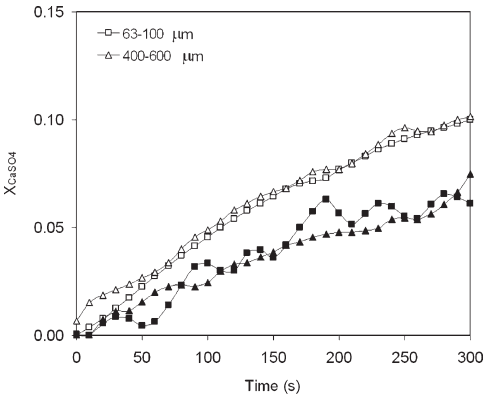

Figure 2. Effect of the particle size on the sulfation of CaO after the first calcination (empty symbols) and 20 calcination/carbonation cycles (filled symbols); T = 650°C, SO_2 concentration = 500 ppmv.

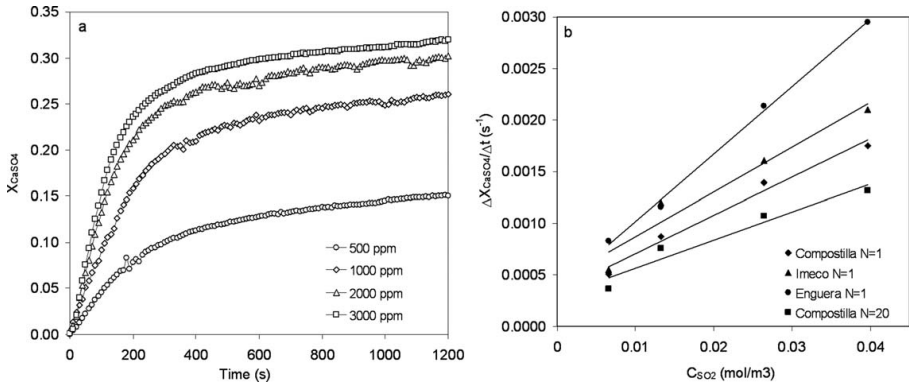

Figure 3. Effect of SO_2 concentration on X_{CaSO_4} for the fresh calcined Compostilla limestone ($N = 1$) (a) and the maximum reaction rate vs. SO_2 concentration (b) ($T = 650°C$).

homogeneous model for these particle size ranges, common in CaL applications with CFB technology. However, this approach should always be reconsidered when using particles of a larger size in other systems.

To study the effect of SO_2 on the sulfation rate of CaO, tests with different concentrations were performed at a temperature of 650°C. The effect of the SO_2 concentration on X_{CaSO_4} in the case of Compostilla limestone after the first calcination cycle is shown in Figure 3a, where the SO_2 concentration ranges from 500 to 3000 ppmv. As can be seen, the SO_2 concentration has a marked effect on the slope of the initial stage of the sulfation process and on the final conversion of the sorbent after 20 min of reaction.

As mentioned earlier, different reaction orders can been found in the literature depending on the sulfation conditions. To determine the reaction order under the sulfation conditions tested in this work, the maximum sulfation rate ($\Delta X/\Delta t$) for the initial period (up to reaction times of 100 s) was represented against the SO_2 concentration. Figure 3b shows the results obtained for the slopes of the curves in the case of the fresh calcined Compostilla limestone. As can be seen, a good linearity is observed indicating a pseudofirst-order reaction respect to SO_2. Figure 3b shows the results obtained for the other limestones ($N = 1$) and for the Compostilla limestone after 20 calcination/carbonation cycles confirming the first reaction order.

The aforementioned experimental results were interpreted in this work using the random pore model (RPM) proposed by Bhatia[36] and recently adapted to the carbonation reaction in CaL systems.[37,38] This model has also been previously applied to freshly calcined limestones to study the diffusion and kinetic resistances involved in the sulfation process.[20] The RPM model has a general expression which is valid for solid–gas reactions and which is also applicable to porous systems with product layer resistance. Thus

$$\frac{dX}{dt} = \frac{k_s SC(1-X)\sqrt{1-\psi\ln(1-X)}}{(1-\varepsilon)\left[1+\frac{\beta Z}{\psi}\left(\sqrt{1-\psi\ln(1-X)}-1\right)\right]} \quad (1)$$

where

$$\beta = \frac{2k_s a\rho(1-\varepsilon)}{bM_{CaO}DS} \quad (2)$$

and k_s is the rate constant for the surface reaction, S is the reaction surface area per unit of volume, ε is the porosity of the particles, D is the effective product layer diffusivity, and C is the SO_2 concentration. In Eq. 2, Ψ is a structural parameter that takes into account the internal particle pore structure which can be calculated as

$$\psi = \frac{4\pi L(1-\varepsilon)}{S^2} \quad (3)$$

where L is the initial pore length in the porous system per unit of volume. For a chemically controlled reaction, the general rate expression from Eq. 1 can be simplified and integrated to yield the following equation [36]

$$\frac{1}{\psi}\left[\sqrt{1-\psi\ln(1-X)}-1\right] = \frac{k_s SCt}{2(1-\varepsilon)} \quad (4)$$

On the other hand, when chemical kinetics and diffusion through the product layer are controlling the overall reaction rate, Eq. 1 can be integrated to the following equation

$$\frac{1}{\psi}\left[\sqrt{1-\psi\ln(1-X)}-1\right] = \frac{S}{(1-\varepsilon)}\sqrt{\frac{DM_{CaO}Ct}{2\rho_{CaO}Z}} \quad (5)$$

Textural parameters, used as inputs in the RPM model (S, L, and ε), can be determined from experimental measurements.[20] In the case of cycled CaO, as the textural properties (S_N, L_N) change during cycling, their values for each cycle need to be known before the model can be applied. To avoid the need for experimental measurement of these parameters and in the absence of a detailed sintering model able to estimate the pore-size distribution during cycling, we adopted a similar methodology to that proposed by Grasa et al.[37] applying the RPM to the carbonation reaction of the cycled particles. Assuming that $CaCO_3$ forms a fairly constant layer at the end of the fast carbonation period[32] and the total pore volume remains constant with the number of cycles, these authors proposed to determine S_N and L_N for each cycle, from the initial values (S_0 and L_0) and the maximum CO_2 carrying capacity of the sorbent (X_N) as follows

$$S_N = S_0 X_N \quad (6)$$

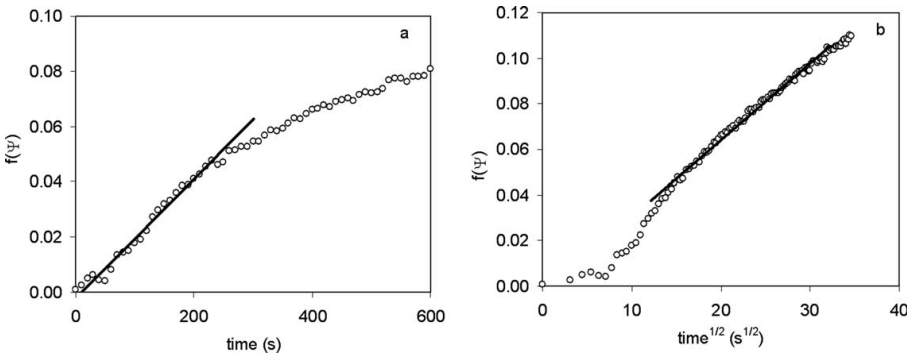

Figure 4. Fitting of Eq. 4 (a) and Eq. 5 (b) to the experimental data obtained for the Enguera limestone at $N = 20$ ($T = 650°C$, SO_2 concentration = 500 ppmv).

$$L_N = L_0 X_N \frac{r_{p_0}}{r_{p_N}} \tag{7}$$

where S_0 and L_0 are the values corresponding to the initial fresh calcined limestones, and r_p is the pore radius (r_{p0} initial value, r_{PN} after N cycles). The maximum carrying capacity (X_N) in each cycle can be calculated using the following equation proposed by Grasa et al.[39]

$$X_N = \left(\frac{1}{\frac{1}{(1-X_r)} + kN} + X_r \right) \tag{8}$$

where k is the deactivation constant, X_r is the residual conversion after an infinite number of cycles and N is the number of cycles. Values of $k = 0.52$ and $X_r = 0.075$ have been proven to be valid for a wide range of sorbents and carbonation conditions and have been used in this work. The values calculated for X_N by means Eq. 8 were compared with the experimental CO_2 carrying capacities obtained during TGA cycling and a good agreement was found. We estimated the initial surface area (S_0) of the fresh calcined limestones from the maximum CO_2 carrying capacity of the sorbent in the first cycle assuming the $CaCO_3$ layer thickness at the end of the fast reaction regimen to be 49 nm.[32] This yields an initial value of 30×10^6 m^2/m^3 assuming an initial CO_2 carrying capacity of 0.7 (using $N = 1$ in Eq. 8). The initial values of pore length (L_0) and porosity (ε) used for the three limestones were 4.16×10^{14} m/m^3 and 0.46, respectively. These values were taken from a study of Grasa et al.[37] in which calcined Imeco limestone was characterized by mercury porosimetry.

Once the evolution of the surface area (S_N) and Ψ_N were calculated with the number of cycles, the reaction parameters, k_s and D, were determined by fitting Eqs. 4 and 5 to the experimental data. Figure 4 shows an example of the fitting of these equations to the experimental data obtained during the sulfation of Enguera limestone after 20 cycles of calcination/carbonation. Figures 4a, b represent the left-hand side of Eqs. 4 and 5 against time and time$^{1/2}$, respectively. From the slopes of the straight lines, k_s and D can be calculated. As can be seen from these figures, there is a clear threshold between the chemical and the diffusion controlled regime that can be easily identified for $f(\Psi) \sim 0.5$ which corresponds approximately to $X_{CaSO_4} = 0.10$. A similar marked threshold was observed for the other samples studied. This indicates that under these experimental conditions and with this particle size, the overall reaction rate is initially controlled by the chemical reaction rate that takes place over the entire surface of the sorbent. However, as the reaction proceeds, the surface is covered by a layer of $CaSO_4$ and diffusion through the product layer becomes the limiting step. No pore diffusion effects were detected in the experiments or used in the model.

Before discussing the values of k_s and D (shown in Table 2), it may be useful to test the suitability of this model for describing the evolution of X_{CaSO_4} with time. CaO conversion to $CaSO_4$ with reaction time can be calculated using the following equations which can be derived from Eqs. 4 and 5:

(a) for the chemically controlled regime

$$X = 1 - \exp\left(\frac{1 - \left(\frac{\tau}{2}\psi_N + 1 \right)^2}{\psi_N} \right) \tag{9}$$

(b) for the diffusion controlled regime

$$X = 1 - \exp\left(\frac{1}{\psi_N} - \frac{\left[\sqrt{1 + \beta Z \tau} - \left(1 - \frac{\beta Z}{\psi_N} \right) \right]^2 \psi_N}{(\beta Z)^2} \right) \tag{10}$$

where

$$\tau = \frac{k_s C S_N t}{(1 - \varepsilon)} \tag{11}$$

Figure 5 compares the experimental values with those calculated for Compostilla limestone for different numbers of cycles. In this figure, the transition between chemically and diffusion controlled regime has been obtained from the

Table 2. Calculated Kinetic Rate Parameters (k_s and D) for the Different Limestones at 650°C

Limestone	k_s (m^4/mol s)	D (m^2/s)	h_{CaSO_4} (nm)
Compostilla	4.32E-09	2.77E-12	8.6
Imeco	4.95E-09	2.41E-12	7.0
Enguera	5.63E-09	4.88E-12	9.9

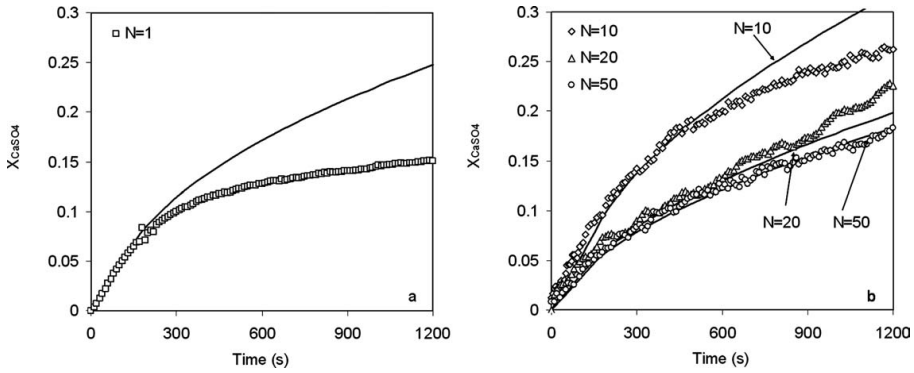

Figure 5. Comparison of experimental and calculated values of X_{CaSO_4} for Compostilla limestone with different numbers of cycles: (a) first cycle and (b) higher cycles (T = 650°C, SO_2 concentration = 500 ppmv; calculated values: solid lines).

experimental results (typically around 120–180 s). Moreover, X_{CaSO_4} has been calculated using the k_s and D values derived for each cycle. As can be seen in the figure, the model only predicts satisfactorily the CaO conversion up to a value of ~0.10 in the case of the fresh calcined limestone ($N = 1$), which corresponds to a reaction time of around 4 min. From this point, the calculated values clearly over predict the experimental ones. By contrast, for the sorbent obtained after 10 calcination/carbonation cycles, the model is able to calculate the sorbent conversion up to values of $X_{CaSO_4} = 0.2$ which corresponds to a reaction time of ~10 min. In the case of the sorbent that has been cycled 20 and 50 times, the X_{CaSO_4} values calculated with the RPM model are in close agreement with the experimental ones over the entire reaction period.

The fact that the model correctly predicts the evolution of the sulfation conversion of the sorbent obtained after many carbonation/calcination cycles is a strong validation of the RPM model when applied to our results. It shows that the product layer of $CaSO_4$ is able to grow around the whole particle without experiencing any geometrical restrictions. The homogeneous model is not valid for particles derived from fresh calcined limestone because they undergo pore plugging as reaction proceeds. In the case of $N = 10$, the pore structure must be in an intermediate stage.

In a postcombustion Ca-looping system, most particles will have been cycling the system 10 s of times depending on the makeup flow ratio of fresh limestone.[34] Therefore, the assumption that the sulfation reaction progresses homogeneously in the particles, as indicated by Eqs. 1–8, will serve as an adequate approximation for practical reactor modeling purposes. A good agreement between the calculated values for cycled particles was found for each limestone, indicating the intrinsic nature of the values of k_s and D. By contrast, the best-fit values for the first cycle were clearly lower than that of the average values for all three limestones, especially in the case of the effective product layer diffusivity (D), which tends to be one order of magnitude lower. This can be explained by taking into account that the reaction surface in the particles has been calculated by means of Eqs. 6 and 8, which will tend to overestimate the reacting surface when small pores (that are prompt to $CaSO_4$ plugging) are present. The average values of k_s and D for each limestone are summarized in Table 2. These have been calculated using the values of k_s and D calculated for each cycle, except those corresponding to the fresh calcined limestone ($N = 1$).

The values presented in Table 2 are in agreement with those found by Bhatia[20] for fresh calcined sorbents at temperatures of around 650°C. From the values of X_{CaSO_4} at which the transition between the chemical and diffusion controlled regime is observed and the surface area (S_N), it is possible to estimate the thickness of the product layer (h) at which the reaction becomes diffusion controlled by means of the following equation

$$h = \frac{X_{CaSO_4}\rho_{CaO}V_{MCaSO_4}}{S_N M_{CaO}} \tag{12}$$

The calculated values of h are shown in Table 2. An average $CaSO_4$ layer thickness of 8.5 nm is obtained. This average value can be used to estimate the sulfate conversion that marks the transition between the kinetic and the diffusion controlled regimes.

Although this work focused on the carbonator reactor, where the operation temperature will be fairly constant at around 650°C, we attempted to determine the influence of the temperature on the kinetic rate parameters by means of the Arrhenius equation

$$k_s = k_{s0}\exp(-E_{ak}/RT) \tag{13}$$

$$D = D_0\exp(-E_{aD}/RT) \tag{14}$$

For this purpose, we performed tests at higher temperatures to determine k_s and D. However, diffusional resistances were observed during the tests at higher temperatures, which could not be avoided in our experimental setup. To overcome this

Table 3. Kinetic Parameters of Eqs. 13 and 146 for the Three Limestones

	Compostilla	Imeco	Enguera
k_{s0} (m^4/mol s)	6.38E−06	7.31E−06	8.31E−06
E_{ak} (kJ/mol)	56	56	56
D_0 (m^2/s)	1.71E−05	1.49E−05	3.02E−05
E_{aD} (kJ/mol)	120	120	120

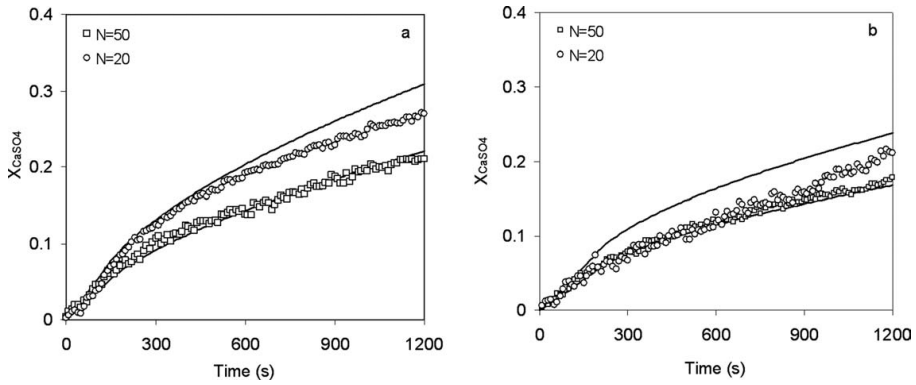

Figure 6. Comparison of experimental values of X_{CaSO_4} of Enguera (a) and Compostilla (b) limestones for $N = 20$ and 50 with those calculated by means of the model and the average values shown in Table 2 (solid lines); $T = 650°C$, SO_2 concentration = 500 ppmv.

problem and to reduce the number of adjustable parameters, we determined the values of the pre-exponential factors, assuming an activation energy of 56 kJ/mol and 120 kJ/mol as calculated by Bhatia[20] for k_s and D, respectively. The results obtained are shown in Table 3.

Figure 6 shows the experimental evolution of X_{CaSO_4} with sulfation time together with those calculated using the average values of Table 2 and assuming a layer thickness of 8.5 nm for Enguera and Compostilla limestone with different numbers of cycles. As can be seen, there is reasonable agreement between the experimental and calculated values, confirming the suitability of the model for determining the sulfation rates of cycled sorbents.

When applying the RPM model to design Ca-looping systems, it will be found that for the typically low sulfation conversions of solids in these systems, the particles will react mainly under the chemical controlled regime. Therefore, the sulfation rate can be calculated using the simplified form of Eq. 1 for this regime together with the parameters reported in Table 3

$$\frac{dX}{dt} = \frac{k_s S C (1-X)\sqrt{1-\psi \ln(1-X)}}{(1-\varepsilon)} \tag{15}$$

The high reaction rate achieved for SO_2 capture under typical carbonator conditions in postcombustion Ca-looping systems, confirms that these reactors are suitable as SO_2 absorbers and as high-temperature CO_2 capture devices.

Conclusions

The RPM has been applied to study the sulfation behavior of cycled CaO particles at a temperature of 650°C (typical of carbonator reactors in Ca-looping CO_2 capture systems). Under these conditions, the sulfation proceeds through an initial chemically controlled step followed by second period where chemical reaction and diffusion through the product layer are the controlling resistances. Sulfation has been found to be a first reaction order with respect to SO_2 under the experimental conditions tested. The rate constants for surface reaction (k_s) between 4.32×10^{-9} and 5.63×10^{-9} m^4/mol s were calculated at 650°C for the three limestones used. The calculated values of effective product layer diffusivity (D) range from 2.43×10^{-12} to 4.88×10^{-12} m^2/s. These values are in agreement with those found in the literature under similar conditions. The results obtained with RPM indicate that cycled sorbents do not undergo pore plugging due to the growth of a layer of $CaSO_4$ (for reaction times of up to 20 min). For low CaO conversion ($X_{CaSO_4} < 0.05$), sulfation is a chemically controlled reaction. The high sulfation rates measured with highly cycled (carbonation/calcination) particles seem to indicate that postcombustion Ca-looping carbonator reactors will be effective reactors for capturing SO_2 from flue gases.

Acknowledgments

This work is partially funded by the European Commission (FP7-CaOling project).

Notation

a, b = stoichiometric coefficients for sulfation reaction
C = concentration of SO_2, kmol/m^3
D = effective product layer diffusivity, m^2/s
D_0 = pre-exponential factor in Eq. 14, m^2/s
E_{ak} = activation energy for the kinetic regime, kJ/mol
E_{aD} = activation energy for the combined diffusion and kinetic regime, kJ/mol
h = product layer thickness, m
k = sorbent deactivation constant
k_s = rate constant for surface reaction, m^4/mol s
k_{s0} = pre-exponential factor in Eq. 13, m^4/mol s
L = total length of pore system, m/m^3
M = molecular weight, kg/kmol
N = number of calcination/carbonation cycles
r_{PN} = radius of the pore after N cycles, m
S = reaction surface per unit of volume, m^2/m^3
t = reaction time, s
V_M = molar volume, m^3/kmol
X_N = CaO molar conversion to $CaCO_3$ in each cycle
X_{CaSO_4} = CaO molar conversion to $CaSO_4$
X_r = residual CaO conversion
Z = ratio volume fraction after and before reaction

Greek letters

$\beta = 2k_s a\rho(1-\varepsilon)/M_{CaO}bDS$
ε = porosity
ρ = density, kg/m^3

$\psi = 4\pi L(1 - \varepsilon)/S^2$
$\tau = k_s CSt/(1 - \varepsilon)$

Literature Cited

1. Anthony EJ. Solid looping cycles: a new technology for coal conversion. *Ind Eng Chem Res*. 2008;47:1747–1754.
2. Blamey J, Anthony EJ, Wang J, Fennel PS. The calcium looping cycle for large-scale CO_2 capture. *Progr Energ Combust Sci*. 2010;36:260–279.
3. Shimizu T, Hirama T, Hosoda H, Kitano K, Inagaki M, Tejima K. A twin fluid-bed reactor for removal of CO_2 from combustion processes. *Trans IChemE*. 1999;77:62–68.
4. Romeo LM, Abanades JC, Escosa JM, Paño J, Jiménez A, Sánchez-Biezma A, Ballesteros JC. Oxyfuel carbonation/calcination cycle for low cost CO_2 capture in existing power plants. *Energ Convers Manag*. 2008;49:2809–2814.
5. Romano M. Coal-fired power plant with calcium oxide carbonation for post-combustion CO_2 capture. *Energy Procedia*. 2009;1:1099–1006.
6. Ströle J, Lasheras A, Galloy A, Epple B. Simulation of the carbonate looping process for post-combustion CO_2 capture from a coal-fired power plant. *Chem Eng Technol*. 2009;32:435–442.
7. Yongping Y, Rongrong Z, Liqiang D, Kavosh M, Patchigolla K, Oakey J. Integration and evaluation of a power plant with a CaO-based CO_2 capture system. *Int J Greenhouse Gas Control*. 2010;4:603–612.
8. Martínez I, Murillo R, Grasa G, Abanades JC. Integration of Ca looping system for CO_2 capture in existing power plants. *AIChE J*. 2011;57:2599–2607.
9. Anthony EJ, Granatstein DL. Sulfation phenomena in fluidized bed combustion systems. *Progr Energ Combust Sci*. 2001;27:215–236.
10. Li Y, Buchi S, Grace JR, Lim CJ. SO_2 removal and CO_2 capture by limestone resulting from calcination/sulfation/carbonation cycles. *Energy Fuels*. 2005;19:1927–1934.
11. Ryu HJ, Grace JR, Lim CJ. Simultaneous CO_2/SO_2 capture characteristics of three limestones in a fluidized-bed reactor. *Energy Fuels*. 2006;20:1621–1628.
12. Sun P, Grace JR, Lim CJ, Anthony EJ. Removal of CO_2 by calcium-based sorbents in presence of SO_2. *Energy Fuels*. 2007;21:163–170.
13. Grasa GS, Alonso M, Abanades JC. Sulfation in a carbonation/calcination loop to capture CO_2. *Ind Eng Chem Res*. 2008;47:1630–1635.
14. Manovic V, Anthony EJ. Sequential SO_2/CO_2 capture enhanced by steam reactivation of CaO-based sorbent. *Fuel*. 2008;87:1564–1573.
15. Manovic V, Anthony EJ, Loncarevic D. SO_2 retention by CaO-based sorbent spent in CO_2 looping cycles. *Ind Eng Chem Res*. 2009;48:6617–6632.
16. Pacciani R, Müller CR, Davidson JF, Dennis JS, Hayhurst AN. Performance of novel synthetic Ca-based sorbent suitable for desulfurizing flue gases in a fluidized bed. *Ind Eng Chem Res*. 2009;48:7016–7024.
17. Manovic M, Anthony EJ. Competition of sulphation and carbonation reactions during looping cycles for CO_2 capture by CaO-based sorbents. *J Phys Chem A*. 2010;114:3397–4002.
18. Abanades JC, Anthony EJ, Wang J, Oakey JE. Fluidized bed combustion systems integrating CO_2 capture with CaO. *Environ Sci Technol*. 2005;39:2861–2866.
19. Georgakis C, Chang CW, Szekely J. A changing grain size model for gas–solid reactions. *Chem Eng Sci*. 1979;34:1072–1075.
20. Bhatia SK, Perlmutter DD. The effect of pore structure on fluid–solid reactions: application to the SO_2-lime reaction. *AIChE J*. 1981;27:226–234.
21. Borgwardt RH, Bruce KR. Effect of specific surface area on the reactivity of CaO with SO_2. *AIChE J*. 1986;32:239–246.
22. Borgward RH, Bruce KR, Blake J. An investigation of product-layer diffusivity for CaO sulfation. *Ind Eng Chem Res*. 1987;26:1993–1998.
23. Dennis JS, Hayhurst AN. Mechanism of the sulphation of calcined limestone particles in combustion gases. *Chem Eng Sci*. 1990;45:1175–1187.
24. Hartman M, Coughlin RW. Reaction of sulfur dioxide with limestone and the grain model. *AIChE·J*. 1976;22:490–498.
25. Adánez J, García-Labiano F, Fierro V. Modelling for the high-temperature sulphation of calcium-based sorbents with cylindrical and plate-like geometries. *Chem Eng Sci*. 2000;55:3665–3683.
26. Borgwardt RH. Kinetics of the reaction of SO_2 with calcined limestone. *Environ Sci Technol*. 1970;4:59–61.
27. Hartman M, Coughlin RW. Reaction of sulfur dioxide with limestone and the influence of pore structure. *Ind Eng Chem Process Des Dev*. 1974;13:248–253.
28. Pigford RL, Sliger G. Rate of diffusion-controlled reaction between gas and a porous solid sphere. Reaction of SO_2 with $CaCO_3$. *Ind Eng Chem Process Des Dev*. 1973;12:85–91.
29. Adánez J, Gayán P, García-Labiano F. Comparison of mechanistic models for the sulfation reaction in a broad range of particle sized of sorbents. *Ind Eng Chem Res*. 1996;35:2190–2197.
30. Curran GP, Fink CE, Gorin E. CO_2 acceptor gasification process. Studies of acceptor properties. *Adv Chem Ser*. 1967;69:141–161.
31. Barker R. Reversibility of the reaction $CaCO_3 = CaO + CO_2$. *J Appl Chem Biotechnol*. 1973;23:733–742.
32. Alvarez D, Abanades JC. Determination of the critical product layer thickness in the reaction of CaO with CO_2. *Ind Eng Chem Res*. 2005;44:5608–5615.
33. González B, Grasa GS, Alonso M, Abanades JC. Modeling of the deactivation in a carbonate loop at high temperatures calcination. *Ind Eng Chem Res*. 2008;45:9256–9262.
34. Abanades JC. The maximum capture efficiency of CO_2 using a carbonation/calcination cycle of $CaO/CaCO_3$. *Chem Eng J*. 2002;60:303–306.
35. Abanades JC, Álvarez D. Conversion limits in the reaction of CO_2 with lime. *Energy Fuels*. 2003;17:308–315.
36. Bhatia SK, Perlmutter DD. A random pore model for fluid-solid reactions. I. Isothermal, kinetic control. *AIChE J*. 1980;26:379–386.
37. Grasa G, Murillo R, Alonso M, Abanades JC. Application of the random pore model to the carbonation cyclic reaction. *AIChE J*. 2009;55:1246–1255.
38. Arias B, Abanades JC, Grasa GS. An analysis of the effect of carbonation conditions on CaO deactivation curves. *Chem Eng J*. 2011;167:255–261.
39. Grasa GS, Abanades JC. CO_2 capture capacity of CaO in long series of carbonation/calcination cycles. *Ind Eng Chem Res*. 2006;45:8846–8851.

Manuscript received May 18, 2011, and revision received July 25, 2011.

4.6.2 Publicación II

Investigation of SO_2 Capture in a Circulating Fluidized Bed Carbonator of a Ca Looping Cycle

Publicado en:

I&EC research

Volumen 52

Año 2013

Índice de Impacto: 2.235

I&EC research
Industrial & Engineering Chemistry Research

Article

pubs.acs.org/IECR

Investigation of SO_2 Capture in a Circulating Fluidized Bed Carbonator of a Ca Looping Cycle

Borja Arias,* Jose Maria Cordero, Mónica Alonso, Maria Elena Diego, and Juan Carlos Abanades

Instituto Nacional del Carbón (CSIC), C/Francisco Pintado Fe, No. 26, 33011 Oviedo, Spain

ABSTRACT: Calcium looping is a postcombustion CO_2 capture technology that uses CaO as a regenerable solid sorbent. One potential advantage of this technology is that it allows flue gases to be treated with SO_2, avoiding the need for a costly desulfurization step. In this work, we study the desulfurization capacity of a circulating fluidized bed (CFB) carbonator reactor in a 30 kW_{th} pilot plant that has been used to test CO_2 and SO_2 cocapture. A simple reactor model is applied to analyze the experimental results obtained and to study the effect of the main variables involved in the process: i.e., the circulation rates of solids and the inventory of active material in the CFB reactor. The results obtained have shown that SO_2 capture efficiencies above 0.95 can be achieved in a CFB carbonator even when using a low inventory of active material in the bed. Extreme desulfurization (SO_2 emissions below 5−10 ppmv) is thought to be achievable in large scale CFB carbonators designed to capture CO_2 with CaO.

INTRODUCTION

Calcium looping is an emerging postcombustion CO_2 capture technology that uses CaO as a regenerable solid sorbent. In this system, CO_2 from the combustion flue gas of a power plant is captured by using CaO as sorbent in a circulating fluidized bed (CFB) carbonator operating between 600 and 700 °C. The stream of partially carbonated solids leaving the carbonator is directed to the CFB calciner, where the solids are calcined by burning coal under oxy-fuel conditions at temperatures above 900 °C, allowing the release of the CO_2 captured from the power plant and the regeneration of the sorbent (CaO). The CFB reactors used in Ca looping operate with solid materials (mainly CaO particles and ashes) and key operating conditions (gas velocities and solid circulation rates) very similar to those present in large scale CFB combustors. This advantage explains the rapid development of this technology in recent years from small laboratory scale pilot plants[1−6] to larger pilot plants with scales of 200 kW_{th}[7] and 1 MW_{th}.[8−10]

Other features of the process are that the heat supplied to the calciner can be recovered from different high temperatures sources, thus ensuring an efficient heat integration through the entire power plant and a lower energy penalty.[11−16] Another important aspect of CaL compared to other postcombustion CO_2 capture technologies (e.g., amine systems) is that the flue gas treated can contain a certain amount of SO_2 since CaO from calcined limestones is used in many commercial scale power plants.[17] Several works on sulfation phenomena in CaL systems have been published although these focus mainly on the effect of SO_2 on CO_2 carrying capacity during cycling.[18−25] These studies have referred to the negative impact of SO_2 on sorbent capacity and the increasing decay of CO_2 carrying capacity of the sorbent during cycling due to the irreversible sulfation reaction of CaO. Some researchers[18,20,23] have shown that the SO_2 absorption capacity of cycled CaO is higher than that of the fresh calcined limestone due to fact that the sintering process causes the pores to open. These researchers have also suggested the idea of using the spent sorbent from calcium looping as feedstock material for SO_2 retention in CFB boilers during coal combustion. However, it should be noted that a simple mass balance on the continuous operation of Ca looping[26] reveals that the large makeup flows of limestone required to purge the ash and maintain sorbent activity result in very low average particle sulfation values (sulfation conversions below 5 mol %). In any case, the loss of activity due to the irreversible reaction between CaO and SO_2 can be compensated for by adding fresh sorbent due to the low cost of limestone and by taking advantage of synergy with the cement industry.[27,28] Other aspects of the presence of SO_2 in Ca looping is the effect on sorbent attrition. Different trends have been reported in the literature. Some authors[29] have found that the presence of SO_2 can reduce the attrition of the sorbent during CO_2 capture in CFB reactor. However, a recent work carried out by Coppola et al.[30] has reported that SO_2 has little impact on sorbent attrition during CO_2 capture in a fluidized bed reactor.

The fact that Ca looping allows flue gases to be treated with SO_2 offers the possibility of avoiding the desulfurization step and removing the SO_2 during CO_2 capture process. However, to our knowledge, no experiment has demonstrated the ability of a CFB carbonator to retain SO_2 under the typical conditions expected of a carbonator in a calcium looping system. The aim of this work is to study the desulfurization capacity of a CFB carbonator in a small pilot plant composed of two interconnected fluidized beds during CO_2 capture operating in continuous mode (i.e., continuous circulation of solid between the calciner and carbonator). A simple reactor model is proposed to analyze the experimental results obtained and to study the effect of the main variables involved in the process.

Received: October 2, 2012
Revised: December 21, 2012
Accepted: January 14, 2013
Published: January 14, 2013

dx.doi.org/10.1021/ie3026828 | *Ind. Eng. Chem. Res.* 2013, 52, 2700−2706

EXPERIMENTAL SECTION

The tests shown in this work were carried out in the 30 kW pilot plant at INCAR-CSIC which has been described elsewhere.[5] Figure 1 outlines the Ca looping process and the main variables analyzed during an experimental campaign to test SO_2 capture in the carbonator. This facility consists of two interconnected CFB reactors: a carbonator 6.5 m in height and a calciner 6.0 m in height. Both reactors have an internal diameter of 0.1 m. The facility is electrically heated by independently controlled ovens. Each reactor is equipped with a primary cyclone which separates the solids and flue gases leaving the risers. In order to close the pressure balance and to return the solids to the riser, each reactor is equipped with a loop seal which consists of a bubbling fluidized-bed aerated with air. A simulated flue gas is supplied to the carbonator by mixing air, CO_2, and SO_2 by means three mass flow controllers. For this study, the calciner was operated burning coal with air. The composition of the flue gas leaving both reactors was measured by two continuous gas analysers. The inventory of solids in each reactor was calculated from the pressure drop in the risers. During the tests, samples of solids from the risers were taken using sampling ports. The conversion of CaO to $CaCO_3$ and $CaSO_4$ was calculated by determining the carbon and sulfur content of the samples of solids using a LECO CS 230. The samples were also tested in a TG equipment to determine their maximum CO_2 carrying capacity (X_{ave}).

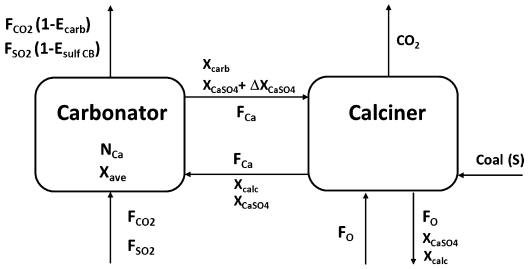

Figure 1. Scheme and main variables in the calcium looping process for CO_2 capture incorporating SO_2 cocapture.

Compostilla limestone was used in all the experiments (main components of calcined limestone: 95.4 wt % CaO, 2.6 wt % Fe_2O_3, 0.8 wt % MgO, 0.5 wt % K_2O) the initial average size of the particles being 105 μm. The main input of sulfur into the system was the flue gas fed into the carbonator. A low ash and sulfur coal was used during the tests (71.0% C, 4.4% H, 0.2% S, 3.9% ash) to facilitate the analysis of SO_2 capture in the carbonator. The experimental procedure applied is similar to that described by Rodríguez et al.[5] For each test an initial batch of 20 kg of limestone was used. The solids were calcined by burning coal in the carbonator and calciner. After this initial calcination, the coal fed into the carbonator was stopped to allow the temperature to fall to a value between 600 and 700 °C. Once this temperature had been reached, synthetic flue gas was fed into the carbonator in order to start the cocapture test.

Table 1 resumes the main parameters involved in the carbonator reactor and the range of operating conditions. Initial tests showed that a high inventory of active solids in the carbonator (as needed for an efficient capture of CO_2)[5] leads to extremely high SO_2 capture efficiencies (close to 1). Since the information from these tests is of little use for model validation purposes or to elucidate the effect of the variables involved in the SO_2 capture process, most of the tests were carried out under experimental conditions that lead to SO_2 capture efficiencies well below 1, even though in these conditions, CO_2 capture efficiencies were unacceptably low. This was achieved by using an unrealistically high SO_2 concentration in the flue gas fed into the reactor and lower than usual inventories in the carbonator and lower solids circulation rates from the calciner.

Table 1. Range of Operation Conditions and Range of Main Parameters

carbonator temperature (°C)	575−685
carbonator superficial gas velocity (m s^{-1})	2.1−2.9
inlet CO_2 volume fraction	0.06−0.15
inlet SO_2 concentration (ppmv)	1300−6250
inventory of solids in the carbonator (kg m^{-2})	20−255
maximum CO_2 carrying capacity of the solids	0.04−0.18
CO_2 capture efficiency	0.10−0.50
SO_2 capture efficiency	0.70−1.00

Figure 2 shows an example of an experimental testing period of 40 min. The O_2, CO_2, and SO_2 concentration at the exit of the carbonator are shown in the first graph. The second graph shows the inventory of solids in the carbonator and the reactor temperature. The carbonator temperature shown in the second graph of Figure 2 corresponds to the average value calculated from the temperatures measured at the bottom of the carbonator where the dense bed is located. The third graph shows the CO_2 and SO_2 capture efficiencies calculated from the gas composition measured at the exit of the carbonator reactor.

The experimental run illustrated in Figure 2 is divided into four periods with different SO_2 inlet concentrations and solids inventories of solids. During this experimental run, the total flow to the carbonator and the CO_2 molar fraction at the inlet was kept constant at 0.12. The SO_2 inlet concentration to the carbonator during the initial period (1) was kept at 1900 ppmv. The SO_2 capture efficiency during this period was around 0.98, since the SO_2 concentration at the exit of the carbonator was around 40 ppmv. After this period, the SO_2 inlet concentration was increased to 3800 ppmv. This increase in the inlet concentration led to an increase in the SO_2 concentration at the exit of the carbonator and a reduction in SO_2 capture efficiency to a value of around 0.95. During the third period, the SO_2 inlet concentration to the carbonator was set to 1800 ppmv. A reduction in the SO_2 at the exit of the carbonator was observed at this point which stabilized to a value close to 60 ppmv. The SO_2 capture efficiency during this period was 0.97, slightly lower than during the initial period due to a small reduction in the inventory of solids. In the last period shown in Figure 2, the inventory of solids in the system was increased by reinjecting solids taken from the secondary cyclones. This increased the SO_2 capture efficiency to a value of 1 as no SO_2 was detected at the exit of the carbonator. At the beginning of this period, CO_2 capture efficiency also increased. The carbonator temperature then rose, as a result of which a decrease in CO_2 capture efficiency was observed.

The experimental results shown in the Results and Discussion section correspond to steady states of at least 10 min, such as those shown in Figure 2. These steady periods are characterized by the average reactor temperatures (carbonator and calciner), the inventory of solids in the risers (carbonator and calciner), the CO_2 and SO_2 concentration at the carbonator

dx.doi.org/10.1021/ie3026828 | Ind. Eng. Chem. Res. 2013, 52, 2700−2706

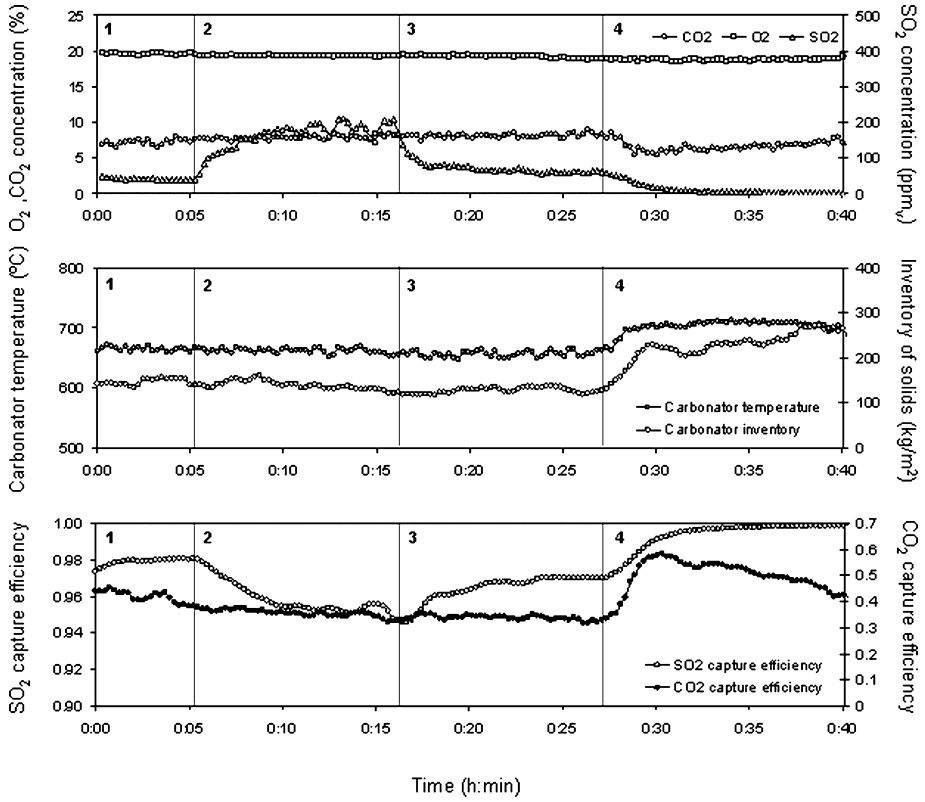

Figure 2. Results of an experimental run during a SO_2–CO_2 cocapture test (average gas velocity = 2.5 m/s, CO_2 inlet fraction = 0.12, X_{ave} = 0.06).

inlet, the carbonate content of the solids leaving the carbonator (X_{carb}) and the calciner (X_{calc}), the sulfate content of the solids (X_{CaSO4}), the average CO_2 carrying capacity of the solids in the system (X_{ave}), and the circulation rate of the solids in the carbonator. A total of 40 h of useful operation in SO_2 and CO_2 capture mode was achieved.

RESULTS AND DISCUSSION

To analyze SO_2 capture in the carbonator, we followed a similar approach to that used by Alonso et al.,[31] Rodríguez el al.,[5] and Charitos et al.[6] when analyzing CO_2 capture in a CFB carbonator. These previous studies demonstrated that the assumptions of instantaneous and perfect mixing of solids and plug flow in the gas phase are sufficient for interpreting the results obtained in the 30 kW dual fluidized bed pilot plant. The overall mass balance in the carbonator for SO_2 can be expressed as

$$\begin{pmatrix} SO_2 \text{ reacting} \\ \text{with CaO in the bed} \end{pmatrix} = \begin{pmatrix} SO_2 \text{ removed} \\ \text{from the gas phase} \end{pmatrix} = \begin{pmatrix} CaSO_4 \text{ formed in the} \\ \text{circulating stream of CaO} \end{pmatrix} \quad (1)$$

According to this mass balance, the SO_2 that is removed from the flue gas fed to the carbonator is equal to the $CaSO_4$ formed in the circulating stream of CaO. Therefore, in a stationary state:

$$F_{Ca}\Delta X_{CaSO4} = E_{sulfCB}F_{SO2} \quad (2)$$

where F_{SO2} is the molar flow of SO_2 fed into the carbonator (mol s^{-1}), E_{sulfCB} is the SO_2 capture efficiency in the carbonator, F_{Ca} is the Ca molar circulation rate (mol s^{-1}) through the carbonator, and ΔX_{CaSO4} is the increment in molar sulfate content between the inlet and the outlet of the carbonator. The closure of this mass balance is difficult to verify in practice as ΔX_{CaSO4} is very small, due to the incremental concentration of $CaSO_4$ per cycle considering the high circulation of solids compared to the amount of SO_2 fed into the carbonator.[20] However, in a continuous system, where there is a makeup flow of fresh limestone and a purge of spent sorbent, a similar mass balance can be applied to the whole Ca looping system:

$$F_0X_{CaSO4} = E_{sulfCB}F_{SO2} + E_{sulfCC}F_{SO2comb} \quad (3)$$

where F_0 is the molar flow of make up flow (mol s^{-1}), X_{CaSO4} is the $CaSO_4$ content in the purge of solids, $F_{SO2comb}$ is the molar flow of SO_2 produced during the combustion of coal in the calciner (mol s^{-1}), and E_{sulfCC} is the SO_2 capture efficiency in the calciner. In the case of the test carried out in the 30 kW dual fluidized pilot plant, there is no continuous addition of fresh limestone to the system which would result in an increase

dx.doi.org/10.1021/ie3026828 | Ind. Eng. Chem. Res. 2013, 52, 2700−2706

in $CaSO_4$ content of the solids circulating in the system. Therefore, the evolution of the X_{CaSO4} with time during a given experiment with a stable inventory of material in the system can be calculated by using the following expression:

$$X_{CaSO4} = \int_0^t \frac{F_{SO2}E_{sulfCB} + F_{SO2comb}E_{sulfCC}}{N_{Ca,total}}\,dt \quad (4)$$

where $N_{Ca,total}$ is the amount of Ca present the system (mol). Figure 3 shows a comparison of the experimental sulfate

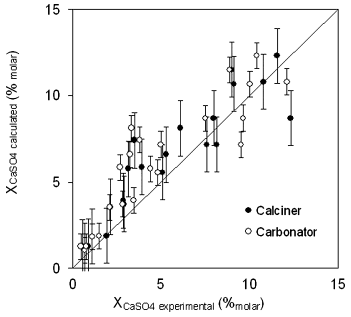

Figure 3. SO_2 mass balance closure. Comparison of the experimental and calculated X_{CaSO4} in the particles taken from the system during an experimental run.

content of samples taken periodically during an experimental run using a batch of limestone with the sulfate content calculated using eq 4. As can be seen from this figure, there is a good agreement between the experimental and calculated values, which indicates that there is an adequate mass balance closure between the SO_2 disappearing from the gas phase and the $CaSO_4$ formed inside the mass of solids present in the system. Figure 3 also indicates a good overall mixing of the solids in the system (with a time scale of minutes to tens of minutes affecting the total inventory of the solids in the system). It should also be noted that $CaSO_4$ is mainly formed in the carbonator, due to low surfur content of the coal used and that the X_{CaSO4} content in the solids taken from calciner and carbonator are similar.

To analyze the influence of the variables involved in SO_2 capture with a view to the designing of the carbonator, the most interesting mass balance is that of the SO_2 reacting with the bed of solids. This can be written as

$$E_{sulfCB}F_{SO2} = N_{Ca\ active}\left(\frac{dX_{CaSO4}}{dt}\right)_{reactor} \quad (5)$$

where $N_{Ca\ active}$ is the inventory of Ca (mol) reacting in the carbonator bed and $(dX_{CaSO4}/dt)_{reactor}$ is the average reaction rate of the solids (s^{-1}). Regarding the reaction term, we have shown in a previous work[32] that the layer of $CaSO_4$ is able to grow around the particle surface of cycled CaO without experiencing any geometrical restrictions for low conversion and that the sulfation conversion can be described adequately using a homogeneous model as the random pore model. We also have shown that the surface area available for the sulfation reaction can be correlated adequately with the CO_2 carrying capacity of the sorbent. In order to simplify the reaction term, we have assumed that the solids react in the carbonator bed according to the following expression:

$$\left(\frac{dX_{CaSO4}}{dt}\right)_{reactor} = k_{sulf}\varphi_{SO2}X_{ave}\overline{\nu_{SO_2}} \quad (6)$$

where k_{sulf} is the sulfation rate constant, φ_{SO2} is the gas−solid contacting effectivity factor (similar to that defined by Rodríguez et al.[5] for the CO_2 reaction rate in the carbonator), X_{ave} is the average CO_2 carrying capacity of the solids and $\overline{\nu_{SO_2}}$ is the average SO_2 molar fraction in the carbonator. This expression used for the reaction rate term is consistent with the results obtained in a TGA during the sulfation of cycled CaO under carbonation conditions reported by Arias et al.[32] for low sulfation conversions when particles react in a chemically controlled regime.

Regarding the inventory of Ca reacting with SO_2 in the carbonator, it is assumed that the fraction of partially carbonated CaO does not play an active role in SO_2 capture since it is unlikely that SO_2 will react directly with $CaCO_3$ to produce $CaSO_4$ at carbonator temperatures of around 650 °C.[33] Moreover, the particles that are covered by the layer of $CaCO_3$ cannot be considered active as the low diffusivity of SO_2 through the carbonate layer at the relatively low temperature of the carbonator would prevent any conversion of the inner CaO inside the particles. On the basis of these assumptions, it is inferred that only those particles that do not reach their maximum CO_2 carrying capacity in the carbonator bed are active for SO_2 retention. This definition of our active inventory is similar to that used by Alonso et al.[31] and Charitos et al.[6] for analyzing the CO_2 in a CFB carbonator. Assuming a perfect mixing of the solids in the carbonator, Alonso et al.[31] defined in a previous work a characteristic time, t^* (which depends on the reactivity of the particles toward CO_2 in the carbonator). According to their definition, this parameter is the time needed for the particles to reach X_{ave} under the reaction conditions in the carbonator and can be calculated using the equation:

$$t^* = \frac{X_{ave} - X_{calc}}{k_{carb}\varphi_{CO2}X_{ave}(\overline{\nu_{CO2}} - \nu_{CO2eq})} \quad (7)$$

where k_{carb} is the carbonation rate constant (s^{-1}) and φ_{CO2} is the gas−solid contacting effectivity factor for the CO_2 (see refs 6 and 31 for more details). It is assumed that those particles with a residence time in the carbonator higher than t^* have achieved their maximum CO_2 carrying capacity and do not react with SO_2. Assuming a perfect mixing of the solids in the carbonator reactor, a fraction of active solids (f_a), defined as those solids with a residence time in the carbonator lower than t^*, can be calculated using the following equation:

$$f_a = 1 - e^{(-t*/(N_{Ca}/F_{Ca}))} \quad (8)$$

where N_{Ca} is the amount of Ca (mol) in the carbonator and F_{Ca} is the circulation of Ca between the reactors (mol s^{-1}). Using this approach, Charitos et al.[6] defined an active space time as $\tau_{aCO2} = N_{Ca}f_aX_{ave}/F_{CO2}$, from which it follows that the CO_2 capture efficiency parameter is

$$E_{carb} = k_{carb}\varphi_{CO2}(\overline{\nu_{CO2}} - \nu_{CO2eq})\tau_{aCO2} \quad (9)$$

From the SO_2 mass balance and the definition of the active inventory of solids as $N_{Ca\ active} = N_{Ca}f_a$, eq 5 can be rewritten in a similar form to that defined for CO_2 to give the following expression:

$$E_{sulfCB} = k_{sulf}\varphi_{SO2}\overline{\nu_{SO2}}\tau_{aSO2} \quad (10)$$

dx.doi.org/10.1021/ie3026828 | Ind. Eng. Chem. Res. 2013, 52, 2700−2706

where τ_{aSO_2} is the active space time for the SO_2 and is defined as

$$\tau_{aSO_2} = \frac{N_{Ca} f_a X_{ave}}{F_{SO2}} \quad (11)$$

The term $k_{sulf}\varphi_{SO2}$ was calculated by comparing both terms of the SO_2 mass balance in eq 5. Figure 4 shows a comparison of the SO_2 removed from the gas phase (y-axis) and the SO_2 that reacts with CaO in the carbonator bed of solids (x-axis).

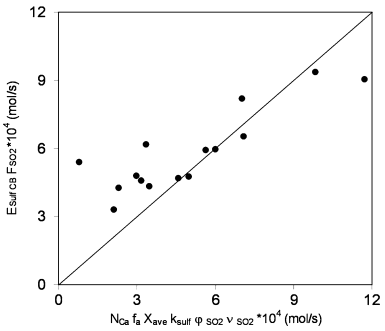

Figure 4. Comparison of the SO_2 removed from the gas phase with the SO_2 that reacts with CaO in the bed of the carbonator.

The apparent sulfation reaction constant, $k_{sulf}\varphi_{SO2}$, obtained from the fitting of the results shown in Figure 4 is 3.22 s^{-1}. To determine $k_{sulf}\varphi_{SO2}$, only those points with an E_{sulfCB} below 1 were used. In order to calculate the value of φ_{SO2}, we employed a value of k_{sulf} from the experimental data presented by Arias et al.[32] for Compostilla limestone which has a value of 3.78 s^{-1} at a temperature of 630 °C (average temperature for the experimental data obtained in this work). This yields a φ_{SO2} value of 0.85 which indicates that SO_2 capture in the carbonator in the presence of CO_2 is mainly controlled by the sulfation reaction rate of the particles in the bed.

In Figure 5, SO_2 capture efficiency is plotted against SO_2 active space time. As can be seen, there is reasonable agreement between the experimental results and the values predicted with

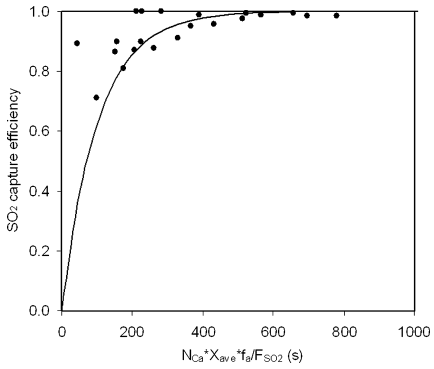

Figure 5. Comparison of experimental SO_2 capture efficiency vs active space time for SO_2 (solid line calculated from eq 10 and the following average conditions; carbonator temperature = 630 °C; SO_2 inlet concentration = 3000 ppmv, gas velocity inlet = 2.7 m/s).

eq 10. From this plot, it is deduced that a minimum value of τ_{aSO_2} is needed to achieve certain SO_2 capture efficiency. For example, in order to remove 99% of the SO_2 fed into the carbonator, an active SO_2 space time of 480 s is needed.

It may also be worthwhile to consider the relationships between CO_2 capture efficiency and SO_2 capture efficiency arising from the mass balance equations that lead to eqs 9 and 10. As mentioned above, the experimental CO_2 capture efficiency results obtained in this work in the cocapture SO_2 tests were not the main subject of the present work, as the reactor conditions selected for measuring SO_2 capture efficiencies lower than 1 lead to very modest CO_2 capture efficiencies. Nevertheless, the data on CO_2 capture efficiencies obtained during these tests were analyzed using the methodology proposed by Charitos et al.[6] and eq 9 in order to obtain an apparent carbonation reaction constant, $k_{carb}\varphi_{CO2}$. This constant was 0.33 s^{-1}, which is consistent with the value reported by Charitos et al.[6] of 0.43 s^{-1} using experimental data acquired in the 30-kW INCAR-CSIC pilot plant using a different batch of the same limestone. Combining eqs 9 and 10, we obtain

$$E_{sulfCB} = \frac{k_{sulf}\varphi_{SO2}\overline{\nu_{SO2}}F_{CO2}}{k_{carb}\varphi_{CO2}(\overline{\nu_{CO2} - \nu_{CO2eq}})F_{SO2}} E_{carb} \quad (12)$$

Figure 6 compares the experimentally measured CO_2 and SO_2 capture efficiencies achieved in the 30 kW_{th} pilot plant with

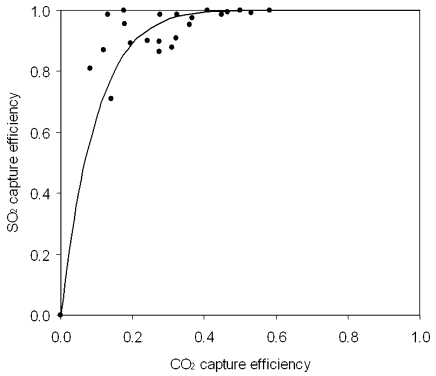

Figure 6. Comparison between the experimental results of SO_2 capture efficiency and CO_2 capture efficiency (line corresponds to the values calculated using eq 12).

this equation, using the constants reported above. As can be seen there is reasonable agreement between the experimental and calculated values. When the carbonator is operating in experimental conditions that allow a typical CO_2 capture efficiency of above 0.8, virtually all the SO_2 fed into this reactor is removed from the flue gas. Only when the operating conditions in the carbonator yield a CO_2 capture efficiency that is well below 0.5 will the SO_2 capture efficiency be lower than 1. Since the main target in the carbonator is to remove CO_2 at high capture efficiencies (even if this is at the expense of large makeup flow of sorbent to ensure the presence of a sufficient inventory of active material in the bed), it can be assumed that almost total desulfurization of the flue gas will take place in the carbonator of a calcium looping CO_2 capture system.

dx.doi.org/10.1021/ie3026828 | Ind. Eng. Chem. Res. 2013, 52, 2700−2706

CONCLUSIONS

The retention of SO_2 during CO_2 capture in a CFB carbonator of dual fluidized bed experimental facility working in continuous mode has been studied. The results obtained show that CFB carbonators are excellent desulfurization units and SO_2 capture efficiencies of above 0.95 can be achieved, even with low inventories of solids in the reacting bed. A good closure of the SO_2 mass balance of the SO_2 during its removal from the gas phase and its reaction with the inventory of solids was found. A simple reactor model was applied to predict SO_2 capture efficiency. The apparent sulfation reaction constant for the limestone used in this work was 3.22 s^{-1}. From this value, it was calculated that a gas−solid contact factor of around 0.85 was calculated, indicating that SO_2 capture efficiency is controlled by the chemical sulfation reaction. The results obtained in this work show that, when the carbonator is working with a typical CO_2 capture efficiency of above 0.8, the SO_2 entering with the flue gas will be removed from the flue gas.

AUTHOR INFORMATION

Corresponding Author

*Telephone: +34 985 11 90 57. Fax: +34 985 29 76 62. E-mail: borja@incar.csic.es.

Notes

The authors declare no competing financial interest.

ACKNOWLEDGMENTS

The research presented in this work has received partial funding from the European Community's Seventh Framework Programme (FP7/2007-2013) under the GA 241302-CaOling Project and from the PCTI Asturias Regional Government. J.M.C. also acknowledges the FYCIT fellowship for a Ph.D. grant.

NOTATION

E_{carb} = CO_2 capture efficiency
E_{sulfCB} = SO_2 capture efficiency in the carbonator
E_{sulfCC} = SO_2 capture efficiency in the calciner
F_0 = molar make up flow of limestone (mol s^{-1})
f_a = fraction of active particles reacting in the carbonator
F_{Ca} = molar flow of Ca circulating between reactors (mol s^{-1})
F_{CO2} = molar flow of CO_2 fed to the carbonator (mol s^{-1})
F_{SO2} = molar flow of SO_2 fed to the carbonator (mol s^{-1})
$F_{SO2comb}$ = molar flow of SO_2 produced during coal combustion (mol s^{-1})
k_{carb} = carbonation rate constant (s^{-1})
k_{sulf} = sulfation rate constant (s^{-1})
N_{Ca} = inventory of Ca in the carbonator bed (mol)
$N_{Ca\ active}$ = inventory of active Ca in the carbonator bed (mol)
$N_{Catotal}$ = total inventory of Ca in the system (mol)
t^* = characteristic time (s)
X_{ave} = maximum CO_2 carrying capacity of the solids
X_{calc} = carbonate content of the solids leaving the calciner
X_{carb} = carbonate content of the solids leaving the carbonator
X_{CaSO4} = sulfate content of the solids

Greek Symbols

ΔX_{CaSO4} = increment of molar sulfate content of the solids in the carbonator
φ = gas−solid contacting effectivity factor
ν = molar fraction
τ_a = active space time (s)

REFERENCES

(1) Abanades, J. C.; Anthony, E. J.; Lu, D. Y.; Salvador, C.; Álvarez, D. Capture of CO_2 from Combustion Gases in a Fluidized Bed of CaO. *AIChE J.* **2004**, *50*, 1614.

(2) Lu, D. Y.; Hughes, R. W.; Anthony, E. J. Ca-based sorbent looping combustion for CO_2 capture in pilot-scale dual fluidized beds. *Fuel Process. Technol.* **2008**, *89*, 1386.

(3) Alonso, M.; Rodríguez, N.; González, B.; Grasa, G.; Murillo, R.; Abanades, J. C. Carbon dioxide capture from combustion flue gases with a calcium oxide Chemicals loop. Experimental results and process development. *Int. J. Greenhouse Gas Control* **2010**, *4*, 167.

(4) Charitos, A.; Hawthorne, C.; Bidwe, A. R.; Sivalingam, S.; Schuster, A.; Spliethoff, H.; Scheffknecht, G. Parametric investigation of the calcium looping process for CO_2 capture in a 10 kW_{th} dual fluidized bed. *Int. J. Greenhouse Gas Control* **2010**, *4*, 776.

(5) Rodríguez, N.; Alonso, M.; Abanades, J. C. Experimental investigation of a circulating fluidized-bed reactor to capture CO_2 with CaO. *AIChE J.* **2011**, *57*, 1356.

(6) Charitos, A.; Rodríguez, N.; Hawthorne, C.; Alonso, M.; Zieba, M.; Arias, B.; Kopanakis, G.; Scheffknecht, G.; Abanades, J. C. Experimental validation of the calcium looping CO_2 capture process with two circulating fluidized bed carbonator reactors. *Ind. Eng. Chem. Res.* **2011**, *50*, 9685.

(7) Hawthorne, C.; Dieter, H.; Bidwe, A.; Schuster, A.; Scheffknecht, G.; Unterberger, S.; Käß, M. CO_2 Capture with CaO in a 200 kWth Dual Fluidized Bed Pilot Plant. *Energy Procedia* **2011**, *4*, 441.

(8) Sánchez-Biezma, A.; Ballesteros, J. C.; Diaz, L.; de Zárraga, E.; Álvarez, F. J.; López, J.; Arias, B.; Grasa, G.; Abanades, J. C. Postcombustion CO_2 capture with CaO. Status of the technology and next steps towards large scale demonstration. *Energy Procedia* **2011**, *4*, 852.

(9) Sánchez-Biezma, A.; Díaz, L.; López, J.; Arias, B.; Paniagua, J.; De Zárraga, E.; Álvarez, F. J.; Abanades, J. C. La Pereda CO_2: a 1.7 MW pilot to test post-combustion CO_2 capture with CaO. *21st International Conference on Fluidized Bed Combustion*, Naples, Italy, June 3−6, 2012.

(10) Plötz, S.; Bayrak, A.; Galloy, A.; Kremer, J.; Orth, M.; Wieczorek, M.; Ströhle, J.; Epple, B. First Carbonate Looping Experiments with a 1 MWth Test Facility Consisting of Two Interconnected CFBs. *21st Conference on Fluidized Bed combustion*, Naples, Italy, June 3−6, 2012.

(11) Shimizu, T.; Hirama, T.; Hosoda, H.; Kitani, K.; Inagaki, M.; Tejima, K. A twin fluid-bed reactor for removal of CO_2 from combustion processes. *Trans. Inst. Chem. Eng.* **1999**, *77*, 63.

(12) Romeo, L. M.; Abanades, J. C.; Escosa, J. M.; Paño, J.; Jiménez, A.; Sánchez-Biezma, A.; Ballesteros, J. C. Oxyfuel carbonation/calcination cycle for low cost CO_2 capture in existing power plants. *Energy Conversion Manage.* **2008**, *49*, 2809.

(13) Romano, M. Coal-fired power plant with calcium oxide carbonation for post-combustion CO_2 capture. *Energy Procedia* **2009**, *1*, 1099.

(14) Ströhle, J.; Lasheras, A.; Galloy, A.; Epple, B. Simulation of the carbonate looping process for post-combustion CO_2 capture from a coal-fired power plant. *Chem. Eng. Technol.* **2009**, *32*, 435.

(15) Yongping, Y.; Rongrong, Z.; Liqiang, D.; Kavosh, M.; Patchigolla, K.; Oakey, J. Integration and evaluation of a power plant with a CaO-based CO_2 capture system. *Int. J. Greenhouse Gas Control* **2010**, *4*, 603.

(16) Martínez, I.; Murillo, R.; Grasa, G.; Abanades, J. C. Integration of Ca looping system for CO_2 capture in existing power plants. *AIChE J.* **2010**, *57*, 2599.

(17) Anthony, E. J.; Granatstein, D. L. Sulfation phenomena in fluidized bed combustion systems. *Prog. Energy Combust. Sci.* **2001**, *27*, 215.

(18) Li, Y.; Buchi, S.; Grace, J. R.; Lim, C. J. SO_2 removal and CO_2 capture by limestone resulting from calcination/sulfation/carbonation cycles. *Energy Fuels* **2005**, *19*, 1927.

(19) Ryu, H.-J.; Grace, J. R.; Lim, C. J. Simultaneous CO_2/SO_2 capture characteristics of three limestones in a fluidized-bed reactor. *Energy Fuels* **2006**, *20*, 1621.
(20) Grasa, G. S.; Alonso, M.; Abanades, J. C. Sulfation in a carbonation/calcination loop to capture CO_2. *Ind. Eng. Chem. Res.* **2008**, *47*, 1630.
(21) Sun, P.; Grace, J. R.; Lim, C. J.; Anthony, E. J. Removal of CO_2 by calcium-based sorbents in presence of SO_2. *Energy Fuel* **2007**, *21*, 163.
(22) Manovic, V.; Anthony, E. J. Sequential SO_2/CO_2 capture enhanced by steam reactivation of CaO-based sorbent. *Fuel* **2008**, *87*, 1564.
(23) Manovic, V.; Anthony, E. J.; Loncarevic, D. SO_2 retention by CaO-based sorbent spent in CO_2 looping cycles. *Ind. Eng. Chem. Res.* **2009**, *48*, 6617.
(24) Pacciani, R.; Müller, C. R.; Davidson, J. F.; Dennis, J. S.; Hayhurst, A. N. Performance of novel synthetic Ca-based sorbent suitable for desulfurizing flue gases in a fluidized bed. *Ind. Eng. Chem. Res.* **2009**, *48*, 7016.
(25) Manovic, M.; Anthony, E. J. Competition of sulphation and carbonation reactions during looping cycles for CO_2 capture by CaO-based sorbents. *J. Phys. Chem. A* **2010**, *114*, 3397.
(26) Abanades, J. C.; Rubin, E. S.; Anthony, E. J. Sorbent cost and performance in CO_2 capture systems. *Ind. Eng. Chem. Res.* **2004**, *43*, 3462.
(27) Dean, C. C.; Blamey, J.; Florin, N. H.; Al-Jeboori, M. J.; Fennell, P. S. The calcium looping cycle for CO_2 capture from power generation, cement manufacture and hydrogen production. *Chem. Eng. Res. Des.* **2011**, *89*, 836.
(28) Dean, C. C.; Dugwell, D.; Fennell, P. S. Investigation into potential synergy between power generation, cement manufacture and CO_2 abatement using the calcium looping cycle. *Energy Environ. Sci.* **2011**, *4*, 2050.
(29) Jia, L.; Hughes, R.; Lu, D.; Anthony, E. J.; Lau, I. Attrition of calcining limestones in circulating fluidized-bed systems. *Ind. Eng. Chem. Res.* **2007**, *46*, 5199.
(30) Coppola, A.; Montagnaro, F.; Salatino, P.; Scala, F. Fluidized bed calcium looping: The effect of SO_2 on sorbent attrition and CO_2 capture capacity. *Chem. Eng. J.* **2012**, *207−208*, 445.
(31) Alonso, M.; Rodríguez, N.; Grasa, G.; Abanades, J. C. Modelling of a fluidized bed carbonator reactor to capture CO_2. *Chem. Eng. Sci.* **2009**, *64*, 883.
(32) Arias, B.; Cordero, J. M.; Alonso, M.; Abanades, J. C. Sulfation Rates of Cycled CaO Particles in the Carbonator of a Ca-Looping Cycle for Postcombustion CO_2 Capture. *AIChE J.* **2012**, *58*, 2262.
(33) Hu, G.; Dam-Johansen, K.; Wedel, S.; Hansen, J. P. Review of the direct sulfation reaction of limestone. *Prog. Energy Combust. Sci.* **2006**, *32*, 386.

4.6.3 Publicación III

Sulfation Rates of Particles in Calcium Looping Reactors

Publicado en:

Chemical Engineering & Technology

Volumen 37

Año 2014

Índice de Impacto: 2.175

Chemical Engineering & Technology

Mónica Alonso
José M. Cordero
Borja Arias
Juan C. Abanades

CSIC-INCAR, Oviedo, Spain.

Review

Sulfation Rates of Particles in Calcium Looping Reactors

The sulfation reaction rate of CaO particles in three reactors comprising a post-combustion calcium looping system is discussed: a combustion chamber generating flue gases, a carbonator reactor to capture CO_2 and SO_2, and an oxy-fired calciner to regenerate the CO_2 sorbent. Due to its strong impact on the pore size distribution of CaO particles, the number of carbonation/calcination cycles arises as a new important variable to understand sulfation phenomena. Sulfation patterns change as a result of particle cycling, becoming more homogeneous with higher number of cycles. Experimental results from thermogravimetric tests demonstrate that high sulfation rates can be measured under all conditions tested, indicating that the calcium looping systems will be extremely efficient in SO_2 capture.

Keywords: Calcium looping, CO_2 capture, Fluidized bed, Limestone, SO_2 capture

Received: November 12, 2012; *revised:* September 06, 2013; *accepted:* October 29, 2013

DOI: 10.1002/ceat.201200614

1 Introduction

Post-combustion calcium looping (CaL) systems are increasingly applied in different pilots in Europe and elsewhere [1]. The largest one is a 1.7-MW_{th} pilot successfully running under the EU project CaOling [2, 3], another 1-MW_{th} pilot is operated in Darmstadt [4]. Valuable experience has been gained in recent years in laboratory-scale units [5] operating in continuous mode. In a post-combustion CaL system, the CO_2 from the flue gas is captured by CaO in a circulating fluidized bed (CFB) carbonator reactor at temperatures between 600 °C and 700 °C. The partially carbonated sorbent regeneration takes place in the calciner reactor where oxycombustion at temperatures above 900 °C is required [6]. The energy penalty associated with this process is low because the high operating temperatures allow for efficient heat integration.

Another advantage of CaL compared with other post-combustion technologies is the tolerance to the SO_2 concentration in the flue gas. This is due to the presence of a very effective desulfurization agent, i.e., calcined limestone, in all the reactors. At the temperatures and atmospheres typical for CaL systems, $CaSO_4$ is formed irreversibly, at the expense of a certain deactivation of CaO for CO_2 capture. A mass balance of a CaL system as indicated in Fig. 1 reveals that the conversion of CaO to $CaSO_4$ in the purge stream is expected to be well below 5 mol % at CO_2 carrying capacities higher than 0.1 when using natural limestones [7]. This low conversion has important implications for the debate of the sulfur effect in CaL systems as this is below the limit of conversion to achieve extensive pore plugging typically found in highly sulfated particles in other circulating fluidized bed combustion (CFBC) environments. Moreover, the characteristic open structure of cycled CaO particles in a CaL system proved to have a positive impact on sorbent utilization during standard sulfation in CFBCs [8–13].

Sulfation of CaO particles in CFBC boilers is an extensively studied reaction [14]. In the absence of pore diffusion resistance, kinetic studies on this reaction [15, 16] established that the reactivity of CaO increases with internal surface area. The overall reaction rate is controlled by the chemical reaction at low conversions and then by the gas diffusion through the $CaSO_4$ layer formed over the CaO that increases with higher sulfation conversion. The reduction in porosity as the reaction proceeds, leads to an incomplete conversion of CaO. The reaction order ranges from 0.6 to 1 [17–20]. It is generally accepted that there are three patterns of sulfation depending on the particle size, morphology, and microstructure of the calcined limestones [21]: unreacted core, network, and uniform. The unreacted core pattern is typical in calcined limestone with large particle size, medium-sized grains, and small micropores. The network pattern is characteristic of calcined limestone particles where there is an interconnected network of microfractures. Finally, the uniform pattern is developed in particles with small grains and small micropores as well as large grains with large micropores, macropores, and fractures.

Several mathematical models have been developed to describe the structure evolution and pore plugging processes under different conditions and for different sorbents [16–18,

Correspondence: Dr. Mónica Alonso (mac@incar.csic.es), CSIC-INCAR, Francisco Pintado Fe 26, 33011 Oviedo, Spain.

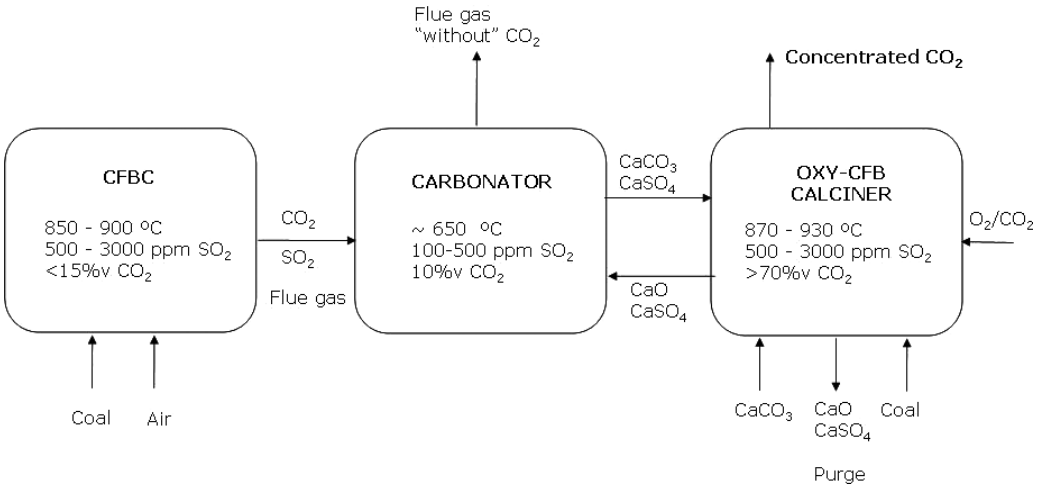

Figure 1. General scheme for a CaL system and relevant sulfation conditions when the reference power plant is an air-fired CFBC.

22–25]. Basically, they are classified into grain models and pore models. Grain models are based on the assumption that the particles are constituted by a matrix of small grains, usually spherical. The pore models are founded on the assumption that the particles are a network of randomly intersecting cylindrical pores. The models increase in complexity when diffusion phenomena of the reactants through the plugged pores are taken into account. Ideally, model parameters at particle level derived from a small laboratory-scale test should be retained when solving reactor models at large scale. However, these model parameters are known to be very sensitive to limestone type and operating conditions during the test and there is no consensus on a methodology to estimate reliable sulfation parameters from lab-scale measurements.

There are recent indications [26] that most of the existing published results on sulfation of CaO may be flawed by the lack of steam during the sulfation test in small laboratory equipment. Stewart et al. [26] found a very strong effect of H_2O (v) on the progress of sulfation particles that leads to an increase of 45 % in sulfation conversions after 10 h of reaction when steam is present in the simulated flue gas. They noted that most of the published papers on sulfation phenomena have ignored this strong effect of steam on sulfation, despite steam being present in all natural combustion flue gases. Particles circulating between carbonator and calciner (Fig. 1) should be less affected by the presence of steam, as the large make-up flow of limestone ensures residence times and average sulfation conversions much lower than those typical in the CFBC. However, the steam effect on CaL systems will require future investigations outside the scope of the present review. Therefore, the aim is to summarize the information available on the sulfation rate of CaO particles at relevant conditions in the carbonator and calciner reactors of a CaL system and discuss the use of CaO purges from the CaL systems as a SO_2 sorbent feed to the CFBC power plant of the system of Fig. 1.

2 SO_2 Capture in the CaL Carbonator

The CaL carbonator operates at optimum temperatures for CO_2 capture between 600 °C and 700 °C which is in principle not ideal for the sulfation reaction. Two competitive reactions can take place simultaneously when a flue gas containing SO_2 is fed to a CaL carbonator of Fig. 1: the CO_2 and the SO_2 capture by the CaO. It is well-known that the maximum CaO conversion to $CaCO_3$ decreases with the number of carbonation/calcination cycles due to a sintering mechanism that reduces the specific surface area when the number of cycles increases. Some of the early works on sulfation in CaL systems [9, 10, 13, 27] have reported the accelerated decay in CO_2 carrying capacity when SO_2 is present in the flue gas because the irreversible formation of a $CaSO_4$ product layer on the free surface available for the carbonation reaction. However, it has to be noted that Ca/CO_2 ratios between 10 and 20 have been confirmed in continuous pilots [5, 28] as an optimum target to run the CO_2 capture system. The presence of SO_2 will require higher make-up flow ratios to maintain these Ca/CO_2 ratios in the CO_2 capture loop. Since the SO_2 partial pressure in the flue gas coming from the existing CFBC power plant will be between two and three orders of magnitude lower than the CO_2 concentration, this means that the Ca/S ratio to the carbonator will always be a very large number for the CaL carbonator reactor and that sulfation levels of CaO particles in the system of Fig. 1 will not exceed a few points of Ca conversion. This fact has to be taken into account when measuring sulfation rates in small lab equipment to derive reaction rate parameters.

Recently, a kinetic study on sulfation of cycled CaO particles at CaL carbonator conditions has been published [29], testing in a thermogravimetric apparatus three limestones with particle sizes of 63–100 μm. Although the three calcined limestones (one calcination) exhibited different sulfation patterns under the conditions of the carbonator, when the cycle number

increases up to 50 cycles, the behavior of all of them becomes quite similar (Fig. 2). This indicates again the strong effect of the number of carbonation/calcination cycles on the pore structure of CaO particles. Under these reaction conditions, the sulfation reaction seems to be chemically controlled below sulfation conversion of 0.1 and then a second stage controlled by the effective diffusion of SO_2 through the product layer takes place [29]. It was observed that the transition between both stages is around 5 min irrespective of the cycle number. After 50 carbonation/calcination cycles, there is a smoother transition between fast and slow reaction regimes for all limestones. This sulfation behavior might be expected in view of the evolution of the sorbent surface toward a more opened texture [10, 13, 29–31] where the pore blockage mechanism should become increasingly negligible.

A pseudo-first-order reaction for the fresh calcined limestones as well as for highly cycled CaO particles was reported to fit sufficiently well the available data, using the random pore model (RPM) [32] following the same procedure as used in previous works [33, 34] to derive model parameters. The reaction parameters k_s and D in the RPM were calculated for each cycle, except those corresponding to the fresh calcined limestone where the pore plugging mechanism distorted the fitting quality (see Fig. 2). The average value of k_s varies between 4.32×10^{-9} and 5.63×10^{-9} $m^4 mol^{-1} s^{-1}$ whereas the average value of D ranges between 2.41×10^{-12} and 4.88×10^{-12} $m^2 s^{-1}$. These values are in agreement with those found by Bathia and Perlmutter [17] for fresh calcined sorbents at temperatures of 650 °C. The transition between the chemically controlled regime and the diffusion-controlled regime was confirmed to occur at a conversion to $CaSO_4$ of 0.1. For CaO particles cycled more than 20 times, model predictions and experimental data are in good agreement. An average $CaSO_4$ thickness layer of 8.5 nm was calculated from the CaO conversion at which the transition between chemically and diffusion-controlled regime is observed.

Under CaL conditions where low CaO conversions (less than 0.05) will be expected, the sulfation reaction is chemically controlled in the carbonator, and extremely high SO_2 capture efficiencies should be expected in view of these reaction rates, the large Ca/S ratios in the carbonator, and the typically large bed inventories of CaO required in the carbonator to achieve high CO_2 capture efficiencies. Future work should test these parameters in the presence of steam that can only make these reactions rates even faster [26].

3 SO_2 Capture in the CaL Calciner

The CaL calciner is an oxy-fired CFBC combustor characterized by high CO_2 concentrations (higher than 60 vol %) and temperatures around 900 °C in order to promote calcination of the $CaCO_3$ formed in the carbonator. In recent years, only a few published works analyzed the sulfation under oxy-fuel combustion conditions [35–38], but most of them are related to noncalcining conditions. As in the case of the CFBCs, none of these studies take into account the effect of the carbonation/calcination cycle number. Moreover, the quantitative information on reaction rates is very limited. Within the CaOling project [2], we are currently investigating the effect of the number of carbonation/calcination cycles, particle size, and the SO_2 concentration on sulfation. Two limestones have been used, and for the same particle size employed in the CaL carbonator studies referred above [32], the final conversion to $CaSO_4$ and the initial slope of the sulfation curves were reduced as the number of cycles decreased. This is in contrast with the reported improvement in final sulfation discussed in previous paragraphs as a result of pore opening along cycling.

Experiments with different particle sizes were carried out: 36–63 μm, 63–100 μm, 100–200 μm, and 400–600 μm. For Compostilla limestone it was found that under these conditions the initial sulfation rates are very similar for all particle sizes at the same number of cycles. Therefore, the sulfation pattern must be homogeneous or network-type [21]. In contrast, for fresh calcined Enguera limestone the sulfation rate and the final conversion to $CaSO_4$ decrease when the particle diameter increases, as revealed in Fig. 3. This is a clear indication of the unreacted core sulfation pattern. When this second limestone is cycled 50 times, it is evident (Fig. 3 b) that the initial sulfation rate is very similar for the three smaller particle sizes, and final conversion to $CaSO_4$ decreases with the particle size at longer times. These results are consistent with recent findings from García-Labiano et al. [38], who studied the particle size effect under oxy-fuel conditions for fresh calcined limestones. Also consistent with their results is that CO_2 concentration did not exert any influence on the initial sulfation rate or final conversion to $CaSO_4$.

In order to find suitable reaction rate parameters, we are applying the RPM model again to fit reaction rate data at high number of cycles with the SO_2 concentration varying in this case between 500 and 3000 ppmv to account for different coal qualities possible in the CaL calciner. The sulfation rate follows apparently a first-order reaction, and the preliminary rate parameters, refer-

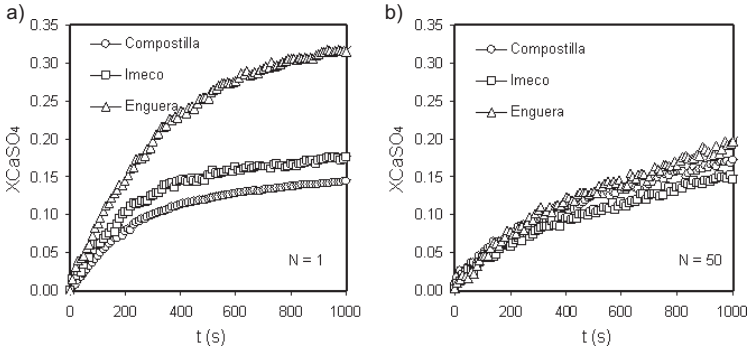

Figure 2. Sulfation conversion at carbonator conditions for three limestones. (a) After one calcination; (b) after 50 carbonation/calcination cycles. Reproduced from Arias et al. [29].

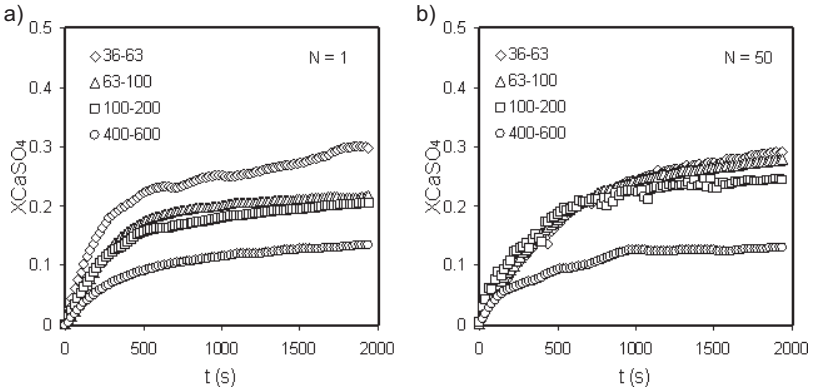

Figure 3. Sulfation conversion as a function of time for Enguera limestone at different particle sizes. (a) After one calcination; (b) after 50 carbonation/calcination cycles at 930 °C, 500 ppmv SO_2, 70 vol % CO_2, and ~ 5 vol % oxygen content.

ring to low sulfation conversions and specific surface areas characteristic in the CaL particles, do not differ much from those observed for standard sulfation conditions at 850 °C.

The high sulfation rates measured with highly cycled CaO particles indicate that post-combustion CaL system reactors will be effective reactors for SO_2 capture from flue gases. Fig. 4 compares the two limestones (calcined-carbonated 50 times) used in this study under the conditions of the three reactors of Fig. 1. The results presented in Fig. 4 exhibit an increase in the reaction rate with higher temperatures for the initial times as it would be expected. However, for longer times, the final conversion to $CaSO_4$ is higher at 850 °C than at 930 °C for both limestones. The optimum temperature conditions for sulfation of highly cycled particles are still around 850 °C as it is the case for most limestones calcined (once) in a CFBC. The open pore network characterics of highly cycled particles leads to pseudo-homogeneous sulfation patterns even when the first calcination follows a core-shell pattern.

4 Conclusions

A review on the sulfation of CaO under relevant conditions in the reactors of a CaL system reveals that

- the number of carbonation/calcination cycles affects the sulfation pattern, becoming more homogeneous with higher N. No core-shell pattern has been detected for $N > 2$ even when limestones follow such a pattern when $N = 1$ for particle sizes below 200 µm;
- the apparent order of the sulfation reaction is close to unity for both carbonator and calciner reactors;
- the CO_2 concentration does not affect the sulfation rates for highly cycled particles and particle diameters below 200 µm;
- the high sulfation rates measured for the cycled CaO particles indicate that the post-combustion CaL system would be effective for capturing SO_2 from flue gases. This can only improve if recent reports on the effect of H_2O (v) on sulfation are confirmed for the fast early stages of this reaction.

Acknowledgment

This work is partially funded by the European Commission (FP7-CaOling project). J. M. Cordero also acknowledges a FYCIT fellowship.

The authors have declared no conflict of interest.

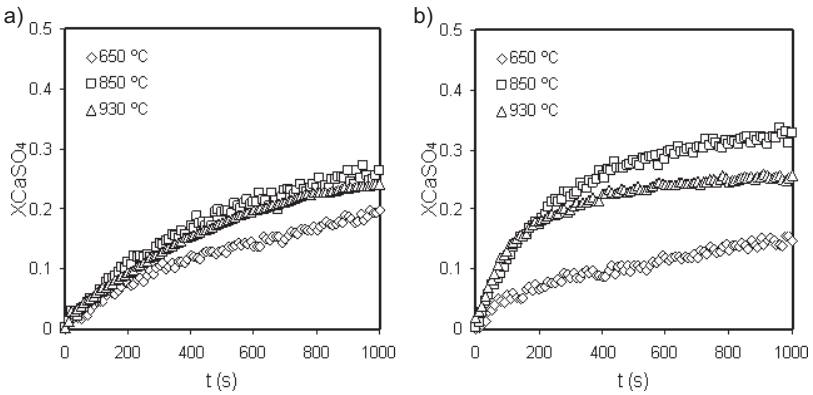

Figure 4. Sulfation conversion as a function of time after 50 carbonation/calcination cycles at different temperatures of sulfation. (a) Enguera limestone; (b) Compostilla limestone. Conditions: 2000 ppmv SO_2 (balance air), particle size 63–100 µm.

References

[1] C. C. Dean, J. Blamey, N. H. Florin, M. J. Al-Jeboory, P. S. Fennell, *Chem. Eng. Res. Des.* **2011**, *89 (6A)*, 836.

[2] *Development of Postcombustion CO_2 Capture with CaO in a Large Testing Facility*. www.caoling.eu

[3] A. Sánchez-Biezma, L. Diaz, J. López, B. Arias, J. Paniagua, E. De Zarraga, J. Alvarez, J. C. Abanades, *Proc. of the 21st Int. Conf. on Fluidized Bed Combustion*, Enzo Albano Editore, Naples **2012**.

[4] A. Galloy, J. Ströhle, B. Epple, *VGB PowerTech.* **2011**, *91 (6)*, 64.

[5] A. Charitos, N. Rodriguez, C. Hawthorne, M. Alonso, M. Zieba, B. Arias, G. Kopanakis, G. Scheffknecht, J. C. Abanades, *Ind. Eng. Chem. Res.* **2011**, *50 (16)*, 9685.

[6] T. Shimizu, T. Hirama, H. Hosoda, K. Kitano, M. Inagaki, K. Tejima, *Chem. Eng. Res. Des.* **1999**, *77 (1)*, 62.

[7] J. C. Abanades, E. J. Anthony, J. S. Wang, J. E. Oakey, *Environ. Sci. Technol.* **2005**, *39 (8)*, 2861.

[8] Y. Li, S. Buchi, J. R. Grace, C. J. Lim, *Energy Fuels* **2005**, *19 (5)*, 1927.

[9] H. J. Ryu, J. R. Grace, C. J. Lim, *Energy Fuels* **2006**, *20 (4)*, 1621.

[10] G. S. Grasa, M. Alonso, J. C. Abanades, *Ind. Eng. Chem. Res.* **2008**, *47 (5)*, 1630.

[11] V. Manovic, E. J. Anthony, D. Loncarevic, *Ind. Eng. Chem. Res.* **2009**, *48 (14)*, 6627.

[12] R. Pacciani, C. R. Muller, J. F. Davidson, J. S. Dennis, A. N. Hayhurst, *Ind. Eng. Chem. Res.* **2009**, *48 (15)*, 7016.

[13] V. Manovic, E. J. Anthony, *J. Phys. Chem. A* **2010**, *114 (11)*, 3997.

[14] E. J. Anthony, D. L. Granatstein, *Prog. Energy Combust. Sci.* **2001**, *27 (2)*, 215.

[15] R. H. Borgwardt, *Environ. Sci. Technol.* **1970**, *4 (1)*, 59.

[16] M. Hartman, R. W. Coughlin, *Ind. Eng. Chem. Process Des. Dev.* **1974**, *13 (3)*, 248.

[17] S. K. Bhatia, D. D. Perlmutter, *AIChE J.* **1981**, *27 (2)*, 226.

[18] R. H. Borgwardt, K. R. Bruce, J. Blake, *Ind. Eng. Chem. Res.* **1987**, *26 (10)*, 1993.

[19] R. L. Pigford, G. Sliger, *Ind. Eng. Chem. Process Des. Dev.* **1973**, *12 (1)*, 85.

[20] J. Adanez, P. Gayan, F. Garcia-Labiano, *Ind. Eng. Chem. Res.* **1996**, *35 (7)*, 2190.

[21] K. Laursen, W. Duo, J. R. Grace, J. Lim, *Fuel* **2000**, *79 (2)*, 153.

[22] C. Georgakis, C. W. Chang, J. Szekely, *Chem. Eng. Sci.* **1979**, *34 (8)*, 1072.

[23] R. H. Borgwardt, K. R. Bruce, *AIChE J.* **1986**, *32 (2)*, 239.

[24] J. S. Dennis, A. N. Hayhurst, *Chem. Eng. Sci.* **1990**, *45 (5)*, 1175.

[25] J. Adanez, F. Garcia-Labiano, V. Fierro, *Chem. Eng. Sci.* **2000**, *55 (18)*, 3665.

[26] M. C. Stewart, V. Manovic, E. J. Anthony, A. Macchi, *Environ. Sci. Technol.* **2010**, *44 (22)*, 8781.

[27] P. Sun, J. R. Grace, C. J. Lim, E. J. Anthony, *Energy Fuels* **2007**, *21 (1)*, 163.

[28] N. Rodriguez, M. Alonso, J. C. Abanades, *AIChE J.* **2011**, *57 (5)*, 1356.

[29] B. Arias, J. M. Cordero, M. Alonso, J. C. Abanades, *AIChE J.* **2012**, *58 (7)*, 2262.

[30] D. Alvarez, J. C. Abanades, *Ind. Eng. Chem. Res.* **2005**, *44 (15)*, 5608.

[31] J. C. Abanades, D. Alvarez, *Energy Fuels* **2003**, *17 (2)*, 308.

[32] S. K. Bhatia, D. D. Perlmutter, *AIChE J.* **1980**, *26 (3)*, 379.

[33] G. Grasa, R. Murillo, M. Alonso, J. C. Abanades, *AIChE J.* **2009**, *55 (5)*, 1246.

[34] B. Arias, J. C. Abanades, G. S. Grasa, *Chem. Eng. J.* **2011**, *167 (1)*, 255.

[35] M. Rahmani, M. Sohrabi, *Chem. Eng. Technol.* **2006**, *29 (12)*, 1496.

[36] H. Liu, S. Katagiri, U. Kaneko, K. Okazaki, *Fuel* **2000**, *79 (8)*, 945.

[37] C. M. Chen, C. S. Zhao, *Ind. Eng. Chem. Res.* **2006**, *45 (14)*, 5078.

[38] F. Garcia-Labiano, A. Rufas, L. F. de Diego, M. de las Obras-Loscertales, P. Gayan, A. Abad, J. Adanez, *Fuel* **2011**, *90 (10)*, 3100.

4.6.4 Publicación IV

Modeling of the kinetics of sulphation of CaO Particles under CaL Reactor Conditions

Enviado a:

Chemical Engineering Journal

Índice de Impacto: 4.181

Modeling of the kinetics of sulphation of CaO particles under CaL reactor conditions

J.M. Cordero[a], *M. Alonso*[b]*

Instituto Nacional del Carbón, CSIC, C/Francisco Pintado Fe, No. 26, 33011 Oviedo, Spain

*Corresponding author, mac@incar.csic.es

ABSTRACT

CO_2 capture in a calcium looping (CaL) system is one of the most promising technologies for climate change mitigation. The main reactors in these systems (carbonator and calciner) operate in conditions where the reaction of CaO with the SO_2 resulting from the combustion of coal is inevitable. It has also been suggested that the CaO-rich purges from CaL could serve as effective SO_2 sorbents in fluidized bed combustor power plants (CFBC). This work reports on the sulphation of CaO under a range of variables that are typical of reactors in CaL systems. Furthermore it is demonstrated that the number of calcination carbonation cycles changes the sulphation patterns of the CaO from heterogeneous to homogeneous in all the limestones tested. For 50 carbonation calcination cycles and for particle sizes below 200 μm, the sulphation pattern is in all cases homogeneous. The sulphation rates were found to be first order with respect to SO_2, and zero with respect to CO_2. Steam was observed to have a positive effect only in the diffusion through

the product layer controlled regime, as it leads to an improvement in the sulfation rates and effectiveness of the sorbent. Most of the experimental results of sulfation of highly cycled sorbents under all conditions can be fitted by means of the Random Pore Model (RPM) assuming that the kinetics and diffusion through the product layer of the $CaSO_4$ are the controlling regimes.

Keywords: sulphation kinetics, SO_2 capture, calcium looping, CO_2 capture, RPM, CFB

1. Introduction

CO_2 capture and storage is one of the best options for mitigating CO_2 emissions to the atmosphere and climate change [1]. Among the technologies developed, the post-combustion calcium looping (CaL) system is one of the most promising due to the economic benefits it offers and experience acquired with similar systems already operating at industrial scale [2-7]). One of the main advantages of these emerging CaL technologies is the low cost of the sorbent since natural limestone is used as the preferred source of CaO. A full post-combustion CaL system consists of two circulating fluidized bed reactors (CFB). One of them is the carbonator, which operates at around 650 °C. In this reactor the flue gas from an existing power plant comes into contact with CaO particles, causing a reaction that yields $CaCO_3$. The $CaCO_3$ then goes to a second CFB reactor, the calciner which operates at temperatures of around 900 °C, where the $CaCO_3$ is calcined, producing a highly concentrated stream of CO_2 [2]. In order to achieve calcination conditions, the oxy-fuel combustion of coal is conducted in this reactor. The high temperatures at which both the CFB carbonator and CFB calciner operate allow efficient heat integration by generating different

streams of solids and gases at high temperatures. The rapid development of this technology can be attributed to its similarity to existing CFBC power plants.

The viability of this technology has been demonstrated in several pilot plants including La Pereda (Spain) which produces 1.7 MWth and is the largest CaL for CO_2 capture installed so far [8, 9]. Other pilots that have achieved promising results are the 1 MWth pilot plant in Darmstadt (Germany) [10], the 0.3 MWth pilot in La Robla [11], the 0.2 MWth pilot at Stuttgart University (Germany) [12] and the 1.9 MWth pilot that is being constructed in Taiwan [13], apart from smaller projects that have also reported positive results [14-16].

Figure 1 represents one of the possible configurations of a CaL system for capturing CO_2 consisting of three main reactors functioning as CFBs (including in this diagram the CFBC power plant as the source of flue gases).

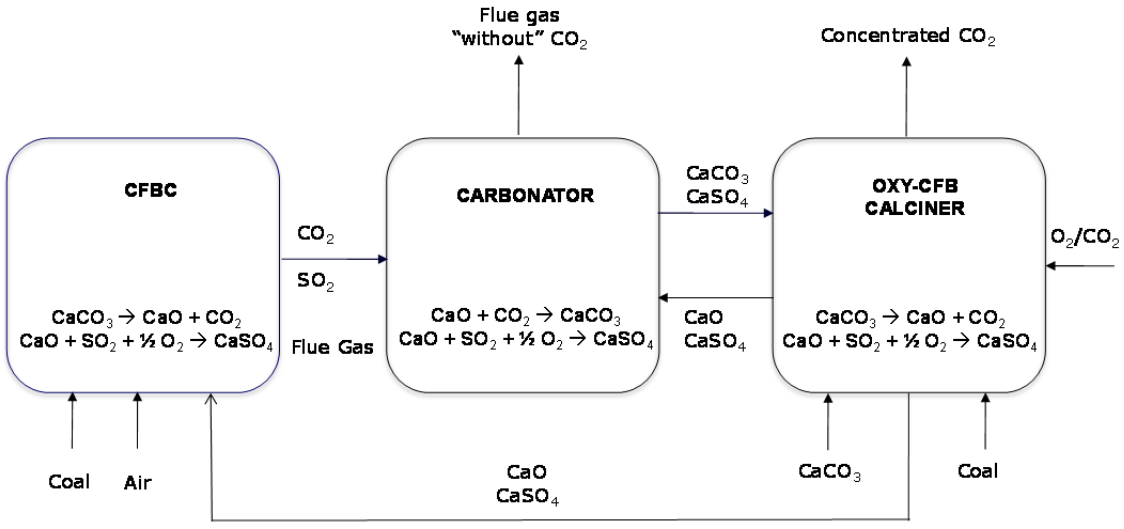

Figure 1. Principal reactors of a CaL system integrated with a CFBC and its main variables.

In the schematic of Figure 1, coal is burned in air in the CFBC, generating a stream of gases that is fed to the CFB carbonator. It is here that CO_2 capture takes place since the CaO reacts with CO_2 to form $CaCO_3$. The carbonated solids then enter the CFB calciner, where CaO is regenerated to form a rich CO_2 atmosphere typical of oxy combustion. A synergy can be exploited in this scheme if the purge extracted from the CaL CO_2 capture system is injected into the CFBC to be used as a calcium support in substitution for the fresh limestone that is routinely used for desulfurization [17-19]. A recent paper [20] illustrates with mass and energy balances the operational and fuel composition windows that make this synergy possible. SO_2 is produced in the CFBC as well as in the oxy CFB calciner due to the combustion of coal. It can also enter into the CFB carbonator depending on the power plant's SO_2 removal efficiency. Under the operating conditions of all three main CFB reactors, SO_2 will react with CaO to form $CaSO_4$ which will not decompose at these working temperatures due to its thermodynamic equilibrium. Furthermore, a certain quantity of $CaSO_4$ in the CaL system is guaranteed depending on the amount of fresh makeup limestone and purge. Therefore, SO_2 will deactivate the CaO available for CO_2 capture [21-23]. The deactivation would be enhanced if methods of reactivation like recarbonation [24] or hydration [25] were used to reduce the make-up.

There is a large background of literature on the sulphation of CaO particles under combustion conditions [26-39]. However, there are several novel features in the CaL system of Figure 1 that have not yet been sufficiently dealt with in the literature. The main novelty is that the particles of a CaL undergo a certain number of calcination carbonation cycles that promote a sintering mechanism characterized by a widening of the pores and a reduction of the surface area [40]. This effect could lead to an enhancement

of SO_2 capture as there is more effective space available for housing the $CaSO_4$ formed, leading to higher CaO conversions [26, 41]. Another difference is related to the operating temperatures of the system schematized in Figure 1. These can vary from 650 °C in the CFB carbonator to 930 °C in the oxy CFB calciner, whereas most sulphation studies are conducted at temperatures of around 850 ºC (the typical temperature in CFBC power plants). The reaction atmosphere also varies from one reactor to another: in CFBCs an average CO_2 concentration of 10% vol. is usual whereas a CO_2 concentration higher than 70 % vol. is to be expected in an oxy-fired CFB calciner. Finally, the conversions of CaO to $CaSO_4$ predicted by the mass balance applied to the CaL system will not exceed 0.1 due to the Ca/S ratio in these systems is larger than in a desulfuration system. This will avoid the extensive pore blockage typical of sulphation in FB combustors, where the aim is to ensure maximum sorbent conversion for sulphation to occur.

The sulphation of CaO has been extensively investigated using many limestones, particle sizes and reaction conditions. Consequently several authors have developed particle sulfation models with the objective of integrating them into larger reactor models. These particle models can be basically divided into two types: grain and pore models. The original grain models assumed that particles are formed by smaller blocks called grains (sometimes referred to as micro grains) [29, 42]. These grains are assumed to be of uniform size, spherically shaped and non-porous. The reaction follows the shrinking core model and no structural changes are taken into consideration. The regimes that usually control the reaction are diffusional in the gas phase or diffusional and kinetic combined, or diffusional through the product layer formed around the grains [29, 34, 43, 44]. Later, the grain models evolved, taking into consideration other grain or micro-grain geometries such as cylindrical or flat [42, 45], structural changes in the grains [31, 46-49], and grain size distribution [45, 50].

The initial pore models assumed that the particles were traversed by pores that are usually cylindrically shaped. These pores were supposedly of uniform size and randomly intersected [51, 52]. This type of model developed taking into account the initial pore structure and its transformation as the reaction proceeds. The pore structure in this model was explained in terms of the evolution of the pore size distribution. Simons et al. [53] assumed that the distribution is like a complex tree where the pore size decreases the further inside the particle the pore is. One of the most widely used pore models is the model developed by Bhatia and Perlmutter [54, 55]: the random pore model (RPM), which assumes that the particle is traversed by random size cylindrical pores with intersecting and overlapping surfaces as reaction proceeds. This model was applied successfully to gas solid reactions [56] including the carbonation and sulphation of CaO [33, 56-59].

The present work focuses on the modelling of the sulphation rates and retention capacities of CaO in the three main reactors involved in CaL, taking into account the special features of these systems and the fact that the sorbent is composed of particles with a specific number of cycles.

2. Experimental

Three different limestones with particle sizes of 36-63 μm, 63-100 μm, 100-200 μm and 400-600 μm were used to study the sulphation reaction of the CaO particles under different conditions. Their chemical composition is shown in Table 1.

Table 1. Chemical composition (wt %) of the limestones used in this work

	Al_2O_3	CaO	Fe_2O_3	K_2O	MgO	Na_2O	SiO_2	TiO_2
Compostilla	0.16	89.7	2.5	0.46	0.76	<0.01	0.07	0.37
Enguera	0.18	98.9	<0.01	0.03	0.62	0.00	0.43	0.02
Brecal	0.00	98.4	0.10	0.00	0.78	0.00	0.69	0.00

Enguera and Brecal are high purity limestones from the point of view of composition in CaO (close to 100% w. on a calcined basis). Compostilla is the limestone of lowest purity, with a CaO composition of 89.7 % w. This limestone also contains a high amount of impurities, the most prominent of which are Fe_2O_3, K_2O and TiO_2.

For the sulphation tests, the thermogravimetric analyzer system illustrated in Figure 2a was used. It consists of a microbalance from CI Instruments, which continuously measures the weight of the sample suspended on a flat platinum pan inside a quartz tube. A special characteristic of its design is the two-zone furnace that can be moved up and down by means of a pneumatic piston. This allows a rapid change between carbonating and calcining temperatures when performing calcination carbonation cycles. The movement of the piston can be synchronized with changes in the gas fed to the TGA by means of mass flow controllers. The temperature of the sample is measured with a thermocouple located very close to the platinum basket and is continuously recorded, as is the weight of the sample by a computer.

In the experimental procedure employed in this study before the sulphation tests the sample was subjected to the desired number of calcination carbonation cycles. The carbonation of the samples was carried out in an

atmosphere of 10% vol. CO_2 in air, at 650 °C, and the calcination was conducted in air at 930 °C (a blank test confirmed that the use of pure CO_2 is unnecessary during calcination to obtain a specific texture linked to a certain cycle number). Each stage of calcination or carbonation was 10 minutes long as the kinetics of these reactions were not the subject of this study. Finally, after the temperature had stabilized, the sulphation stage was initiated. A preliminary study was conducted in order to avoid external diffusional effects. The superficial gas velocity was set at 0.06 m/s (650 °C) for both the sulphation and carbonation reactions since experiments performed at half of this superficial gas velocity had no effect on the rates measured. It is well known that the initial sample mass influences the external diffusional effects. A sample mass of 2-3 mg was small enough to neutralise the diffusional effects as no appreciable changes were detected in the initial sulphation rate, as can be seen in Figure 2b. The conversion of CaO to $CaSO_4$ was calculated from the weight gain of the samples.

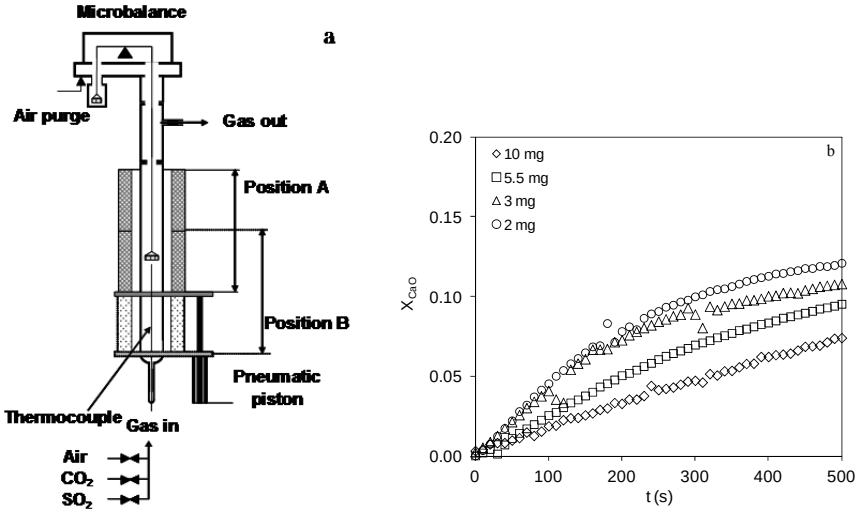

Figure 2. Schematic of the experimental setup used in this work (a). Effect of the initial sample mass on the experimental sulphation rate (b); particles of 63-100 µm, 500 ppmv SO_2 in air, 650 °C, with sulphation occurring after only one calcination (N = 1).

In order to obtain the initial pore parameters of the materials shown in Table 2, a mercury porosimeter Autopore IV 9500 by Micromeritics was used. The samples were previously calcined in a furnace in air at 930 °C. All the sorbents were mesoporous, with the average pore size ranging from 33 to 40.7 nm. The measured porosities indicate that all the sorbents underwent shrinkage during calcination. It was this shrinkage that gave place to a maximum sulphation conversion in the interior of the particles of 0.32 to 0.39, as calculated from the mass balance equation (1) [33]:

$$X^{*}_{CaO} = \frac{\varepsilon_0}{(1-\varepsilon_0)(Z-1)} \qquad (1)$$

Some samples were selected to examine the $CaSO_4$ distribution in the particles. For this purpose a Quanta FEG 650 scanning electron microscope (SEM) coupled to an energy dispersive X ray (EDX) analyser Ametek EDAX equipped with an Apollo X detector was used. The samples were embedded in a Recapoli 2196 resin, cross sectioned and polished.

Table 2. Porous structural parameters for the limestones used in this work.

	S_0 (m^2/m^3) x 10^7	ε	L_0 (m/m^3) x 10^{14}	d_{pm} (nm)	ψ	X^*_{CaO}
Compostilla	4.58	0.40	4.79	33.0	1.7	0.32
Enguera	3.90	0.45	3.29	40.7	1.5	0.39
Brecal	4.37	0.42	4.12	35.6	1.6	0.35

3. Description of the reaction model

In order to determine the sulphation pattern of the CaO particles, a SEM-EDX analysis was conducted on selected samples. Back scattered electrons (BSE) were used because they show differences in chemical composition by displaying higher molecular weight compounds in brighter colours than lower molecular weight compounds. Consequently, $CaSO_4$ can be expected to be distributed in the brightest zones. The BSE-SEM photographs (left side) are supported by EDX mapping to show the sulphur distribution (right side).

Figure 3a shows particles obtained from a calcined limestone sulphated under a CFB calciner conditions. BSE-SEM shows the brightest colour to be on the exterior of the particles, while the core is of a darker colour. This indicates that the $CaSO_4$ is concentrated on the external surface, as is

confirmed by EDX, the sulphur spots being more thinly scattered in the centre of the particles. The sulphation pattern follows the unreacted core pattern. However, for sulphated particles after 50 cycles (Figure 3b-c) there are no appreciable differences in colours in the BSE-SEM, and the EDX indicates a homogeneous distribution of the sulphur throughout the particles. These semi-quantitative results reveal that the sulphation pattern is of the unreacted core type when the number of cycles is low and close to 1 and homogeneous when the number of cycles is sufficiently high.

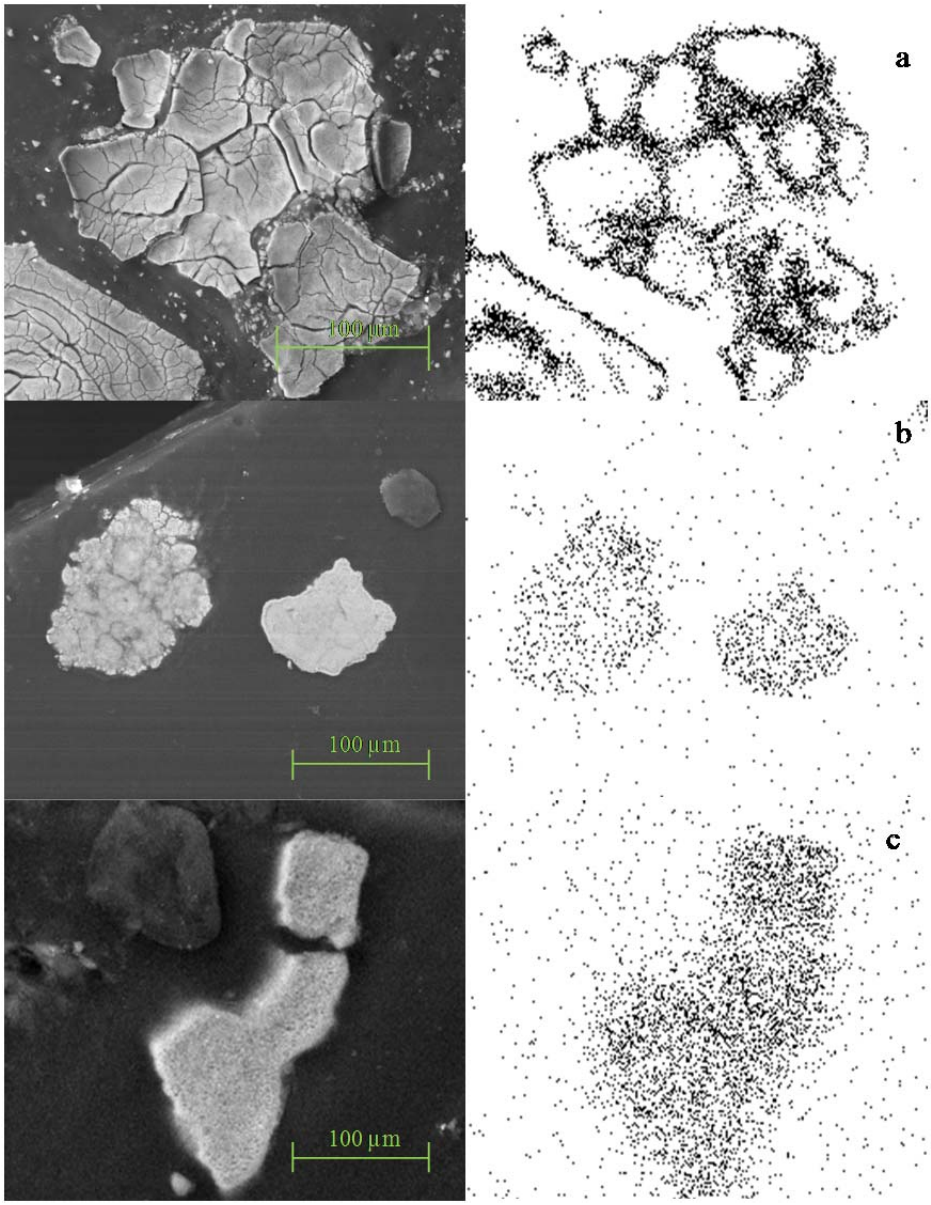

Figure 3. SEM EDX for (a) lime with a $CaSO_4$ conversion of 0.12 sulphated after one calcination, showing an unreacted core sulphation pattern (b) lime with a sulphation conversion of 0.32 after 50 calcination-carbonation cycles and (c) lime with a conversion of 0.25 after 50 calcination-carbonation cycles showing homogeneous $CaSO_4$ distributions.

In order to provide a reasonable interpretation of the experimental results and scalable information on the kinetic parameters derived from the experiments conducted in this study, a discussion of the sulphation patterns and key model assumptions is presented. Several different sulphation patterns have been described in relation to the $CaSO_4$ distributions in the particles. These patterns are related to the morphology and textural properties of the particles [41]. There are three basic sulphation patterns. The unreacted core pattern is characterized by external pore blockage of the surface due to differences in the molar volumes of the $CaSO_4$ and CaO (52.2 and 16.9 cm^3/mol respectively). This pore blockage hinders further sulphation of the inner core of the particles, thus inhibiting the conversion of CaO to $CaSO_4$. The unreacted core pattern is characteristic of sorbents with micro-pores that have no fractures, so only the external surface becomes sulphated, the inner part of the particles remaining unsulphated or only slightly sulphated. The network pattern is characteristic of particles of sorbent with an interconnected network of micro-fractures that allows SO_2 to penetrate inside the particles and to form sulphate inside them in the proximity of the fractures. In this pattern, the particles are divided by the fractures into blocks, each block behaving like an unreacted core since only the external surface, corresponding to the fractures, achieves a high degree of sulphation. Finally, the homogeneous pattern is typical of small particles with wide pores and interconnected fractures. The SO_2 can reach all the surfaces, ensuring a uniform sulphation of the particles. All of these patterns were found in the sulphation of fresh calcined limestones depending on the initial structural properties of the calcined sorbent [26, 41, 60]. However, in a postcombustion CaL system, there are other factors that can change the expected sulphation pattern. One of these factors is the number of calcination-carbonation cycles since they modify the initial porous structure

of the particles. Cycling of the sorbent produces sintering: a reduction of the surface area and an enlargement of the pore size [40]. Another factor is the temperature at which the reaction takes place since each reactor has a different temperature. High temperatures increase the diffusional resistance of the reactant in the pores, and as a consequence pore blockage is more likely to occur. Another limitation is the particle size, since the higher the particle size is, the more likely it is that a core sulphation pattern will occur. Therefore, unreacted core sulphation patterns are more likely for low numbers of calcination carbonation cycles and in the calciner, whereas pseudo or homogeneous sulphation patterns are more likely to occur with highly cycled particles and in the carbonator, as shown in Figure 4.

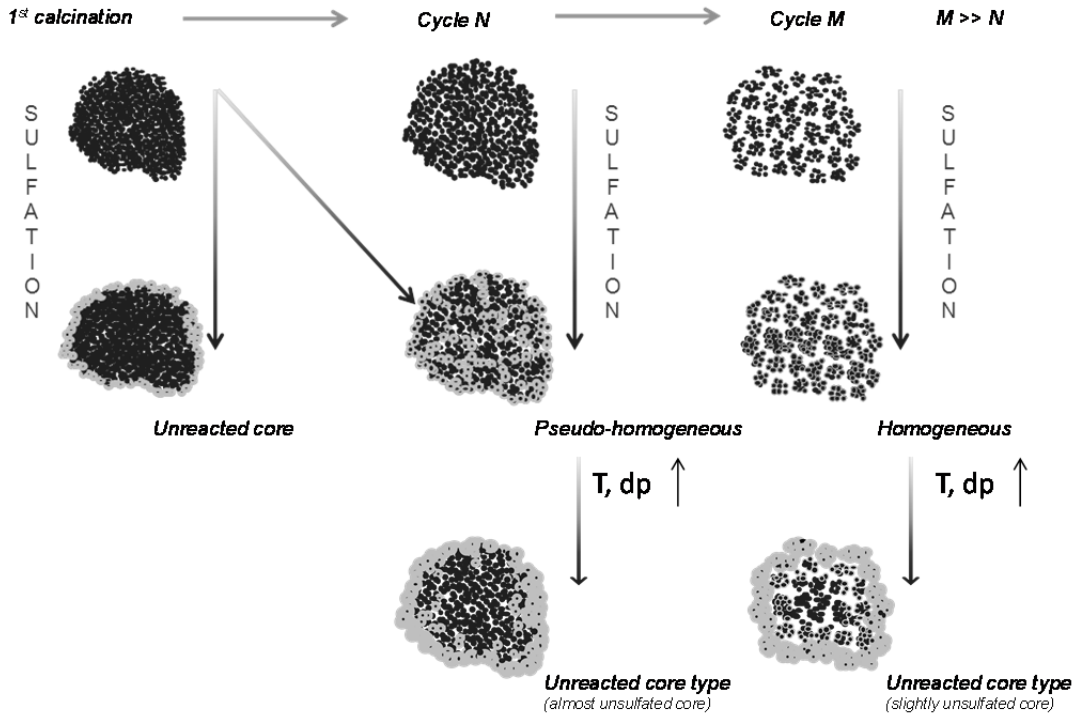

Figure 4. Schematic of the distribution of CaSO4in the particles as a function of the number of calcination carbonation cycles (N), the temperature (T) and the particle diameter (dp).

From the above qualitative discussion of sulfation patterns it is clear that the Random Pore Model is a suitable model for fitting the kinetic parameters and for developing the mathematical expressions to predict the experimental conversion curves of CaO to $CaSO_4$ in the range of operation of the three main reactors involved in post combustion CaL systems. The main reactions to be considered are:

$$CaCO_3 \rightarrow CaO + CO_2 \quad (1)$$

$$CaO + SO_2 + 1/2O_2 \rightarrow CaSO_4 \quad (2)$$

$$CaO + CO_2 \rightarrow CaCO_3 \quad (3)$$

where reactions (1) and (2) take place in the CFBC and in the oxy CFB calciner, while reactions (2) and (3) occur in the CFB carbonator, as shown in Figure 1.

Further assumptions for the RPM are that:

-The particles are isotherm.

-The diffusional effects in the pores are negligible (no radial concentration profiles).

-The sulphation reaction is first order with respect to the SO_2 concentration.

In these conditions, the expression of the RPM model that is valid for the kinetic control and diffusional control of the reactant SO_2 through the product layer of $CaSO_4$ is [55]:

$$\frac{dX_{CaO}}{dt} = \frac{k_S S C_S \left(1 - X_{CaO}\right)\sqrt{1 - \psi LN\left(1 - X_{CaO}\right)}}{\left(1-\varepsilon\right)\left[1 + \frac{\beta Z}{\psi}\left(\sqrt{1 - \psi LN\left(1 - X_{CaO}\right)} - 1\right)\right]} \quad (2)$$

where ψ is the internal structure parameter that accounts for the internal structure of the particle and is expressed as:

$$\psi = \frac{4\pi L(1-\varepsilon)}{S^2} \quad (3)$$

and β is:

$$\beta = \frac{2 k_s a \rho (1-\varepsilon)}{b M_{CaO} D_P S} \quad (4)$$

There are two extreme cases for equation (2) where the kinetic equation can be further simplified. Under the fast kinetic regime (i.e. $\beta = 0$) [54]:

$$\frac{dX_{CaO}}{dt} = \frac{k_s\, S\, C_S (1 - X_{CaO}) \sqrt{1 - \psi \ln(1 - X_{CaO})}}{(1 - \varepsilon)} \tag{5}$$

which, when integrated, yields an explicit expression for the kinetic regime:

$$\frac{1}{\psi}\left[\sqrt{1 - \psi LN(1 - X_{CaO})} - 1\right] = \frac{k_S S C_S t}{2(1 - \varepsilon)} \tag{6}$$

At the other limit, under diffusion through the product layer regime:

$$\frac{\beta Z}{\psi}\left(\sqrt{1 - \psi \ln(1 - X_{CaO})} - 1\right) >> 1 \tag{7}$$

which allows the equation (2) to be integrated to:

$$\frac{1}{\psi}\left[\sqrt{1 - \psi LN(1 - X_{CaO})} - 1\right] = \frac{S}{(1 - \varepsilon)} \sqrt{\frac{D_P M_{CaO} C_S t}{2 \rho_{CaO} Z}} \tag{8}$$

The reaction rate parameters, k_s and D_p, can be obtained by fitting equations (6) and (8) to the experimental data for each regime.

The structural parameters at different cycle numbers were calculated following a method similar to that presented in previous works [56, 58]. This methodology allows the structural parameters of cycled sorbents to be estimated as a function of those corresponding to the fresh calcined limestone and the maximum CO_2 conversion after cycling. These values can

then be used to calculate the specific surface area (S_N) and the length of the porous system (L_N) associated with every mixture of particles by means of the following equations:

$$S_N = S_0 \; X_N \tag{9}$$

$$L_N = L_0 \; X_N \frac{rp_0}{rp_N} \tag{10}$$

The maximum carrying capacity of CO_2 (X_N) can be calculated using the following equation proposed by Grasa et al. [61]

$$X_N = \left(\frac{1}{\frac{1}{(1-X_r)} + kN} + X_r \right) \tag{11}$$

if the deactivation constant (k) and the residual conversion (x_r) for the limestones are known. Moreover, assuming that the sulfation is homogeneous, it is possible to calculate the product layer thickness from the conversion to $CaSO_4$ using the following expression [55]:

$$\Delta = \frac{2Z(1-\varepsilon)}{\psi S}\left(\sqrt{1-\psi LN\left(1-X_{CaO}\right)}-1\right) \tag{12}$$

Equations (6)-(12) will be applied to fit the experimental results following the methodology of section 2.

4. Results and Discussion

The effect of the different variables on the sulphation rates in the CaL reactors have been studied previously [19, 58, 62, 63], including an investigation of the sulphation of the purges from a pilot [19], with the samples being taken from the calciner of the CaL. In these studies it was concluded that the number of calcination carbonation cycles is a variable of special interest. In the present study the experimental work has been broadened to include more limestones and ranges of variables, while the number of calcination carbonation cycles has been strictly controlled in the TG, since it affects the sulphation pattern (surface area, diameter of the pores), in contrast with the previous studies [19, 63]. In the following paragraphs the effect of the main variables (i.e. the SO_2 concentration, the number of calcination carbonation cycles, the reaction temperature, the average particle size, and the presence of other gases such as CO_2 or steam) is described.

The concentration of SO_2 varies depending on the reactors incorporated into the CaL system. For example, the SO_2 concentration of the flue gas produced by the power plant combustor will depend on the sulphur content of the coal being burned in the CFBC and on the efficiency of the SO_2 removal process inside the boiler. These factors will directly affect the SO_2 concentration that is fed to the CFB carbonator to capture CO_2. The maximum SO_2 concentration in the oxy CFB calciner depends on the composition of the coal burned to achieve the high calcination temperatures. A typical range of inlet concentrations of SO_2 in the entire CaL system can change by about one order of magnitude between 500-3000 ppmv. In the literature [33, 34] a variety of reaction orders generally in the range 0.6-1 have been reported depending on the experimental parameters, although there is relatively general consensus about an apparent first order reaction with respect to the SO_2 reactant. Figure 5a is an example of sulfation experiments carried out with highly cycled materials (N=50 in this case) to investigate the effect of

the SO_2 concentration. As can be seen, as the SO_2 concentration in the bulk gas increases from 500 to 3000 ppmv (with a 70% vol. CO_2, in air at 930 °C), the increase in SO_2 concentration has a proportional effect on the initial slope of sulphation as well as certain impact on the final conversion of CaO to $CaSO_4$. This proportionality is consistent with other similar experiments conducted at other key temperatures and cycle numbers, as represented in Figure 5b.

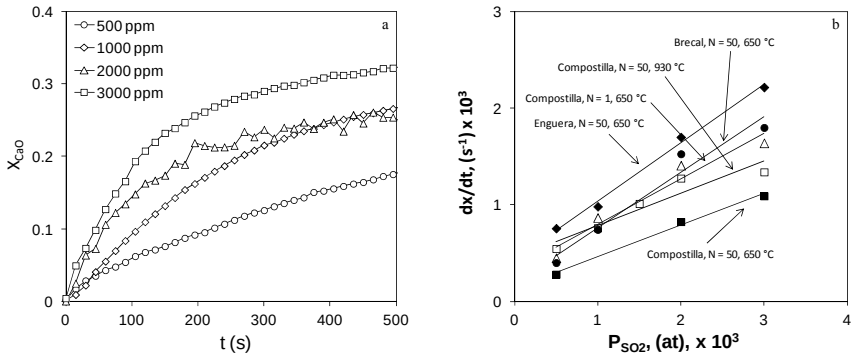

Figure 5. Effect of SO_2 concentration on sulfation of cycled CaO particles. a) conversion curves of Enguera (dp=63-100 µm, 930 °C, N=50) (b) effect of SO_2 concentration on the initial reaction rates for different limes, at two stages of sintering (N = 1,50) and two temperatures (650, 930 °C)

As discussed previously, the number of calcination carbonation cycles, N, has a strong influence on the pore structure of the CaO particles that may cause a change in the sulphation pattern (Figure 4). It is therefore very important to understand and to be able to quantify the impact of N on the kinetics of the sulphation reactions. The results of experiments conducted for this purpose are represented in Figure 6, which shows the sulphation curves obtained for Enguera lime, cut to a size of 63-100 µm, sulphated under two different sulphation atmospheres (the first representative of a CFB

carbonator and the second representative of CFBC conditions). The experiments were carried out with 500 ppm SO_2 in air; with 10% vol. CO_2 in the case of the combustor, and at 650 and 850 ºC respectively.

In the carbonator conditions (Figure 6a) it can be seen that as the number of calcination carbonation cycles increases, the sulphation rates and the final conversion of the CaO to $CaSO_4$ at the end of the sulphation test decrease. Maximum sulphation capacity is achieved after one calcination with a X_{CaO} at approximately 0.34 which is very close to the maximum possible sulphation conversion for this sorbent, 0.39. This effect could be due to the reaction surface reduction associated with the increase in the number of calcination carbonation cycles. However, when the reaction temperature increases to 850 ºC (in a simulated CFBC atmosphere), Figure 6b, the trend is quite the opposite. The sulphation conversion increases as the number of calcination carbonation cycles increases despite the reduction in surface area. This is consistent with the pore blockage mechanism as the sulfation conversion after only one calcination is only 0.17 compared with maximum sulfation conversion. As the pore structure opens up due to the effect of the number of cycles, the inner surface becomes accessible for the reaction to occur and the sulphation conversion increases. Another example of the effect of the number of calcination carbonation cycles on the sulphation curves is shown in Figure 7 for Brecal limestone under the conditions of the CFB carbonator (Figure 7a) and the oxy CFB calciner (Figure 7b). The sulphation in the oxy CFB calciner conditions takes place at 500 ppm SO_2, 70% vol. CO_2 in air at 930 ºC. Under the CFB carbonator conditions (Figure 7a) the initial reaction rate as well as the final sulphation conversion is almost the same after one cycle and after 50 cycles, despite the fact that the surface area has been reduced by around six times after this high number of cycles. This suggests that there is an unreacted core sulphation pattern for the fresh calcined sorbent. As in the previous example, when the reaction temperature

increases (CFB calciner conditions), Figure 7b, the sulphation conversion increases when the number of calcination carbonation cycles increases because the pattern tends to become more homogeneous. However, when the cycle number increases to a number as high as 150 cycles, the reduction in surface area predominates over the opening up of the structure, and as a consequence the sulphation conversion is lower than that achieved after 50 cycles.

To summarize, the increase in temperature tends to favour the unreacted core type due to an increase in the internal pore diffusion resistance to the reactant SO_2. By contrast, the carbonation/calcination number tends to favour the homogeneous pattern due to the sintering of the surface that promotes opened-structures.

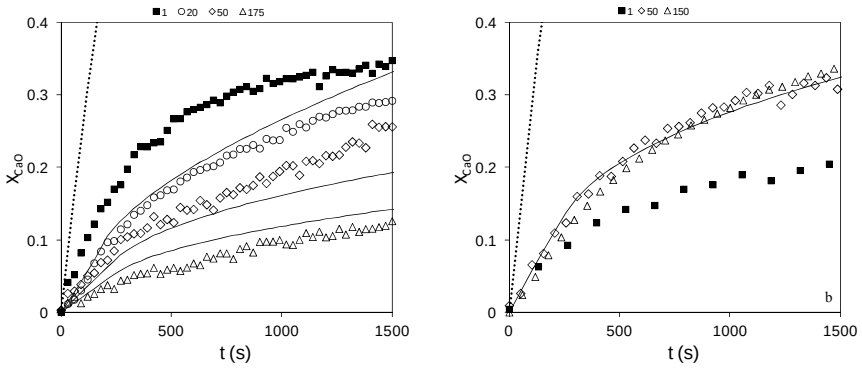

Figure 6. Comparison of the experimental X_{CaO} values of Enguera lime with different numbers of calcination carbonation cycles under the conditions of a CFB carbonator (a) and a CFBC (b). The solid lines correspond to the predictions of the model.

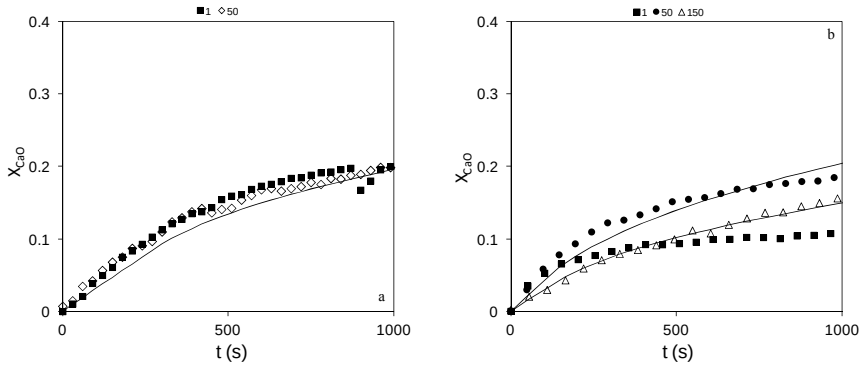

Figure 7. Comparison of X_{CaO} experimental values of Brecal lime with different numbers of calcination carbonation cycles in the conditions of a CFB carbonator (a) and a CFB calciner (b). The solid lines correspond to the predictions of the model.

The RPM was applied to the experimental data yielding the rate constants presented in Table 3. However, cycle 1 was not used for this calculation because of its non-homogeneous nature which is not considered in our model proposal. The kinetic constants (k_s) were obtained by fitting equation (6) to the experimental X_{CaO} vs time data, in the fast stage of the reaction, whereas the diffusional coefficients through the product layer (D_p) were obtained by fitting equation (8) to the slow regime of the sulphation curves.

Table 3. Kinetic and diffusional constants for the three limestones tested.

	T (°C)	ks (m^4/mol s)	Dp (m^2/s)	EaK (kJ/mol)	k_0 (m^4/mol s)	EaD (kJ/mol)*/**	Dp_0 (m^2/s)[a/b]
	650	4.48E-09	3.53E-12				
Compostilla	850	8.23E-09	4.14E-12	26.2	1.36E-07	120/53.96	2.18E-5/1.34E-9
	930	9.90E-09	6.08E-12				
	650	5.75E-09	4.03E-12				
Enguera	850	1.03E-08	7.82E-12	21.9	1.01E-07	120/110.7	2.49E-5/1.1E-6
	930	1.08E-08	1.72E-11				
	650	3.76E-09	1.51E-12				
Brecal	850	5.15E-09	2.84E-12	24.9	9.18E-08	120/150.9	9.34E-6/2.97E-5
	930	8.96E-09	8.32E-12				

[a/b] Below/Above Tammann temperature

For the diffusion through the product layer regime, we applied the Arrhenius equation above 850 ºC but below 850 ºC separately because a slight variation in the E_{aD} fitted under these conditions was detected. This effect has been reported elsewhere in relation with the carbonation reaction of lime [59]. The explanation given in that case was that above the Tammann temperature (861 ºC [64]), there is a change in the properties of the solid $CaSO_4$ formed, which affects the diffusivity of SO_2 through the product layer, and therefore the E_{aD}. The critical point of regime change is characterized by a experimental X_{CaO}. Consequently, this value was employed in equation (12) to estimate the product layer thicknesses of the regime change, (see Table 4).

Table 4. Estimated thicknesses corresponding to the regime changes.

	650 (°C)	850 (°C)	930 (°C)
Compostilla	34.3	13.4	35.4
Enguera	29.3	42.1	20.3
Brecal	29.1	32.2	17.5

As can be seen from Figures 6 and 7, the RPM predicts reasonably well all of the sulphation curves under all the CaL conditions when the cycle number is higher than 20. As might be expected, for cycle 1, the RPM overpredicts the experimental results due to the sulphation pattern and the limitation of our model proposal. However, when the sulphation pattern is homogeneous, as in the case of cycles 50 and 150, it fits reasonably well.

The effect of the particle size is directly related to the sulphation pattern. If the particle size increases, the pore diffusion resistance also increases and consequently unreacted core sulphation patterns are more likely to occur. Because the typical sulphation pattern for the limestones tested in this work for the sorbent after a single calcination was not homogeneous, cycles 20 (in the conditions of a CFB carbonator) and 50 (in the conditions of an oxy CFB calciner) of the Enguera limestone were selected to perform the corresponding sulphation tests under the two extreme conditions. In addition, the experimental results obtained for Compostilla after a single calcination in the conditions of an oxy CFB calciner are shown for comparison purposes. After 20 calcination carbonation cycles the sulphation pattern of Enguera was homogeneous for particle sizes below 100 μm sulphated under the conditions of a CFB carbonator, as is shown in Figure 8a. Moreover, the sulphation curve for 36-63 μm is almost identical to that of 63-100 μm. However, when the particle size increases to 400-600 μm the sulphation rate clearly decreases, indicating an unreacted core type sulphation pattern for this size. As expected, as the reaction temperature increases, this effect for the sulfation pattern to become non-homogeneous becomes more apparent, as in the case of the sulphation reaction under oxy CFB calciner conditions (Figure 8b). The difference in sulphation conversion between the lower particle sizes and the highest one increases. The model predicts reasonably

well the experimental results corresponding to the three smaller particle sizes, where the pattern is homogeneous. Figure 8c shows an unreacted sulphation pattern, as can be seen from the different X_{CaO} vs time curves obtained for the three different particle sizes of Compostilla lime. This result was to be expected, since the higher particle sizes give rise to a maximum X_{CaO} that is lower than that indicated by its porosity: a value of 0.34 should have been obtained in the absence of pore diffusion resistances.

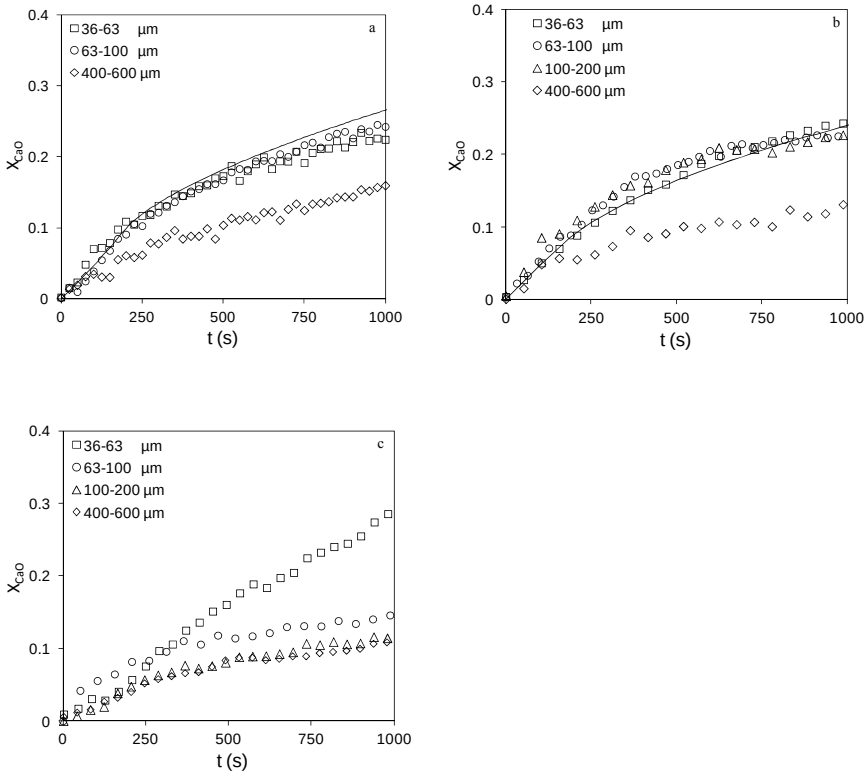

Figure 8. Comparison of the experimental X_{CaO} values of cycled Enguera lime for different particle sizes in the conditions of a CFB carbonator (a) and of a CFB calciner (b). Also the effect of the particle size on the sulphation of Compostilla lime after a single calcination is shown in the conditions of an oxy CFB calciner (c). The solid lines correspond to the predictions of the model.

The effect on the sulphation rates of the CO_2 and H_2O contents in the gas feed in relation to the differences between the reacting atmospheres in the main reactors was also taken into consideration. It can be seen from the results that there is a variation in the concentration of CO_2 depending on the reactor that is being considered. Under CFBC conditions, a typical CO_2 concentration of around 10% vol. was used. In the oxy CFB calciner, an atmosphere rich in CO_2 can be expected due to its highly effective design, which is capable of producing a high purity stream of CO_2 that can be compressed and stored. In this study, a CO_2 concentration of 70% vol. was selected to perform the sulphation tests under CFB calciner conditions. CO_2 is a very effective sintering agent [65], so it might affect the internal pore structure available for sulphation, depending on the time of exposure and the temperature. However, as the sorbent in a CaL will have undergone several cycles of calcination carbonation, the effect of further sintering will be negligible. To test the effect of the CO_2 on the sulphation X_{CaO} vs time curves, two cycled (N = 50) limes were selected and sulphated in CFBC and oxy CFB calciner conditions, with 10% vol. and 70% vol. CO_2 respectively, and 500 ppm SO_2 in air, and compared to the corresponding curves with 0% CO_2. The particle size was 63-100 μm, (see Figure 9). No relevant effects of the CO_2 concentration on the initial sulphation rates of the cycled sorbent can be observed indicating that CO_2 does not affect the sulphation of the cycled lime.

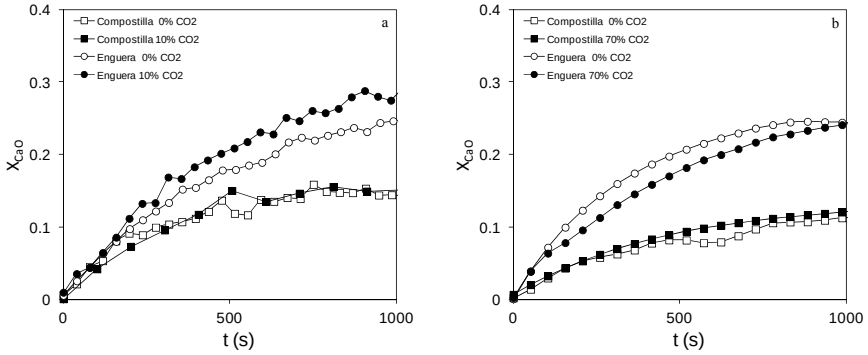

Figure 9. Effect of the CO_2 concentration on the X_{CaO} vs time curves for Enguera and Compostilla limes after 50 cycles of calcination carbonation in the conditions of (a) a CFBC and (b) a CFB calciner.

The experimental data presented until now on the sulphation of CaO were obtained without considering steam. However, steam is a common component of the gas streams produced in power generation. Recently some works [66, 67] have been published that take into account the influence of steam on the sulphation of CaO. They found an enhancement of the sulphur carrying capacities of the limes tested because of an improvement in the rates of diffusion through the product layer. Nevertheless, no appreciable effects were observed on the initial fast step of sulphation. This improvement in the sulphation of CaO is often attributed to a change in the mechanism of reaction or to a reduction in the resistance to diffusion through the product layer. In this work, the effect of steam was tested using two limestones, Enguera and Compostilla. The CFBC conditions (Figure 10a) were simulated using a mixed gas consisting of 10% vol. CO_2, 500 ppm SO_2, 15 and 30% vol. H_2O in air at 850 ºC. Under oxy CFB calciner conditions (Figure 10b) two reaction mixtures were used: 49% vol. CO_2, 15% vol. H_2O, 500 ppm SO_2 in air, and 36% vol. CO_2, 30% vol. H_2O, 500 ppm SO_2 in air at 930 ºC. The particle size was 63-100 µm and the sulphation tests were

performed after 50 calcination carbonation cycles. From the Figure 10a it can be seen that the concentration of steam did not have any effect on the sulphation rates of Compostilla lime. The slopes are essentially the same, and the slight deviations in the final X_{CaO} are only due to experimental errors. Nevertheless, in the case of Enguera lime and the highest steam concentration used (30%), the maximum X_{CaO} increased to the point where it exceeded the maximum calculated for the porosity i.e., approximately 0.39. On the other hand, both limes showed the same behaviour under the oxy CFB calciner conditions during the first step of reaction where the kinetic controlled regime was predominant (Figure 10b). The steam content had no effect on sulphation conversion during the fast stage, which is consistent with the data reported by other authors [66, 67]. However, the maximum X_{CaO} achieved increased with the steam content. It must be concluded therefore that steam enhances the mechanism of diffusion through the product layer of $CaSO_4$. The X_{CaO} value at which the sulphation rate starts to increase due to the steam is well above 0.1 which is considered as the maximum for CaL systems. Thus in these systems the effect of steam will be negligible.

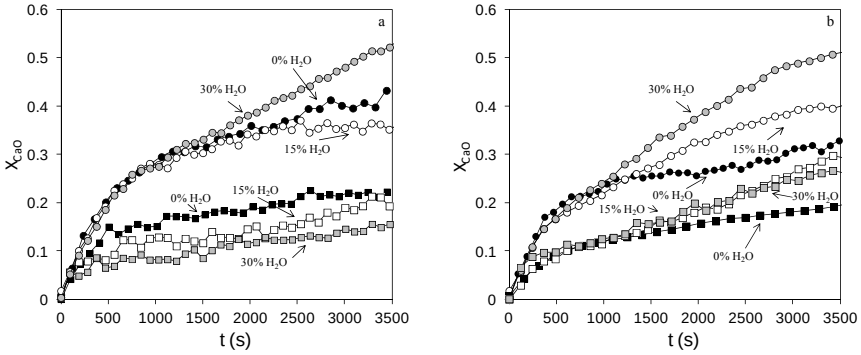

Figure 10. Effect of the H_2O concentration on the X_{CaO} vs time curves for Enguera (○) and Compostilla (□) limes after 50 cycles of calcination carbonation under the conditions of a CFBC (a) and a CFB calciner (b).

5. Conclusions

The sulphation reaction of CaO was studied under conditions typical of the three main reactors incorporated into the CaL system. The reaction order with respect to SO_2 was always 1 regardless of the reactor conditions. The effect of the number of calcination carbonation cycles produces a change in the sulphation pattern. When the number of cycles is increased, the sulphation pattern tends to become more homogeneous. Moreover, as the reaction temperature increases the sulphation pattern tends to resemble that of the unreacted core type due to an increase in diffusional resistance in the pores. Hence the number of carbonation/calcination cycles necessary for the pattern to become homogeneous increases. The increase in the particle size leads to non-homogeneous sulphation patterns since the length of the pores increases, as does pore diffusional resistance. Nevertheless, for particle sizes below 200 μm and highly cycled sorbents a homogeneous sulphation pattern can be expected at any temperature up to 930 ºC. Dependence on the CO_2

concentration is negligible considering the low conversions to $CaSO_4$ achieved and the high number of cycles to which the sorbent has been subjected. The presence of steam improves the sulphation rates in the slow regime of reaction presumably due to an enhancement of the diffusion through the product layer. The Random Pore Model was found to be valid for predicting the experimental sulphation rates and capacities of a sorbent sulphated according to a homogeneous pattern.

A final point worth mentioning is that the use of purges from the oxy CFB calciner as desulfurizing agent in a FB combustor would be beneficial since the sorbent extracted is sintered and it would become more sulphated before pore blockage occurred than if fresh limestone were used.

6. Acknowledgements

The research presented in this work has received partial funding from the European Community Research Fund for Coal and Steel (CaO2 project: RFC-PR-13006). Authors also acknowledge to Prof. J.C. Abanades for his contribution to this article. J.M.C. also acknowledges a Ph.D. fellowship grant awarded by FICYT.

7. Notation

a,b	stoichiometric coefficients for the sulphation reaction
C_S	concentration of SO_2, kmol/m^3
D_P	effective product layer diffusivity, m^2/s
D_{P0}	diffusional pre-exponential factor, m^2/s
d_{pm}	mean pore diameter, nm
E_{ak}	activation energy for the kinetic regime, kJ/mol

E_{aD}	activation energy for the diffusion through the product layer regime, kJ/mol
Δ	product layer thickness, nm
k	sorbent deactivation constant
k_S	rate constant for surface reaction, m^4/mol s
k_{S0}	kinetic pre-exponential factor, m^4/mol s
L	total length of the pore system, m/m^3
M	molecular weight, kg/kmol
N	number of calcination/carbonation cycles
r_{pN}	radius of the pore after N cycles, m
S	reaction surface per unit of volume, m^2/m^3
t	reaction time, s
V_M	molar volume, m^3/kmol
X_{ave}	CaO average molar conversion to $CaCO_3$
X_N	Maximum CaO molar conversion to $CaCO_3$
X_{CaO}	CaO molar conversion to $CaSO_4$
X^*_{CaO}	Maximum CaO molar conversion to $CaSO_4$
Z	volume fraction ratio before and after reaction

Greek letters

β	$2\ k_s\ a\ \rho\ (1-\varepsilon)/M_{CaO}\ b\ D_P\ S$
ε	porosity
ρ	density, kg/m^3
ψ	$4\pi L(1-\varepsilon)/S^2$
τ	$k_s\ C_S\ S\ t/(1-\varepsilon)$

8. Highlights:

- The sulphation of CaO under the three main reactor conditions involved in CaL CO_2 capture systems was studied. The CaL CFB carbonator and the oxy CFB calciner were found to be excellent desulphurization systems.
- The cycled purge from an oxy CFB calciner proved to be a better desulphurization sorbent than fresh limestone under typical FBC/CFBC conditions.
- The RPM applied with the calculated kinetic and diffusional parameters was a suitable model for predicting the sulphation conversions under typical CaL conditions.

9. References

[1] IPCC, Special Report on Carbon Dioxide Capture and Storage, Cambridge University Press, (2005).
[2] T. Shimizu, T. Hirama, H. Hosoda, K. Kitano, M. Inagaki, K. Tejima, A Twin Fluid-Bed Reactor for Removal of CO_2 from Combustion Processes, Chem. Eng. Res. Des. 77 (1999) 62-68.
[3] J.C. Abanades, E.S. Rubin, E.J. Anthony, Sorbent Cost and Performance in CO_2 Capture Systems, Ind. Eng. Chem. Res. 43 (2004) 3462-3466.
[4] L.M. Romeo, J.C. Abanades, J.M. Escosa, J. Paño, A. Giménez, A. Sánchez-Biezma, J.C. Ballesteros, Oxyfuel carbonation/calcination cycle for low cost CO_2 capture in existing power plants, Energy Convers. Manage. 49 (2008) 2809-2814.
[5] J. Blamey, E.J. Anthony, J. Wang, P.S. Fennell, The calcium looping cycle for large-scale CO_2 capture, Prog. Energy Combust. Sci. 36 (2010) 260-279.

[6] I. Martínez, R. Murillo, G. Grasa, J. Carlos Abanades, Integration of a Ca looping system for CO_2 capture in existing power plants, AlChE J. 57 (2011) 2599-2607.
[7] Fluidized bed technologies for near-zero emission combustion and gasification, Woodhead Publishing Limited., Cambridge, (2013).
[8] A. Sánchez-Biezma, J.C. Ballesteros, L. Diaz, E. de Zárraga, F.J. Álvarez, J. López, B. Arias, G. Grasa, J.C. Abanades, Postcombustion CO_2 capture with CaO. Status of the technology and next steps towards large scale demonstration, Energy Procedia 4 (2011) 852-859.
[9] B. Arias, M.E. Diego, J.C. Abanades, M. Lorenzo, L. Diaz, D. Martínez, J. Alvarez, A. Sánchez-Biezma, Demonstration of steady state CO2 capture in a 1.7 MWth calcium looping pilot, Int. J. Greenhouse Gas Control 18 (2013) 237-245.
[10] J. Ströhle, M. Junk, J. Kremer, A. Galloy, B. Epple, Carbonate looping experiments in a 1 MWth pilot plant and model validation, Fuel 127 (2014) 13-22.
[11] M. Alonso, M.E. Diego, J.C. Abanades, C. Perez, J. Chamberlain, In situ CO_2 capture with CaO in a 300 kW fluidized bed biomass combustor, 7th Trondheim CCS Conference, Trondheim, 2013.
[12] C. Hawthorne, H. Dieter, A. Bidwe, A. Schuster, G. Scheffknecht, S. Unterberger, M. Käß, CO_2 capture with CaO in a 200 kWth dual fluidized bed pilot plant, Energy Procedia 4 (2011) 441-448.
[13] M.H. Chang, C.M. Huang, W.H. Liu, W.C. Chen, J.Y. Cheng, W. Chen, T.W. Wen, S. Ouyang, C.H. Shen, H.W. Hsu, Design and Experimental Investigation of Calcium Looping Process for 3-kWth and 1.9-MWth Facilities, Chem. Eng. Technol. 36 (2013) 1525-1532.
[14] D.Y. Lu, R.W. Hughes, E.J. Anthony, Ca-based sorbent looping combustion for CO_2 capture in pilot-scale dual fluidized beds, Fuel Process. Technol. 89 (2008) 1386-1395.
[15] J.C. Abanades, M. Alonso, N. Rodríguez, B. González, G. Grasa, R. Murillo, Capturing CO_2 from combustion flue gases with a carbonation calcination loop. Experimental results and process development, Energy Procedia 1 (2009) 1147-1154.
[16] A. Charitos, N. Rodríguez, C. Hawthorne, M. Alonso, M. Zieba, B. Arias, G. Kopanakis, G. Scheffknecht, J.C. Abanades, Experimental Validation of the Calcium Looping CO_2 Capture Process with Two Circulating Fluidized Bed Carbonator Reactors, Ind. Eng. Chem. Res. 50 (2011) 9685-9695.
[17] V. Manovic, E.J. Anthony, D. Loncarevic, SO_2 Retention by CaO-Based Sorbent Spent in CO_2 Looping Cycles, Ind. Eng. Chem. Res. 48 (2009) 6627-6632.
[18] Y. Li, H. Liu, S. Wu, R. Sun, C. Lu, Sulfation behavior of CaO from long-term carbonation/calcination cycles for CO_2 capture at FBC temperatures, J. Therm. Anal. Calorim. 111 (2013) 1335-1343.

[19] J.M. Cordero, M. Alonso, B. Arias, J.C. Abanades, Sulfation Performance of CaO Purges Derived from Calcium Looping CO_2 Capture Systems, Energy & Fuels 28 (2014) 1325-1330.
[20] M.E. Diego, B. Arias, M. Alonso, J.C. Abanades, The impact of calcium sulfate and inert solids accumulation in post-combustion calcium looping systems, Fuel 109 (2013) 184-190.
[21] P. Sun, J.R. Grace, C.J. Lim, E.J. Anthony, Removal of CO_2 by Calcium-Based Sorbents in the Presence of SO_2, Energy & Fuels 21 (2006) 163-170.
[22] G.S. Grasa, M. Alonso, J.C. Abanades, Sulfation of CaO Particles in a Carbonation/Calcination Loop to Capture CO_2, Ind. Eng. Chem. Res. 47 (2008) 1630-1635.
[23] V. Manovic, E.J. Anthony, Competition of Sulphation and Carbonation Reactions during Looping Cycles for CO_2 Capture by CaO-Based Sorbents, J. Phys. Chem. 114 (2010) 3997-4002.
[24] B. Arias, G.S. Grasa, M. Alonso, J.C. Abanades, Post-combustion calcium looping process with a highly stable sorbent activity by recarbonation, Energy Environ. Sci. 5 (2012) 7353-7359.
[25] V. Manovic, E.J. Anthony, Carbonation of CaO-Based Sorbents Enhanced by Steam Addition, Ind. Eng. Chem. Res. 49 (2010) 9105-9110.
[26] E.J. Anthony, D.L. Granatstein, Sulfation phenomena in fluidized bed combustion systems, Prog. Energy Combust. Sci. 27 (2001) 215-236.
[27] R.H. Borgwardt, Kinetics of the reaction of sulfur dioxide with calcined limestone, Environ. Sci. Technol. 4 (1970) 59-63.
[28] R.H. Borgwardt, R.D. Harvey, Properties of carbonate rocks related to sulfur dioxide reactivity, Environ. Sci. Technol. 6 (1972) 350-360.
[29] R.L. Pigford, G. Sliger, Rate of Diffusion-Controlled Reaction Between a Gas and a Porous Solid Sphere - Reaction of SO_2 with $CaCO_3$, Ind. Eng. Chem. Proc. Des. Dev. 12 (1973) 85-91.
[30] M. Hartman, R.W. Coughlin, Reaction of Sulfur Dioxide with Limestone and the Influence of Pore Structure, Ind. Eng. Chem. Proc. Des. Dev. 13 (1974) 248-253.
[31] M. Hartman, R.W. Coughlin, Reaction of sulfur dioxide with limestone and the grain model, AlChE J. 22 (1976) 490-498.
[32] M. Hartman, O. Trnka, Influence of temperature on the reactivity of limestone particles with sulfur dioxide, Chem. Eng. Sci. 35 (1980) 1189-1194.
[33] S.K. Bhatia, D.D. Perlmutter, The effect of pore structure on fluid-solid reactions: Application to the SO_2-lime reaction, AlChE J. 27 (1981) 226-234.
[34] R.H. Borgwardt, K.R. Bruce, Effect of specific surface area on the reactivity of CaO with SO_2, AlChE J. 32 (1986) 239-246.

[35] J.S. Dennis, A.N. Hayhurst, Mechanism of the sulphation of calcined limestone particles in combustion gases, Chem. Eng. Sci. 45 (1990) 1175-1187.
[36] M. Hartman, O. Trnka, Reactions between calcium oxide and flue gas containing sulfur dioxide at lower temperatures, AlChE J. 39 (1993) 615-624.
[37] J. Adanez, P. Gayan, F. Garcia-Labiano, Comparison of Mechanistic Models for the Sulfation Reaction in a Broad Range of Particle Sizes of Sorbents, Ind. Eng. Chem. Res. 35 (1996) 2190-2197.
[38] J. Adánez, F. García-Labiano, V. Fierro, Modelling for the high-temperature sulphation of calcium-based sorbents with cylindrical and plate-like pore geometries, Chem. Eng. Sci. 55 (2000) 3665-3683.
[39] F. García-Labiano, A. Rufas, L.F. de Diego, M.d.l. Obras-Loscertales, P. Gayán, A. Abad, J. Adánez, Calcium-based sorbents behaviour during sulphation at oxy-fuel fluidised bed combustion conditions, Fuel 90 (2011) 3100-3108.
[40] D. Alvarez, J.C. Abanades, Pore-Size and Shape Effects on the Recarbonation Performance of Calcium Oxide Submitted to Repeated Calcination/Recarbonation Cycles, Energy & Fuels 19 (2004) 270-278.
[41] K. Laursen, W. Duo, J.R. Grace, J. Lim, Sulfation and reactivation characteristics of nine limestones, Fuel 79 (2000) 153-163.
[42] J. Szekely, J.W. Evans, H.Y. Sohn, Gas-solid reactions, (1976).
[43] J. Szekely, J.W. Evans, A structural model for gas—solid reactions with a moving boundary, Chem. Eng. Sci. 25 (1970) 1091-1107.
[44] M. Ishida, C.Y. Wen, Comparison of zone-reaction model and unreacted-core shrinking model in solid—gas reactions—I isothermal analysis, Chem. Eng. Sci. 26 (1971) 1031-1041.
[45] S.V. Sotirchos, H.C. Yu, Overlapping grain models for gas-solid reactions with solid product, Ind. Eng. Chem. Res. 27 (1988) 836-845.
[46] P.A. Ramachandran, J.M. Smith, Effect of sintering and porosity changes on rates of gas—solid reactions, Chem. Eng. J. 14 (1977) 137-146.
[47] C. Georgakis, C.W. Chang, J. Szekely, A changing grain size model for gas--solid reactions, Chem. Eng. Sci. 34 (1979) 1072-1075.
[48] P.V. Ranade, D.P. Harrison, The grain model applied to porous solids with varying structural properties, Chem. Eng. Sci. 34 (1979) 427-432.
[49] K. Dam-Johansen, P.F.B. Hansen, K. Østergaard, High-temperature reaction between sulphur dioxide and limestone—III. A grain-micrograin model and its verification, Chem. Eng. Sci. 46 (1991) 847-853.
[50] J. Szekely, M. Propster, A structural model for gas solid reactions with a moving boundary—VI: The effect of grain size distribution on the conversion of porous solids, Chem. Eng. Sci. 30 (1975) 1049-1055.
[51] E.E. Petersen, Reaction of porous solids, AlChE J. 3 (1957) 443-448.
[52] P.A. Ramachandran, J.M. Smith, A single-pore model for gas-solid noncatalytic reactions, AlChE J. 23 (1977) 353-361.

[53] G.A. Simons, A.R. Garman, A.A. Boni, The kinetic rate of SO_2 sorption by CaO, AlChE J. 33 (1987) 211-217.
[54] S.K. Bhatia, D.D. Perlmutter, A random pore model for fluid-solid reactions: I. Isothermal, kinetic control, AlChE J. 26 (1980) 379-386.
[55] S.K. Bhatia, D.D. Perlmutter, A random pore model for fluid-solid reactions: II. Diffusion and transport effects, AlChE J. 27 (1981) 247-254.
[56] G. Grasa, R. Murillo, M. Alonso, J.C. Abanades, Application of the random pore model to the carbonation cyclic reaction, AlChE J. 55 (2009) 1246-1255.
[57] H. Ale Ebrahim, Application of Random-Pore Model to SO_2 Capture by Lime, Ind. Eng. Chem. Res. 49 (2009) 117-122.
[58] B. Arias, J.M. Cordero, M. Alonso, J.C. Abanades, Sulfation rates of cycled CaO particles in the carbonator of a Ca-looping cycle for postcombustion CO_2 capture, AlChE J. 58 (2012) 2262-2269.
[59] S.K. Bhatia, D.D. Perlmutter, Effect of the product layer on the kinetics of the CO_2-lime reaction, AlChE J. 29 (1983) 79-86.
[60] H.-J. Ryu, J.R. Grace, C.J. Lim, Simultaneous CO_2/SO_2 Capture Characteristics of Three Limestones in a Fluidized-Bed Reactor, Energy & Fuels 20 (2006) 1621-1628.
[61] G.S. Grasa, J.C. Abanades, CO_2 Capture Capacity of CaO in Long Series of Carbonation/Calcination Cycles, Ind. Eng. Chem. Res. 45 (2006) 8846-8851.
[62] M. Alonso, J.M. Cordero, B. Arias, J.C. Abanades, Sulfation Rates of Particles in Calcium Looping Reactors, Chem. Eng. Technol. 37 (2014) 15-19.
[63] B. Arias, J.M. Cordero, M. Alonso, M.E. Diego, J.C. Abanades, Investigation of SO_2 Capture in a Circulating Fluidized Bed Carbonator of a Ca Looping Cycle, Ind. Eng. Chem. Res. 52 (2013) 2700-2706.
[64] A.P. Iribarne, J.V. Iribarne, E.J. Anthony, Reactivity of calcium sulfate from FBC systems, Fuel 76 (1997) 321-327.
[65] R. H. Borgwardt, Sintering of nascent calcium oxide, Chem. Eng. Sci. 44 (1989) 53-60.
[66] C. Wang, L. Jia, Y. Tan, E.J. Anthony, The effect of water on the sulphation of limestone, Fuel 89 (2010) 2628-2632.
[67] M.C. Stewart, V. Manovic, E.J. Anthony, A. Macchi, Enhancement of Indirect Sulphation of Limestone by Steam Addition, Environ. Sci. Technol. 44 (2010) 8781-8786.

4.6.5 Publicación V

Sulfation Performance of CaO Purges Derived from Calcium Looping CO_2 Capture Systems

Publicado en:

Energy & Fuels

Volumen 28

Año 2014

Índice de Impacto: 2.733

energy&fuels

Article

pubs.acs.org/EF

Sulfation Performance of CaO Purges Derived from Calcium Looping CO_2 Capture Systems

Jose M. Cordero,* M. Alonso, B. Arias, and J. C. Abanades

Instituto Nacional del Carbón, Consejo Superior de Investigaciones Científicas (CSIC), Calle Francisco Pintado Fe, 26, 33011 Oviedo, Spain

ABSTRACT: The aim of this work is to investigate the SO_2 capture capacity and sulfation rates of CaO-rich purges from a post-combustion CO_2 capture calcium looping (CaL) large-scale pilot plant (a 1.7 MW_{th} pilot plant operating in continuous mode). The sulfation reaction in simulated flue gas conditions was studied using a thermogravimetric analyzer (TGA), and isothermal sulfation tests were conducted over a range of temperatures to derive the kinetic parameters. It was confirmed that CaO-rich purges from CaL are able to capture more than twice as much SO_2 as the parent fresh calcined limestone. This is because the pore blockage mechanism has less impact on the sulfation of highly cycled CaO purges from the CO_2 capture system. Scanning electron microscopy (SEM)−energy-dispersive X-ray (EDX) analysis confirmed the homogeneous sulfation pattern of the cycled samples obtained from the pilot. A semi-empirical model based on the random pore model (RPM) was used to fit the experimental results. The kinetic parameters k_S and D_P were calculated using the experimental data obtained from TGA tests. The values obtained are consistent with those obtained by other authors for non-cycled materials.

INTRODUCTION

CO_2 capture and storage is a major mitigation option for climate change,[1] and it is the only low-carbon technology currently available for exploiting the vast economic assets represented by fossil fuel reserves or unburnable carbon.[2] Post-combustion calcium looping (CaL) is one of the emerging technologies that is aimed at reducing CO_2 capture costs and energy penalties associated with the separation of CO_2. Post-combustion CaL uses CaO particles to capture CO_2 from a combustion flue gas in a carbonator reactor operating at around 650 °C. $CaCO_3$ formed is decomposed in a calciner operating at temperatures above 900 °C by burning a fuel under oxy-fuel conditions to release CO_2 in a concentrated form.[3] A large fraction of the total heat input is required in the calciner to conduct the endothermic calcination of $CaCO_3$. However, this heat is available at a high temperature in the different mass streams leaving the calciner (>900 °C) and carbonator (650 °C), and it can be used to drive a high-efficiency steam cycle.[3] A distinctive feature of this CO_2 capture process is that it allows for additional power to be produced and reduces the energy penalty for the CO_2 capture.

CaL technology has experienced rapid development in recent years because of its similarities with existing combustion technology in circulating fluidized beds and the advantages that it offers over other post-combustion CO_2 capture technologies[4] (i.e., a lower energy penalty and a low-cost sorbent precursor). The largest demonstration of this technology thus far has been the 1.7 MW_{th} pilot plant in La Pereda (Spain),[5] which entered into operation in January 2012 and obtained the first positive results for a plant operating in continuous mode.[6] Other large pilots that have also achieved encouraging results include the 1 MW_{th} pilot in Darmstadt (Germany)[7] and the 0.2 MW_{th} pilot at Stuttgart University (Germany).[8] A 1.9 MW_{th} pilot is about to be completed in Taiwan,[9] and several smaller pilot trials have produced interesting results in recent years.[10−12]

One possible configuration of a post-combustion CaL system is outlined in Figure 1 and is particularly relevant for the scope

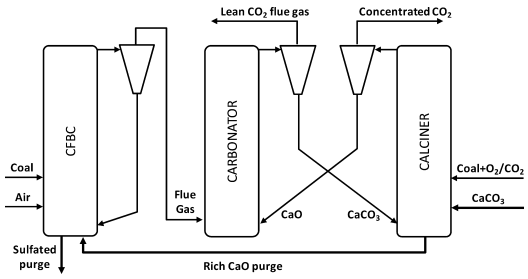

Figure 1. Schematic of a post-combustion CaL system incorporated into an existing CFBC power plant.

of the present work. It consists of an air-fired circulating fluidized-bed combustor (CFBC), followed by a circulating fluidized-bed carbonator for capturing CO_2 with CaO. A third circulating fluidized-bed reactor, the calciner, regenerates CaO by the oxy-combustion of the coal. Figure 1 highlights the mechanical similarity of the key CaL reactor components with existing CFBCs. In addition, the possibility of using the CaO-rich purge of solids from the CO_2 capture system instead of the limestone commonly fed into CFBCs for desulfurization purposes can be observed. Indeed, an ideal synergy would be achieved if the limestone feed for the desulfurization of flue gases in a CFBC could be completely replaced by the feed from the purge of solids leaving the CaL system. In these conditions, the original feed of limestone to the CFBC power plant (now

Received: December 3, 2013
Revised: January 27, 2014
Published: January 28, 2014

   dx.doi.org/10.1021/ef402384z | *Energy Fuels* 2014, 28, 1325−1330

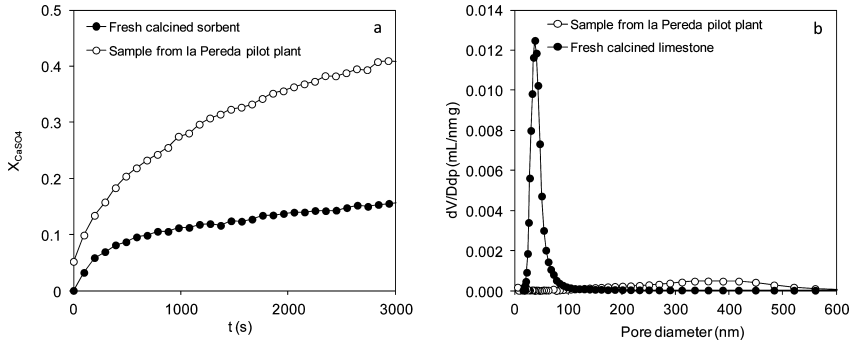

Figure 2. (a) Comparison of the evolution of sulfate conversion with time for the fresh calcined limestone and a sample taken from the La Pereda pilot plant (X_{ave} = 0.12) (sulfation conditions: T = 850 °C, 10% CO_2, 500 ppm SO_2, and balance in air). (b) Pore size distribution of fresh calcined limestone and a sample from the calciner of the La Pereda pilot plant (X_{ave} = 0.12).

supplied as a makeup flow to the CaL system) would have to be sufficient to sustain a certain level of sorbent activity in the calcium loop. Furthermore, when applying sorbent reactivation concepts to the CaL to enhance sorbent activity by the recarbonation[13] or hydration[14] of the solids stream coming from the carbonator, the sulfur mass balance in the system indicates that an accumulation of $CaSO_4$ will take place inside the CaL system as the makeup flow of limestone is reduced thanks to the method of reactivation. A recent paper[15] shows, by means of mass and energy balances in the system, the operating and fuel composition windows that will allow for these reactivation methods to operate in post-combustion systems using CaL. Figure 1 shows that, for very reduced makeup flows of $CaCO_3$ to the calciner on the right-hand side of the figure, assuming perfectly mixed solids in all circulating fluidized-bed (CFB) reactors (CFBC, carbonator, and calciner), the particles in the CaL will go through many carbonation and calcination cycles and will be substantially sulfated in these reactors by sulfur entering with the coal into the calciner and residual SO_2 in the flue gas entering the carbonator.[16] However, to limit the build up of $CaSO_4$ in the CaL in Figure 1, desulfurization in the CFBC with the purged material coming from the CaL must be effective. It has been suggested[17−20] that the practice of using CaO purges for SO_2 capture in existing CFB power plants could be applied because the sulfation of CaO derived from the calcination of limestone in CFB combustion environments has been one of the most studied gas−solid reactions.[21] However, there are substantial differences between CaO present in a CFBC that uses a limestone feed and the CaO-rich purges taken from a CaL cycle to capture CO_2.[18,19,22,23] One common behavior for CaO sorbents of SO_2 with a single calcination is an unreacted core. However, it is well-known that performing several calcination−carbonation cycles produces an opening of the pores by CaO sintering. This pore opening must make the plugging of the external pores more difficult, thus achieving higher conversions to $CaSO_4$ than that obtained for the fresh sorbent.[17,19] The purpose of the present study is to increase our understanding of the sulfation reaction in a CFBC by directly measuring the SO_2 absorption capacity and sulfaltion rates of CaO purge materials obtained from long-duration experiments recently carried out in a 1.7 MW_{th} pilot.[6]

EXPERIMENTAL SECTION

The sulfation experiments carried in this study were conducted in a thermogravimetric analyzer (TGA)[16,24] used in previous works to determine the kinetic parameters of the carbonation and sulfation reactions. Briefly, it consists of a microbalance (CI Instruments) that continuously measures the weight of the sample suspended in a platinum basket. The temperature of the sample is measured by means of a thermocouple, which is located just below the TGA pan and is continuously recorded on a computer.

In this study, small sieved 63−100 μm samples (<3 mg, composed of CaO, $CaCO_3$, $CaSO_4$, and ash) were subjected to an initial calcination step at 930 °C in air. This was followed by carbonation in 10 vol % CO_2 in air at 650 °C for 5 min to check its real and specific activity because the samples are heterogeneous. Sulfation was then performed in typical CFBC conditions: 500 ppmv SO_2 and 10 vol % CO_2 in air at 850 °C. Before the sulfation step, the sample was stabilized for 10 min in air at 850 °C to ensure that sulfation began at the desired temperature. Preliminary tests were carried out to establish the conditions where there was no relevant external diffusional effect.[25] A gas velocity of around 0.07 m/s (at 850 °C) was found to be valid for this purpose (because no effect on the sulfation rates was noted when the velocity was reduced by 50%). It was also established that a sample mass below 3 mg was necessary to eliminate external mass diffusion effects in the most demanding conditions (cycle 1) because of the high surface area. Conversion of CaO to $CaSO_4$ was calculated by measuring the increase in the weight of the samples. The solid samples used in this work were mainly solid purges obtained during recent test campaigns to demonstrate the effectiveness of post-combustion CO_2 capture by CaL (as in Figure 1) in a 1.7 MW_{th} pilot located in "La Pereda", a 50 MW_e CFBC coal power plant located in Mieres (Spain). The pilot has been described in detail elsewhere[5] and is basically made up of two interconnected CFB reactors of height 15 m that are able to treat about 1% (1.7 MW_{th} equivalent) of the flue gas generated in the CFBC power plant. A detailed description of the characteristics of the samples (in terms of equivalent cycle number, ash content, $CaSO_4$ content, etc.) and operating conditions in the pilot has been provided elsewhere.[6] Briefly, the samples were taken during a CO_2 capture test of 1 week duration, which included 80 h of coal/O_2 combustion in the calciner. A local high-purity limestone (>98% $CaCO_3$) was used for the test. During the CO_2 capture experiments, samples of solid material were extracted using isokinetic probes from both the carbonator and calciner reactors. The samples were composed of mainly CaO, $CaCO_3$, and inerts. The inerts are a mixture of $CaSO_4$, which is formed as a result of the SO_2 capture, and ashes from the combustion of the coal. The original limestone was highly pure on CaO (98.4 wt %). Chemical analysis of the samples was carried out to determine their composition by means of X-ray fluorescence spectroscopy (SRS 3000 Bruker) and C/S elemental analysis (LECO 230 CS). The maximum CO_2 carrying capture

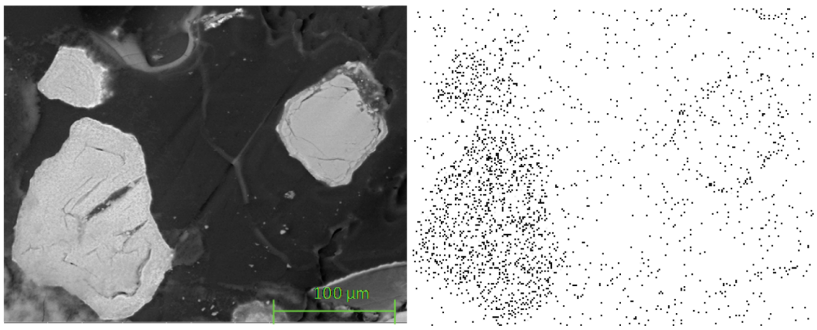

Figure 3. SEM−EDX images of characteristic sorbent particles from the La Pereda pilot plant with a maximum CO_2 carrying capacity of 0.12 and a sulfate conversion of 0.05. The EDX mapping shows uniformly distributed sulfur over the particles.

capacity (maximum conversion of CaO to $CaCO_3$ at the end of the fast CO_2 capture period) was determined to characterize the samples. This parameter was measured using a TGA (Q5000 IR) instrument, which is used routinely for this purpose, because it can automatically handle a large number of samples from the pilot. This test consists of an initial carbonation step in a 10 vol % CO_2 atmosphere, balance in air, for 10 min to calculate the initial degree of conversion to $CaCO_3$, followed by calcination at 850 °C in air for 5 min and then a carbonation step under the same conditions as before. To analyze the texture of the samples, a mercury porosimeter Autopore IV 9500 by Micromeritics was used. Finally, to determine the initial sulfation pattern of the purges from CaL, the cores of selected particles were examined by scanning electron microscopy (SEM), on a Quanta FEG 650 microscope, equipped with an energy-dispersive X-ray (EDX) analyzer Ametek-EDAX and an Apollo X detector. The samples were embedded in a Recapoli 2196 resin, cross-sectioned and polished using water as a lubricant.

A similar experimental procedure was applied in a selected sulfation test conducted on a sample of CaO resulting from the calcination of the fresh limestone used in the pilot for purposes of comparison of sulfation performance with respect to the CaO-rich purges extracted from the pilot. Figure 2a shows the evolution of sulfate conversion with time for a typical sample taken from the La Pereda CaL pilot plant and for a calcined sample of the parent limestone fed into the pilot. The low conversion achieved by the fresh calcined limestone is characteristic of an unreacted core sulfation pattern.[21,26] In contrast to the behavior of the fresh limestone, the highly cycled particles from the pilot (with a CO_2 carrying capacity of about 0.12) are able to sulfate up to a conversion of 0.41 in the same conditions and reaction time. It is well-known that, during calcination−carbonation cycles in the CaL process, the texture of CaO particles is susceptible to sintering that tends to increase the sizes of the pores and reduce the specific surface area of the CaO sorbent.[27−29] The different behaviors of the fresh calcined limestone and the sample from the La Pereda confirm previous observations[16,17,19] that limestones prone to an unreacted core sulfation pattern can evolve toward a more open structure during cycling in a CaL system and display a better sulfation performance. This knowledge has been used recently to quantitatively model the sulfation kinetics of cycled CaO particles under CFB carbonator conditions using a homogeneous (uniform) version of the random pore model (RPM) employed by Arias et al.[16] This model will also be used, in this work, to fit the sulfation kinetics of purges under CFBC conditions to predict the sulfation X_{CaSO_4} versus time curves or, in the future, as a submodel to predict sulfation rates in more general models of the reactors in a CaL process.

Figure 2b shows the pore size distributions of the fresh calcined limestone and the sample from the La Pereda pilot plant with a X_{ave} of 0.12. As seen, the fresh calcined limestone has a narrow pore size distribution, with an average pore diameter of 36 nm, whereas the sample from the La Pereda presents a wider distribution, with an average pore diameter of 327 nm. The La Pereda sample also has a lower porosity (0.31 compared to 0.42 in the case of the fresh calcined limestone) mainly because of the initial conversion to $CaSO_4$ (11 wt %). The differences in the pore size distributions are in agreement with the sulfation performances observed during the TGA tests because the open structure observed in the sample from La Pereda favors the homogeneous growth of $CaSO_4$ over the whole particle without blocking the pores and sealing off the core.

The initial sulfate distribution of the samples from the La Pereda pilot plant was also analyzed using SEM−EDX. Figure 3 shows an example of one of the samples with an initial sulfate conversion of 0.05. As seen, despite the tendency of the fresh calcined limestone to sulfate in an unreacted core pattern, the sulfate is distributed uniformly over the particles from the La Pereda pilot plant.

Determination of Kinetic Parameters. The results obtained from the sulfation of CaL purges in the TGA pilot plant were analyzed using the RPM.[30−32] The general expression of the RPM model that is valid for the kinetic/diffusional control of reactant SO_2 through the product layer of $CaSO_4$ is[32]

$$\frac{dX_{CaSO_4}}{dt} = \frac{k_S S C \sqrt{1 - \psi \ln(1 - X_{CaSO_4})}}{(1-\varepsilon)\left[1 + \frac{\beta Z}{\psi}(1 - \psi \ln(1 - X_{CaSO_4}) - 1)\right]} \quad (1)$$

where ψ is the internal structure parameter that accounts for the internal structure of the particle and is expressed as

$$\psi = \frac{4\pi L(1-\varepsilon)}{S} \quad (2)$$

and β is

$$\beta = \frac{2k_S a \rho (1-\varepsilon)}{bM_{CaO}D_P} \quad (3)$$

There are two boundary cases where eq 1 can be integrated. When the reaction is chemically controlled, β is low and eq 1 can be simplified and integrated to

$$\frac{1}{\psi}\left[\sqrt{1 - \psi \ln(1 - X_{CaSO_4})} - 1\right] = \frac{k_S S C_S t}{(1-\varepsilon)} \quad (4)$$

On the other hand, when diffusion through the product layer formed from $CaSO_4$ has control over the overall reaction, eq 1 can be integrated to give

$$\frac{1}{\psi}\left[\sqrt{1 - \psi \ln(1 - X_{CaSO_4})} - 1\right] = \frac{S}{(1-\varepsilon)}\sqrt{\frac{D_P M_{CaO} C_S t}{2\rho_{CaO} Z}} \quad (5)$$

The reaction rate parameters k_S and D_P can be obtained by fitting eqs 4 and 5 to the experimental data for each regime. From these

dx.doi.org/10.1021/ef402384z | *Energy Fuels* 2014, 28, 1325−1330

equations, the evolution of sulfate conversion with time under the chemically controlled regime (eq 6) and diffusion-controlled regime (eq 7) can be derived as follows:

$$X_{CaSO_4} = 1 - \exp\left(\frac{1 - \left(\frac{\tau}{2}\psi + 1\right)^2}{\psi}\right) \quad (6)$$

$$X_{CaSO_4} = 1 - \exp\left(\frac{1}{\psi} - \frac{\left[\sqrt{1 + \beta Z\tau} - \left(1 - \frac{\beta Z}{\psi}\right)\right]^2 \psi}{(\beta Z)^2}\right) \quad (7)$$

where

$$\tau = \frac{k_S C_S S_N t}{(1 - \varepsilon)} \quad (8)$$

To avoid having to measure the structural parameters for each individual sample, we have adopted a similar methodology to that of previous works.[16,33] This methodology allows for the structural parameters of cycled sorbents to be estimated as a function of those corresponding to the maximum CO_2 conversion of fresh calcined limestone after cycling. As indicated in the Experimental Section, the samples taken during the experimental runs in the La Pereda pilot plant are composed of a mixture of particles that have been subjected to a different number of cycles and have been characterized by an average CO_2 carrying capacity. This value was used to calculate the specific surface area (S_{ave}) and the length of the porous system (L_{ave}) for each mixture of particles using the following equations:

$$S_{ave} = S_0 X_{ave} \quad (9)$$

$$L_{ave} = L_0 X_{ave} \frac{r_{p0}}{r_{pN}} \quad (10)$$

By means of mercury porosimetry, the initial pore structure parameters were measured for the limestone studied and the following results were obtained: $S_0 = 4.37 \times 10^7$ m^2/m^3, $\varepsilon = 0.42$, $L_0 = 4.12 \times 10^{14}$, and $d_{pm} = 36$ nm.

Figure 4 shows the evolution of X_{CaSO_4} with time for some of the samples with different X_{ave}. The figure also shows the values calculated using the RPM and the kinetic parameters shown later in this paper. The starting point during the sulfation tests in TGA corresponds to the X_{CaSO_4} measured during the characterization of the samples from the La Pereda pilot plant. For the sample with a X_{ave} of 0.18, the reaction is faster at the beginning of the sulfation period. The transition to the diffusional regime with a slower reaction rate occurs at a conversion of approximately 20%. However, a progressive decrease in the reaction rate is observed after a conversion of approximately 40% until it almost stops at the end of the sulfation period. This is due to pore blockage from that point on as a consequence of the growth of a product layer of $CaSO_4$. In this case, the RPM is unable to predict the sorbent conversion for high values of X_{CaSO_4} because of the occurrence of pore blockage. For the sample with X_{CaSO_4} of 0.12, the model fits the experimental results with precision. This suggests that the structure of this sample is open enough not to have experienced any pore plugging for the level of conversion to $CaSO_4$ attained. In addition, for the samples with a X_{ave} of 0.10 and 0.08, the RPM is able to predict the experimental values during the entire sulfation period, indicating that the sulfate layer is able to grow without any geometrical restrictions. It can be concluded that the sulfation of CaO goes through an initial homogeneous sulfation period governed first by the kinetic regime. Then, when the product layer of $CaSO_4$ has developed, diffusion through this product layer mechanism takes control of the reaction. However, in the case of insufficiently cycled sorbents, the pores are narrower and, therefore, the effects of pore blockage are noticeable from a certain value of X_{CaSO_4}. It should be noted that the sulfation conversion achieved by the end of the sulfation period descreases with X_{ave}. This is because internal sintering of the CaO structure reduces the reacting surface area. Despite the sintering of the particles during cycling, the purges lead to a higher sulfate conversion than in the case of fresh limestone, even for highly deactivated purges with X_{ave} as low as 0.08.

To test the effect of the temperature on the sulfation reaction, the samples were tested under two additional conditions corresponding to the carbonator and calciner involved in the process depicted in Figure 1. To simulate the calciner conditions, the samples were tested at 930 °C in an atmosphere of 70 vol % CO_2, 500 ppmv SO_2, and balance in air. The carbonator conditions were simulated using a temperature of 650 °C and an air atmosphere with 500 ppmv SO_2. Figure 5 shows the evolution of sulfate conversion in a sample with a X_{ave} of 0.12 at the three temperatures.

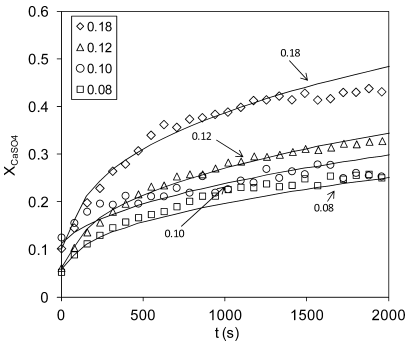

Figure 4. X_{CaSO_4} versus t curves for samples from La Pereda for different X_{ave}. The solid lines correspond to the predictions made by the RPM. Conditions: T = 850 °C, 500 ppm SO_2, 10 vol % CO_2, and balance in air.

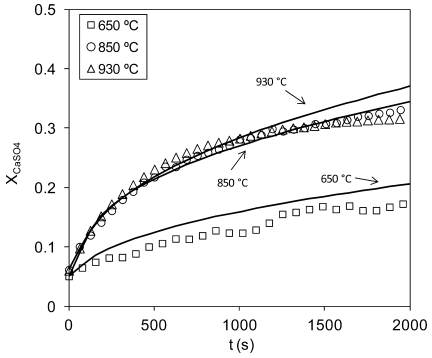

Figure 5. Comparison of experimental values of X_{CaSO_4} of a sample from the La Pereda pilot plant with a X_{ave} of 0.12 to those calculated by the model and calculated reaction constants (solid lines) for three temperatures.

As seen from the experimental results, the optimum sulfation temperatures (in terms of maximum conversions) are in the range of 850−900 °C, which is consistent with the observations reported by other authors.[21] Using the values of k_S and D_P determined for each temperature, the activation energy and pre-exponential factor were calculated. An activation energy of 42 kJ/mol (E_{ak}) was calculated for the kinetic regime, which is in agreement with the value obtained by Bhatia for fresh calcined limestones.[30] The pre-exponential factor calculated (k_{S0}) was 1.02×10^{-6} m^4 mol^{-1} s^{-1}. For the diffusional

regime, we have applied the Arrhenius equation to temperatures above and below 850 °C separately. By means of this procedure, two activation energies were obtained corresponding to the low- and high-temperature ranges. A slight variation was detected in the E_{aD} fitted under these conditions. It has been speculated that the change in the solid properties associated with the operation at temperatures higher than the Tammann temperature, i.e., 861 °C,[34] affects the diffusion of reactant SO_2 through the product layer and, in turn, the E_{aD} value, as demonstrated by other authors for the carbonation reaction of CaO.[35] It is beyond the scope of this work to analyze this effect in more detail. Therefore, the calculated values for the diffusional regime were, for E_{aD}, 138 and 120 kJ/mol for above and below the Tammann temperature, respectively, whereas the calculated values for D_{P0} were 1.56×10^{-5} and 1.45×10^{-5} m^2/s. From a practical point of view, the parameters calculated can be used with sufficient confidence to fit the observed X_{CaSO_4} versus time curves.

CONCLUSION

The performance of purges from a 1.7 MW_{th} CaL pilot plant for SO_2 capture has been tested under typical combustion conditions. The results obtained show that rich CaO purges from the La Pereda pilot plant exhibited a better sulfation performance than the parent fresh calcined limestone. This confirms the suitability of the purges from CaL to be used as feedstock for desulfurization in CFB combustors. The sulfation pattern was found to be homogeneous for a highly cycled sorbent. The results obtained have been interpreted and analyzed using the RPM. The reaction rate parameters measured at 850 °C were 1.10×10^{-8} m^4 mol^{-1} s^{-1} for k_S and 6.80×10^{-12} m^2/s for D_P, which are in agreement with those found in the literature under similar conditions. The RPM is able to calculate adequately the evolution of the sorbent conversion during sulfation, indicating that this particle reaction model and the reaction parameters derived from this work can be integrated into reactor models.

AUTHOR INFORMATION

Corresponding Author

*Telephone: +34-985119090. Fax: +34-985297662. E-mail: jmacod@incar.csic.es.

Notes

The authors declare no competing financial interest.

ACKNOWLEDGMENTS

The research presented in this work has received partial funding from the European Community Research Fund for Coal and Steel (ReCaL Project). Jose M. Cordero also acknowledges the award of a Ph.D. grant by FYCIT.

NOMENCLATURE

a and b = stoichometric coefficients for the sulfation reaction
C_S = concentration of SO_2 ($kmol/m^3$)
D_P = effective product layer diffusivity (m^2/s)
D_{P0} = pre-exponential factor (m^2/s)
d_{pm} = mean pore diameter (nm)
E_{ak} = activation energy for the kinetic regime (kJ/mol)
E_{aD} = activation energy for the diffusion through the product layer regime (kJ/mol)
k_S = rate constant for the surface reaction (m^4 mol^{-1} s^{-1})
k_{S0} = pre-exponential factor (m^4 mol^{-1} s^{-1})
L = total length of the pore system (m/m^3)
M = molecular weight (kg/kmol)
N = number of calcination/carbonation cycles
r_{pN} = radius of the pore after N cycles (m)
S = reaction surface per unit of volume (m^2/m^3)
t = reaction time (s)
V = pore volume (mL/g)
X_{ave} = CaO average conversion to $CaCO_3$
X_{CaSO4} = CaO conversion to $CaSO_4$
Z = volume fraction ratio after and before the reaction

Greek Letters

$\beta = 2k_S a\rho(1-\varepsilon)/M_{CaO} b D_P S$
ε = porosity
ρ = density (kg/m^3)
$\psi = 4\pi L(1-\varepsilon)/S^2$
$\tau = k_S C_S S t/(1-\varepsilon)$

REFERENCES

(1) Intergovernmental Panel on Climate Change (IPCC). *Special Report on Carbon Dioxide Capture and Storage*; Cambridge University Press: New York, 2005.
(2) Carbon Tracker and the Grantham Research Institute. *Unburnable Carbon 2013: Wasted Capital and Stranded Assets*; Carbon Tracker and The Grantham Research Institute: London, U.K., 2013.
(3) Shimizu, T.; Hirama, T.; Hosoda, H.; Kitano, K.; Inagaki, M.; Tejima, K. *Chem. Eng. Res. Des.* **1999**, *77*, 62−68.
(4) Abanades, J. C.; Rubin, E. S.; Anthony, E. J. *Ind. Eng. Chem. Res.* **2004**, *43*, 3462−3466.
(5) Sánchez-Biezma, A.; Ballesteros, J. C.; Diaz, L.; de Zárraga, E.; Álvarez, F. J.; López, J.; Arias, B.; Grasa, G.; Abanades, J. C. *Energy Procedia* **2011**, *4*, 852−859.
(6) Arias, B.; Diego, M. E.; Abanades, J. C.; Lorenzo, M.; Diaz, L.; Martínez, D.; Alvarez, J.; Sánchez-Biezma, A. *Int. J. Greenhouse Gas Control* **2013**, *18*, 237−245.
(7) Galloy, A. *VGB PowerTech* **2011**, *91*, 64−68.
(8) Hawthorne, C.; Dieter, H.; Bidwe, A.; Schuster, A.; Scheffknecht, G.; Unterberger, S.; Käß, M. *Energy Procedia* **2011**, *4*, 441−448.
(9) Chang, M. H.; Huang, C. M.; Liu, W. H.; Chen, W. C.; Cheng, J. Y.; Chen, W.; Wen, T. W.; Ouyang, S.; Shen, C. H.; Hsu, H. W. *Chem. Eng. Technol.* **2013**, *36*, 1525−1532.
(10) Abanades, J. C.; Alonso, M.; Rodríguez, N.; González, B.; Grasa, G.; Murillo, R. *Energy Procedia* **2009**, *1*, 1147−1154.
(11) Charitos, A.; Rodríguez, N.; Hawthorne, C.; Alonso, M.; Zieba, M.; Arias, B.; Kopanakis, G.; Scheffknecht, G.; Abanades, J. C. *Ind. Eng. Chem. Res.* **2011**, *50*, 9685−9695.
(12) Lu, D. Y.; Hughes, R. W.; Anthony, E. J. *Fuel Process. Technol.* **2008**, *89*, 1386−1395.
(13) Arias, B.; Grasa, G. S.; Alonso, M.; Abanades, J. C. *Energy Environ. Sci.* **2012**, *5*, 7353−7359.
(14) Manovic, V.; Anthony, E. J. *Ind. Eng. Chem. Res.* **2010**, *49*, 9105−9110.
(15) Diego, M. E.; Arias, B.; Alonso, M.; Abanades, J. C. *Fuel* **2013**, *109*, 184−190.
(16) Arias, B.; Cordero, J. M.; Alonso, M.; Abanades, J. C. *AIChE J.* **2012**, *58*, 2262−2269.
(17) Li, Y.; Buchi, S.; Grace, J. R.; Lim, C. J. *Energy Fuels* **2005**, *19*, 1927−1934.
(18) Manovic, V.; Anthony, E. J.; Loncarevic, D. *Ind. Eng. Chem. Res.* **2009**, *48*, 6627−6632.
(19) Grasa, G. S.; Alonso, M.; Abanades, J. C. *Ind. Eng. Chem. Res.* **2008**, *47*, 1630−1635.
(20) Li, Y.; Liu, H.; Wu, S.; Sun, R.; Lu, C. *J. Therm. Anal. Calorim.* **2013**, *111*, 1335−1343.
(21) Anthony, E. J.; Granatstein, D. L. *Prog. Energy Combust. Sci.* **2001**, *27*, 215−236.
(22) de las Obras-Loscertales, M.; de Diego, L. F.; García-Labiano, F.; Rufas, A.; Abad, A.; Gayán, P.; Adánez, J. *Energy Fuels* **2013**, *27*, 2266−2274.
(23) Takkinen, S.; Hyppänen, T.; Saastamoinen, J.; Pikkarainen, T. *Energy Fuels* **2011**, *25*, 2968−2979.

(24) González, B.; Grasa, G. S.; Alonso, M.; Abanades, J. C. *Ind. Eng. Chem. Res.* **2008**, *47*, 9256−9262.
(25) Alonso, M.; Criado, Y. A.; Abanades, J. C.; Grasa, G. *Fuel* **2014**, DOI: 10.1016/j.fuel.2013.08.005.
(26) Laursen, K.; Duo, W.; Grace, J. R.; Lim, J. *Fuel* **2000**, *79*, 153−163.
(27) Barker, R. J. *Appl. Chem. Biotechnol.* **1973**, *23*, 733−742.
(28) Abanades, J. C.; Alvarez, D. *Energy Fuels* **2003**, *17*, 308−315.
(29) Alvarez, D.; Abanades, J. C. *Energy Fuels* **2004**, *19*, 270−278.
(30) Bhatia, S. K.; Perlmutter, D. D. *AIChE J.* **1981**, *27*, 226−234.
(31) Bhatia, S. K.; Perlmutter, D. D. *AIChE J.* **1980**, *26*, 379−386.
(32) Bhatia, S. K.; Perlmutter, D. D. *AIChE J.* **1981**, *27*, 247−254.
(33) Grasa, G.; Murillo, R.; Alonso, M.; Abanades, J. C. *AIChE J.* **2009**, *55*, 1246−1255.
(34) Iribarne, A. P.; Iribarne, J. V.; Anthony, E. J. *Fuel* **1997**, *76*, 321−327.
(35) Bhatia, S. K.; Perlmutter, D. D. *AIChE J.* **1983**, *29*, 79−86.

5. Conclusiones

Las principales conclusiones de esta Tesis se resumen a continuación:

- Las altas velocidades y capacidades de sulfatación medidas para las partículas de CaO en las condiciones de operación de sistemas de captura de CO_2 por calcinación/carbonatación (CaL) en régimen de postcombustión, indican que estos sistemas son eficientes para la captura del SO_2. Además, en los carbonatadores en condiciones normales de operación se produce la co-captura de CO_2 y de SO_2 con una elevada eficacia, posibilitando la eliminación de la etapa de desulfuración en el combustor de la central térmica a costa de cierta desactivación de parte del CaO activo como sorbente de CO_2.
- En lo que respecta a los patrones de sulfatación de las partículas en los reactores de un sistema CaL en régimen de post-combustión, éstos serán normalmente homogéneos para diámetros de partícula < 200 μm y un número típico de ciclos de calcinación/carbonatación, independientemente del tipo de caliza. El proceso de calcinación/carbonatación- sinteriza el sorbente aumentando el diámetro de los poros y previniendo el sellado habitual en patrones de núcleo sin reaccionar típicos en la sulfatación de sorbente fresco con una única calcinación.

- Cuando el patrón de sulfatación es homogéneo, la sulfatación del CaO presenta dos etapas básicas: una etapa rápida inicial, controlada por la cinética, y una segunda etapa más lenta, gobernada por la difusión a través de la capa producto de $CaSO_4$ depositada sobre la superficie interna de CaO.
- En lo que respecta al comportamiento de sorbentes obtenidos de las purgas de sistemas CaL, las elevadas capacidades de sulfatación medidas han demostrado que estos sorbentes son más eficientes que la correspondiente caliza fresca calcinada cuando se usan para la captura de SO_2 en un combustor. Por lo tanto, la purga de sistemas CaL es un sorbente más eficaz que la caliza fresca original normalmente utilizada en estos equipos. De esta forma, se puede eliminar la corriente de caliza fresca alimentada para desulfurar en calderas al sustituirse por estas purgas de sólidos ricas en CaO provenientes del sistema de captura de CO_2.
- El modelo RPM ha sido validado para predecir las velocidades y capacidades de sulfatación en un sorbente típico bajo las condiciones de un CaL. Los parámetros cinéticos intrínsecos calculados junto con las ecuaciones desarrolladas a partir del modelo RPM pueden ser integrados con éxito en modelos de reactor y predecir las eficacias de captura de SO_2 de dichos reactores.

Otras conclusiones de esta Tesis son:

- El orden de reacción aparente para la sulfatación del CaO respecto del SO_2 es cercano a uno en todo el intervalo de variables de operación relevantes en reactores dentro de una sistema de CaL.

- Teniendo en cuental las bajas conversiones de CaO a $CaSO_4$ (< 5%) esperables en un CaL, la reacción de sulfatación estará normalmente controlada por la cinética intrínseca.
- La concentración de CO_2 no afecta a la velocidad de sulfatación de sorbentes altamente ciclados.
- La presencia de vapor de agua aumenta la velocidad de sulfatación en el régimen difusional a través de la capa producto de $CaSO_4$, pero no afecta a la etapa rápida controlada por la cinénica.
- Al aumentar la temperatura de reacción, los patrones de sulfatación tienden a ser más heterogéneos debido a un aumento de la resistencia difusional en los poros, y por lo tanto mayor número de ciclos N son necesarios para transformar el patrón en homogéneo.

6. Referencias

[1] IPCC-AR5, Climate Change 2013: The Physical Science Basis, (2013).
[2] IPCC-AR5, Climate Change 2014: Mitigation of Climate Change, (2014).
[3] NOAA, Trends of Atmospheric Carbon Dioxide, 2014.
[4] Global CCS Institute, 2014.
[5] IPCC, Special Report on Carbon Dioxide Capture and Storage, Cambridge University Press, (2005).
[6] A.D. Ebner, J.A. Ritter, State-of-the-art Adsorption and Membrane Separation Processes for Carbon Dioxide Production from Carbon Dioxide Emitting Industries, Separation Science and Technology 44 (2009) 1273-1421.
[7] P. Curran George, E. Fink Carl, E. Gorin, CO_2 Acceptor Gasification Process, Fuel Gasification, American Chemical Society, 1967, pp. 141-165.
[8] T. Shimizu, T. Hirama, H. Hosoda, K. Kitano, M. Inagaki, K. Tejima, A Twin Fluid-Bed Reactor for Removal of CO_2 from Combustion Processes, Chemical Engineering Research and Design 77 (1999) 62-68.
[9] J.C. Abanades, The maximum capture efficiency of CO_2 using a carbonation/calcination cycle of CaO/$CaCO_3$, Chemical Engineering Journal 90 (2002) 303-306.
[10] J.C. Abanades, E.J. Anthony, D.Y. Lu, C. Salvador, D. Alvarez, Capture of CO_2 from combustion gases in a fluidized bed of CaO, AIChE Journal 50 (2004) 1614-1622.
[11] J.C. Abanades, E.J. Anthony, J. Wang, J.E. Oakey, Fluidized Bed Combustion Systems Integrating CO_2 Capture with CaO, Environmental Science and Technology 39 (2005) 2861-2866.
[12] M. Alonso, N. Rodríguez, B. González, G. Grasa, R. Murillo, J.C. Abanades, Carbon dioxide capture from combustion flue gases with a calcium oxide chemical loop. Experimental results and process development, International Journal of Greenhouse Gas Control 4 (2010) 167-173.
[13] J.C. Abanades, M. Alonso, N. Rodríguez, Biomass Combustion with in Situ CO_2 Capture with CaO. I. Process Description and Economics, Industrial & Engineering Chemistry Research 50 (2011) 6972-6981.

[14] M. Alonso, N. Rodríguez, B. González, B. Arias, J.C. Abanades, Biomass Combustion with in Situ CO_2 Capture by CaO. II. Experimental Results, Industrial & Engineering Chemistry Research 50 (2011) 6982-6989.
[15] N. Rodríguez, M. Alonso, J.C. Abanades, Experimental investigation of a circulating fluidized-bed reactor to capture CO_2 with CaO, AIChE Journal 57 (2011) 1356-1366.
[16] B. Arias, M.E. Diego, J.C. Abanades, M. Lorenzo, L. Diaz, D. Martínez, J. Alvarez, A. Sánchez-Biezma, Demonstration of steady state CO_2 capture in a 1.7MWth calcium looping pilot, International Journal of Greenhouse Gas Control 18 (2013) 237-245.
[17] J.C. Abanades, Calcium looping for CO_2 capture in combustion systems.

Fluidized bed technologies for near-zero emission combustion and gasification, 2013, pp. 931-970.
[18] M. Alonso, M.E. Diego, C. Pérez, J.R. Chamberlain, J.C. Abanades, Biomass combustion with in situ CO_2 capture by CaO in a 300kWth circulating fluidized bed facility, International Journal of Greenhouse Gas Control 29 (2014) 142-152.
[19] J.C. Abanades, E.S. Rubin, E.J. Anthony, Sorbent Cost and Performance in CO_2 Capture Systems, Industrial & Engineering Chemistry Research 43 (2004) 3462-3466.
[20] N. Rodríguez, R. Murillo, J.C. Abanades, CO_2 Capture from Cement Plants Using Oxyfired Precalcination and/or Calcium Looping, Environmental Science and Technology 46 (2012) 2460-2466.
[21] V. Manovic, E.J. Anthony, D. Loncarevic, SO_2 Retention by CaO-Based Sorbent Spent in CO_2 Looping Cycles, Industrial & Engineering Chemistry Research 48 (2009) 6627-6632.
[22] I. Martínez, R. Murillo, G. Grasa, J. Carlos Abanades, Integration of a Ca looping system for CO_2 capture in existing power plants, AIChE Journal 57 (2011) 2599-2607.
[23] N. Rodriguez, M. Alonso, G. Grasa, J.C. Abanades, Heat requirements in a calciner of $CaCO_3$ integrated in a CO_2 capture system using CaO, Chemical Engineering Journal 138 (2008) 148-154.
[24] A. Charitos, N. Rodríguez, C. Hawthorne, M. Alonso, M. Zieba, B. Arias, G. Kopanakis, G. Scheffknecht, J.C. Abanades, Experimental Validation of the Calcium Looping CO_2 Capture Process with Two Circulating Fluidized Bed Carbonator Reactors, Industrial & Engineering Chemistry Research 50 (2011) 9685-9695.
[25] J. Ströhle, M. Junk, J. Kremer, A. Galloy, B. Epple, Carbonate looping experiments in a 1MWth pilot plant and model validation, Fuel 127 (2014) 13-22.

[26] M. Alonso, M.E. Diego, J.C. Abanades, C. Perez, J. Chamberlain, In situ CO_2 capture with CaO in a 300 kW fluidized bed biomass combustor, 7th Trondheim CCS Conference, Trondheim, 2013.
[27] C. Hawthorne, H. Dieter, A. Bidwe, A. Schuster, G. Scheffknecht, S. Unterberger, M. Käß, CO_2 capture with CaO in a 200 kWth dual fluidized bed pilot plant, Energy Procedia 4 (2011) 441-448.
[28] M.H. Chang, C.M. Huang, W.H. Liu, W.C. Chen, J.Y. Cheng, W. Chen, T.W. Wen, S. Ouyang, C.H. Shen, H.W. Hsu, Design and Experimental Investigation of Calcium Looping Process for 3-kWth and 1.9-MWth Facilities, Chemical Engineering & Technology 36 (2013) 1525-1532.
[29] D.Y. Lu, R.W. Hughes, E.J. Anthony, Ca-based sorbent looping combustion for CO_2 capture in pilot-scale dual fluidized beds, Fuel Processing Technology 89 (2008) 1386-1395.
[30] J.C. Abanades, M. Alonso, N. Rodríguez, B. González, G. Grasa, R. Murillo, Capturing CO_2 from combustion flue gases with a carbonation calcination loop. Experimental results and process development, Energy Procedia 1 (2009) 1147-1154.
[31] I. Martinez, R. Murillo, G. Grasa, N. Rodriguez, J.C. Abanades, Conceptual design of a three fluidised beds combustion system capturing CO2 with CaO, International Journal of Greenhouse Gas Control 5 (2011) 498-504.
[32] N. Rodríguez, M. Alonso, G. Grasa, J.C. Abanades, Process for Capturing CO_2 Arising from the Calcination of the $CaCO_3$ Used in Cement Manufacture, Environmental Science and Technology 42 (2008) 6980-6984.
[33] J.C. Abanades, M. Alonso, N. Rodriguez, Experimental validation of in situ CO_2 capture with CaO during the low temperature combustion of biomass in a fluidized bed reactor, International Journal of Greenhouse Gas Control 5 (2011) 512-520.
[34] A.W.D. Hills, The mechanism of the thermal decomposition of calcium carbonate, Chemical Engineering Science 23 (1968) 297-320.
[35] I. Martínez, G. Grasa, R. Murillo, B. Arias, J.C. Abanades, Modelling the continuous calcination of $CaCO_3$ in a Ca-looping system, Chemical Engineering Journal 215–216 (2013) 174-181.
[36] R. Barker, The reversibility of the reaction $CaCO_3 \rightleftarrows CaO+CO_2$, Journal of Applied Chemistry and Biotechnology 23 (1973) 733-742.
[37] G.S. Grasa, J.C. Abanades, CO_2 Capture Capacity of CaO in Long Series of Carbonation/Calcination Cycles, Industrial & Engineering Chemistry Research 45 (2006) 8846-8851.
[38] B. Arias, G.S. Grasa, M. Alonso, J.C. Abanades, Post-combustion calcium looping process with a highly stable sorbent activity by recarbonation, Energy & Environmental Science 5 (2012) 7353-7359.
[39] B. Arias, J.C. Abanades, E.J. Anthony, Model for Self-Reactivation of Highly Sintered CaO Particles during CO_2 Capture Looping Cycles, Energy & Fuels 25 (2011) 1926-1930.

[40] B. González, G.S. Grasa, M. Alonso, J.C. Abanades, Modeling of the Deactivation of CaO in a Carbonate Loop at High Temperatures of Calcination, Industrial & Engineering Chemistry Research 47 (2008) 9256-9262.
[41] J.C. Abanades, D. Alvarez, Conversion Limits in the Reaction of CO_2 with Lime, Energy & Fuels 17 (2003) 308-315.
[42] G.S. Grasa, J.C. Abanades, M. Alonso, B. González, Reactivity of highly cycled particles of CaO in a carbonation/calcination loop, Chemical Engineering Journal 137 (2008) 561-567.
[43] D. Alvarez, J.C. Abanades, Determination of the Critical Product Layer Thickness in the Reaction of CaO with CO_2, Industrial & Engineering Chemistry Research 44 (2005) 5608-5615.
[44] D. Alvarez, J.C. Abanades, Pore-Size and Shape Effects on the Recarbonation Performance of Calcium Oxide Submitted to Repeated Calcination/Recarbonation Cycles, Energy & Fuels 19 (2004) 270-278.
[45] S.K. Bhatia, D.D. Perlmutter, A random pore model for fluid-solid reactions: I. Isothermal, kinetic control, AIChE Journal 26 (1980) 379-386.
[46] S.K. Bhatia, D.D. Perlmutter, A random pore model for fluid-solid reactions: II. Diffusion and transport effects, AIChE Journal 27 (1981) 247-254.
[47] S.K. Bhatia, D.D. Perlmutter, Effect of the product layer on the kinetics of the CO_2-lime reaction, AIChE Journal 29 (1983) 79-86.
[48] G. Grasa, R. Murillo, M. Alonso, J.C. Abanades, Application of the random pore model to the carbonation cyclic reaction, AIChE Journal 55 (2009) 1246-1255.
[49] M. Hartman, O. Trnka, Reactions between calcium oxide and flue gas containing sulfur dioxide at lower temperatures, AIChE Journal 39 (1993) 615-624.
[50] E.J. Anthony, D.L. Granatstein, Sulfation phenomena in fluidized bed combustion systems, Progress in Energy and Combustion Science 27 (2001) 215-236.
[51] R.H. Borgwardt, Kinetics of the reaction of sulfur dioxide with calcined limestone, Environmental Science and Technology 4 (1970) 59-63.
[52] R.H. Borgwardt, R.D. Harvey, Properties of carbonate rocks related to sulfur dioxide reactivity, Environmental Science and Technology 6 (1972) 350-360.
[53] S.K. Bhatia, D.D. Perlmutter, The effect of pore structure on fluid-solid reactions: Application to the SO_2-lime reaction, AIChE Journal 27 (1981) 226-234.
[54] K. Laursen, W. Duo, J.R. Grace, J. Lim, Sulfation and reactivation characteristics of nine limestones, Fuel 79 (2000) 153-163.
[55] M. Hartman, R.W. Coughlin, Reaction of Sulfur Dioxide with Limestone and the Influence of Pore Structure, Industrial & Engineering Chemistry Process Design and Development 13 (1974) 248-253.

[56] S.V. Sotirchos, H.-C. Yu, Mathematical modelling of gas-solid reactions with solid product, Chemical Engineering Science 40 (1985) 2039-2052.
[57] R.H. Borgwardt, K.R. Bruce, Effect of specific surface area on the reactivity of CaO with SO_2, AIChE Journal 32 (1986) 239-246.
[58] M.Z. Haji-Sulaiman, A.W. Scaroni, S. Yavuzkurt, Optimum sulfation temperature for sorbents used in fluidized bed coal combustion, Fuel Processing Technology 25 (1990) 227-240.
[59] S. Zarkanitis, S.V. Sotirchos, Pore structure and particle size effects on limestone capacity for SO_2 removal, AIChE Journal 35 (1989) 821-830.
[60] J. Adanez, P. Gayan, F. Garcia-Labiano, Comparison of Mechanistic Models for the Sulfation Reaction in a Broad Range of Particle Sizes of Sorbents, Industrial & Engineering Chemistry Research 35 (1996) 2190-2197.
[61] F. García-Labiano, A. Rufas, L.F. de Diego, M.d.l. Obras-Loscertales, P. Gayán, A. Abad, J. Adánez, Calcium-based sorbents behaviour during sulphation at oxy-fuel fluidised bed combustion conditions, Fuel 90 (2011) 3100-3108.
[62] C. Wang, L. Jia, Y. Tan, E.J. Anthony, The effect of water on the sulphation of limestone, Fuel 89 (2010) 2628-2632.
[63] M.C. Stewart, V. Manovic, E.J. Anthony, A. Macchi, Enhancement of Indirect Sulphation of Limestone by Steam Addition, Environmental Science and Technology 44 (2010) 8781-8786.
[64] R.L. Pigford, G. Sliger, Rate of Diffusion-Controlled Reaction Between a Gas and a Porous Solid Sphere - Reaction of SO_2 with $CaCO_3$, Industrial & Engineering Chemistry Process Design and Development 12 (1973) 85-91.
[65] J. Szekely, J.W. Evans, H.Y. Sohn, Gas-solid reactions, Academic Press, (1976).
[66] J. Szekely, J.W. Evans, A structural model for gas—solid reactions with a moving boundary, Chemical Engineering Science 25 (1970) 1091-1107.
[67] M. Ishida, C.Y. Wen, Comparison of zone-reaction model and unreacted-core shrinking model in solid—gas reactions—I isothermal analysis, Chemical Engineering Science 26 (1971) 1031-1041.
[68] S.V. Sotirchos, H.C. Yu, Overlapping grain models for gas-solid reactions with solid product, Industrial & Engineering Chemistry Research 27 (1988) 836-845.
[69] M. Hartman, R.W. Coughlin, Reaction of sulfur dioxide with limestone and the grain model, AIChE Journal 22 (1976) 490-498.
[70] P.A. Ramachandran, J.M. Smith, Effect of sintering and porosity changes on rates of gas—solid reactions, The Chemical Engineering Journal 14 (1977) 137-146.
[71] C. Georgakis, C.W. Chang, J. Szekely, A changing grain size model for gas--solid reactions, Chemical Engineering Science 34 (1979) 1072-1075.

[72] P.V. Ranade, D.P. Harrison, The grain model applied to porous solids with varying structural properties, Chemical Engineering Science 34 (1979) 427-432.
[73] J. Szekely, M. Propster, A structural model for gas solid reactions with a moving boundary—VI: The effect of grain size distribution on the conversion of porous solids, Chemical Engineering Science 30 (1975) 1049-1055.
[74] E.E. Petersen, Reaction of porous solids, AIChE Journal 3 (1957) 443-448.
[75] P.A. Ramachandran, J.M. Smith, A single-pore model for gas-solid noncatalytic reactions, AIChE Journal 23 (1977) 353-361.
[76] G.A. Simons, A.R. Garman, A.A. Boni, The kinetic rate of SO_2 sorption by CaO, AIChE Journal 33 (1987) 211-217.
[77] H. Ale Ebrahim, Application of Random-Pore Model to SO_2 Capture by Lime, Industrial & Engineering Chemistry Research 49 (2009) 117-122.
[78] Y. Li, S. Buchi, J.R. Grace, C.J. Lim, SO_2 Removal and CO_2 Capture by Limestone Resulting from Calcination/Sulfation/Carbonation Cycles, Energy & Fuels 19 (2005) 1927-1934.
[79] H.-J. Ryu, J.R. Grace, C.J. Lim, Simultaneous CO_2/SO_2 Capture Characteristics of Three Limestones in a Fluidized-Bed Reactor, Energy & Fuels 20 (2006) 1621-1628.
[80] P. Sun, J.R. Grace, C.J. Lim, E.J. Anthony, Removal of CO_2 by Calcium-Based Sorbents in the Presence of SO_2, Energy & Fuels 21 (2006) 163-170.
[81] G.S. Grasa, M. Alonso, J.C. Abanades, Sulfation of CaO Particles in a Carbonation/Calcination Loop to Capture CO_2, Industrial & Engineering Chemistry Research 47 (2008) 1630-1635.
[82] V. Manovic, E.J. Anthony, Competition of Sulphation and Carbonation Reactions during Looping Cycles for CO_2 Capture by CaO-Based Sorbents, The Journal of Physical Chemistry A 114 (2010) 3997-4002.